

Role of DNA-topoisomerase I in mtDNA maintenance

Relevance of a distinct, mitochondria-targeted enzyme
version in vertebrates

Inaugural-Dissertation

zur Erlangung des Doktorgrades
der Mathematisch-Naturwissenschaftlichen Fakultät
der Heinrich-Heine-Universität Düsseldorf

vorgelegt von

Ilaria Dalla Rosa

aus Bolzano

Düsseldorf, Januar 2009

Aus dem Institut für Klinische Chemie und Laboratoriumsdiagnostik
des Universitätsklinikums Düsseldorf

Gedruckt mit der Genehmigung der
Mathematisch-Naturwissenschaftlichen Fakultät der
Heinrich-Heine-Universität Düsseldorf

Referent: Prof. Dr. Fritz Boege
Koreferent: Prof. Dr. Johannes H. Hegemann

Tag der mündlichen Prüfung: 5.6.2009

Contents

Summary	I
Zusammenfassung.....	III
1. Introduction	1
1.1 Mitochondria	2
1.1.1 Mitochondrial structure	2
1.1.2 Mitochondrial import.....	2
1.1.3 The mitochondrial respiratory chain.....	3
1.1.4 MtDNA.....	4
1.1.4.1 MtDNA organisation	5
1.1.4.2 MtDNA metabolism.....	6
1.1.5 Mitochondrial dysfunctions	11
1.1.5.1 Mitochondria and ageing	12
1.1.5.2 Mitochondria and diseases.....	14
1.1.5.3 Molecular basis of mitochondrial disfunctions	15
1.2 DNA topoisomerases	16
1.2.1 Classification and cellular functions.....	17
1.2.1.1 Type I topoisomerases	18
1.2.1.2 Type II topoisomerases	19
1.2.2. Mitochondrial topoisomerases.....	20
1.2.2.1 Vertebrates	20
1.2.2.2. Non-vertebrate eukaryotes.....	21
1.2.3. Human nuclear topoisomerase I (Top1).....	23
1.2.3.1 Structure.....	23
1.2.3.2 Cellular roles.....	25
1.2.4. Mitochondrial topoisomerase I (Top1mt).....	25
1.3 Aims of study.....	28
2. Materials	29
2.1 Available plasmids	29
2.1.1 Expression vectors.....	29
2.1.2 Viral vector.....	29
2.1.3 cDNAs	29
2.1.4 cDNAs used as PCR standards or Northern and Southern blot probes ...	30

2.2 Microbiology	30
2.2.1 E.coli strains.....	30
2.2.2 Bacterial growth media	31
2.3 Cell culture	31
2.3.1 Cell lines.....	31
2.3.2 Supplements & Antibiotics	31
2.3.3 Media.....	32
2.4 Buffers and Stock Solutions	32
2.5 Enzymes	33
2.6 Chemicals	33
2.7 Antibodies	34
2.7.1 Primary antibodies.....	34
2.7.2 Secondary antibodies	34
2.8 Consumable items	35
2.9 Kits	35
2.10 Instruments	35
3. Methods	37
3.1 Cloning	37
3.1.1 Plasmids construction	37
3.1.1.1 Basic construct	37
3.1.1.2 Mitochondria-targeted YFP chimera	37
3.1.1.3 Nuclear targeted chimera	39
3.1.1.4 Untagged Top1mt	39
3.1.1.5 Viral constructs.....	40
3.1.1.6 Swap constructs.....	40
3.1.1.7 Overlap extension PCR.....	42
3.1.1.8 Standard PCR	43
3.1.2 Restriction nucleases digestion, gel electrophoresis and recovery of DNA from agarose gels	43
3.1.3 Ligation	44
3.1.4 Transformation and isolation of plasmid DNA	44
3.1.4.1 Generation of competent E.Coli cells.....	44
3.1.4.2 Transformation of E.coli	44
3.1.4.3 Plasmid preparation at a small scale (Minipreps)	44
3.1.4.4 Plasmid preparation at a large scale (Maxipreps)	45
3.1.4.5 Sequencing of plasmids	45
3.2 Cell culture	45

3.2.1 Maintenance of mammalian cells	45
3.2.2 Transfection and selection of HT-1080 cells	45
3.2.3 Viral transduction	46
3.2.3.1 Lentivirus production.....	46
3.2.3.2 HT1080 transduction.....	46
3.2.4 Cell cycle analysis	47
3.2.5 β-galactosidase staining	47
3.3 Microscopy	47
3.3.1 Fluorescence microscopy.....	47
3.3.2 Confocal microscopy	47
3.4 Proteins analysis	48
3.4.1 Preparation of mitoplasts.....	48
3.4.2 Preparation of whole cells lysates.....	48
3.4.3 Preparation of mitoplast lysates.....	49
3.4.4 Polyacrylamide gel electrophoresis	49
3.4.4.1 Gel run.....	49
3.4.4.2 Blotting	49
3.4.4.3 Western Blot.....	49
3.4.5 Catalytic activity of topoisomerase I	50
3.4.5.1 Mitoplast protein extracts.....	50
3.4.5.2 Relaxation assay	50
3.5 MtDNA analysis	50
3.5.1 Quantification of mtDNA copy number and mtDNA deletions.....	50
3.5.1.1 DNA extraction	50
3.5.1.2 Quantitative Real-Time PCR (qPCR).....	50
3.5.2 Southern Blot.....	52
3.5.2.1 DNA preparation	52
3.5.2.2. DNA separation and transfer	52
3.5.2.3. Probe generation	52
3.5.2.4. Labelling and hybridization	53
3.5.3 Analysis of mitochondrial transcripts.....	53
3.5.3.1 Total RNA isolation.....	53
3.5.3.2 Semiquantitative analysis of mtDNA transcripts: Northern Blotting ...	53
3.5.3.3 Quantitative analysis of mtDNA transcripts: Real-Time Reverse-	
Transcription PCR (qRT-PCR)	54
3.5.3.4 Quantitative analysis of nuclear transcripts for mitochondria-targeted	
proteins	56
3.6 Investigation of mitochondrial functions	56
3.6.1 Mitochondrial reactive oxygen species (ROS) production.....	56
3.6.2 Mitochondrial respiration.....	57

3.6.3 Lactate production	57
3.7 Statistics.....	57
4. Results.....	59
4.1 Deregulated Top1mt expression	59
4.1.1 Mitochondrial targeting of transgenic Top1mt variants.....	59
4.1.2 Deregulated expression of Top1mt increases topoisomerase I activity in mitochondria	62
4.1.3 MTS-YFP-Top1mt associates with mitochondrial nucleoids without changing the overall topological state of mtDNA.....	64
4.1.4 Effect of increased Top1mt activity on mtDNA metabolism and mtDNA stability	66
4.1.4.1 Deregulated Top1mt expression does not affect the mtDNA replication and stability	67
4.1.4.2 MTS-YFP-Top1mt activity decreases steady-state levels of mtDNA transcripts.....	68
4.1.5 Modest decrease of mtDNA transcripts drastically reduces the respiratory chain proteins.....	70
4.1.6 Defective respiratory chain assembly inhibits cell respiration and induces a metabolic switch to anaerobic glycolysis.....	73
4.1.7 Defects of the respiratory chain lead to increased oxidative stress in mitochondria	74
4.2 Mitochondrial targeting of nuclear Top1	77
4.2.1 The MTS of COX subunit VII is able to import Top1 into mitochondria	77
4.2.2 Top1 maintains its biochemical activity in mitochondria	79
4.2.3 Mitochondrial targeting of Top1 leads to mtDNA depletion	80
4.2.4 Mitochondrial targeting of Top1 alters mitochondrial shape.....	80
4.2.5 Mitochondrial targeting of Top1 depletes respiratory chain	82
4.2.6 Mitochondrial targeting of Top1 compromises cell respiration.....	84
4.2.7 Mitochondrial targeting of Top1 causes uridine auxotrophy	85
4.2.8 Mitochondrial targeting of Top1 induces cell senescence.....	86
4.2.9 mtDNA depletion induced by mitochondrial targeting of Top1 is a passive process.....	86
4.2.10 Mitochondrial targeting of Top1 blocks mtDNA replication initiation.	89
4.3 The effects of Top1mt/Top1 hybrids.....	91
4.3.1 Targeting of Top1mt/Top1 hybrids to mitochondria	91
4.3.2 Top1mt/Top1 hybrids maintain their catalytic properties	94
4.3.3 mtDNA transcription-repressive properties reside in the core domain of Top1.....	95

4.3.4 Top1 ¹⁹¹⁻³⁵¹ manifests its repressive effect only in the context of a complete topoisomerase I enzyme.	96
4.3.5 Top1 and Top1mt differ in their interaction with nuclear genomic DNA	98
4.3.6 Evolutional change of Top1mt occurs in a highly conserved region	99
5. Discussion	105
5.1 Mitochondrial targeting of Top1 is incompatible with a correct mtDNA metabolism in human cells.....	105
5.1.1 Effects on cell-physiology of Top1 mitochondrial targeting	106
5.1.2 Which evolutionary changes have generated or defused the mtDNA repressive potential of Top1 or Top1mt, respectively?.....	107
5.1.3 How does Top1 deplete mtDNA?.....	108
5.2 Heterologous expression of Top1mt.....	112
5.2.1 Top1mt possesses an inherent potential to inhibit transcription of mitochondrial genes	112
5.1.2 <i>In vivo</i> effects of attenuated mtDNA transcription.....	113
5.1.3 Top1mt associates with mitochondrial nucleoids	115
5.3 Concluding remarks	115
6.References	119
7. Abbreviations	139
8. Appendix.....	143
8.1 Plasmid maps	143
8.1.A pMC-2PS-delta HindIII-P	143
8.1.B pMC-EYFP-P-N.....	144
8.1.C pCL1P3.....	145
8.1.D pMC-EYFP-P-N	146
8.2 Top1/Top1mt alignment.....	147
9. Acknowledgments	149
10. Curriculum Vitae	151
11. Erklärung.....	153

Summary

In vertebrate cells, mitochondrial DNA represents the only genetic material outside the nucleus. The mitochondrial genome (mtDNA) encodes an essential protein subset of the respiratory chain. Transcription and replication generate topological tensions in the circular mtDNA molecule that must be removed to enable progression of mtDNA metabolism. The only enzymes capable of releasing topological stress from double helical DNA are DNA topoisomerases. Therefore, topoisomerase activity is believed to be an essential cofactor of mtDNA metabolism. In fact, all three topoisomerase sub-families present in the vertebrate nucleus (IA, IB and IIA) are also present in mitochondria. Vertebrate evolution has split the type IB topoisomerase into two genetically distinct but catalytically similar variants: one dedicated to the nucleus (Top1) and one dedicated to the mitochondrial compartment (Top1mt). Top1mt paralogues are present in all vertebrates, but not found in invertebrates, suggesting important role(s) of this enzyme in vertebrate mtDNA metabolism. On the other hand, Top1mt was found to be dispensable for mouse development. Thus, the significance of this separately encoded enzyme remains unknown. One possible explanation would be that in long-lived vertebral species prolonged exposure to Top1 compromises mtDNA integrity and that the development of Top1mt provided a type IB enzyme version able to safely handle the mitochondrial genome. In this work, I tested this hypothesis by aberrant targeting of nuclear Top1 to mitochondria of human cells and investigating the effects of this manipulation on mtDNA metabolism.

Mitochondrial targeting of YFP tagged Top1 strongly inhibited mtDNA transcription. As a consequence, the primers necessary for mtDNA replication were depleted, which ultimately led to a complete loss of mtDNA. This effect was independent of Top1 catalytic activity, since it was also induced by inactive (Y723F) mutants. In contrast, heterologous expression of YFP tagged Top1mt did not affect replication and average copy number of mtDNA. To identify which evolutionary changes in Top1mt enable safe handling of mtDNA, several regions of the two enzyme variants were inter-changed and the resulting Top1/Top1mt hybrids were then tested for their effect on mtDNA copy number. The domain swapping strategy revealed that mtDNA-destructive properties of Top1 are fully retained in all hybrids presenting residues 191-286 of the nuclear enzyme. Importantly, this region

Summary

manifests its repressive effect only in the context of a functional enzyme. Finally it should be noted that expression of YFP fused Top1mt caused a slight decrease of mtDNA transcripts level, an effect not inflicted by the active site mutant (Y559F), the YFP tag alone or overexpression of the untagged enzyme. This moderate decrease of mtDNA transcripts resulted in severe mitochondrial dysfunction.

In conclusion, targeting of the nuclear variant Top1 to human mitochondria is incompatible with stable mtDNA propagation and the development of Top1mt was necessary to ensure safe handling of mtDNA. Despite these evolutionary changes, Top1mt still harbours a potential to inhibit mtDNA transcription.

Zusammenfassung

Das einzige genetische Material außerhalb des Zellkernes in Vertebratenzellen ist das mitochondriale Genom (mtDNA), welches die Information für einen essentiellen Teil der Atmungskettenproteine enthält. Die Transkription und Replikation der zirkulären mtDNA-Moleküle generieren topologischen Stress, der beseitigt werden muss, um einen korrekten Verlauf des mtDNA-Metabolismus zu erlauben. DNA-Topoisomerasen sind die einzigen Enzyme, die in der Lage sind, Torsionsspannungen einer DNA-Doppelhelix zu beseitigen, und die Aktivität dieser Enzyme wird daher als wesentliche Cofaktor des mtDNA-Metabolismus angesehen. Alle drei im Zellkern von Vertebraten auftretenden Unterfamilien der Topoisomerasen (IA, IB und IIA) sind auch in den Mitochondrien vorhanden. Die Evolution von Vertebraten hat die Typ-IB Topoisomerase in zwei verschiedene Varianten aufgespalten: die eine ist zuständig für den Kern (Top1) und die andere für die Mitochondrien (Top1mt). Alle Vertebraten besitzen ein Top1mt-Paralog, Invertebraten jedoch nicht, was eine wichtige Rolle(n) von diesem Enzym im mtDNA-Metabolismus von Wirbeltieren vermuten lässt. Andererseits ist Top1mt für die Entwicklung der Maus entbehrlich, so dass die Relevanz dieses separat kodierten Enzyms bislang unklar ist. Eine mögliche Erklärung wäre, dass in lang lebenden Organismen die Integrität der mtDNA durch die Aktivität der nukleären Top1-Variante gefährdet ist, und dass deshalb im Laufe der Evolution eine Typ-IB-Topoisomerase entstanden ist, die in der Lage ist, mtDNA sicher zu metabolisieren. Um diese Hypothese zu überprüfen, habe ich in der vorliegenden Arbeit nukleäre Top1 artifiziell in den Mitochondrien humaner Zellen exprimiert und die Auswirkungen dieser Manipulation auf den mtDNA Metabolismus untersucht.

Diese mitochondriale Adressierung YFP-fusionierter Top1 führte zu einer ausgeprägten Hemmung der mtDNA-Transkription. Die daraus resultierende Verminderung von Primern, welche für die mtDNA-Replikation notwendig sind, resultierte schließlich zu einem kompletten Verlust der mtDNA. Da auch inaktive Top1-Mutanten (Y723F) denselben Effekt auslösten, ist die schädliche Wirkung der Top1 unabhängig von ihrer katalytischen Aktivität. Im Gegensatz dazu beeinflusste die heterologe Überexpression einer YFP-fusionierten Top1mt weder die Replikation noch die Kopienanzahl der mtDNA. Um herauszufinden, welche evolutionären Veränderungen der Top1mt den sicheren Umgang mit der mtDNA ermöglichen,

wurden verschiedenen Regionen von Top1 und Top1mt untereinander ausgetauscht und die resultierenden Hybrid-Proteine auf ihren Einfluss auf die Kopienanzahl der mtDNA untersucht. Diese Austauschstrategie zeigte, dass die schädigenden Eigenschaften der Top1 in allen Hybriden, die die Aminosäurereste 191-286 des nukleären Enzyms beinhalten, auftreten. Diese Region zeigte ihre hemmenden Eigenschaften nur im Kontext eines funktionalen Enzyms. Hierbei ist die Tatsache bemerkenswert, dass die Expression einer YFP-fusionierten Top1mt eine leichte Abnahme der mitochondrialen Transkripte verursachte. Im Gegensatz dazu trat dieser Effekt weder bei der Expression der katalytisch inaktiven Mutante (Y723F), noch bei unfusioniertem YFP oder unfusioniertem Enzym auf. Allerdings führte diese leichte Reduktion der mtDNA Transkripte zu schweren mitochondrialen Dysfunktionen.

Zusammenfassend ergibt sich ein Bild, in dem eine Adressierung der nukleären Variante Top1 in humanen Mitochondrien mit einer stabilen mtDNA Übertragung unvereinbar ist, und in dem die Entwicklung einer mitochondrialen Top1mt im Sinne eines sicheren Umgangs mit der mtDNA notwendig war. Allerdings besitzt die Top1mt trotz dieser evolutionären Anpassungen immer noch das Potential, die mtDNA Transkription zu hemmen.

1. Introduction

Mitochondria are essential organelles of eukaryotic cells involved in a wide spectrum of functions. They play a prominent role in various anabolic and catabolic processes, including Krebs and urea cycle, β -oxidation and the biosynthesis of heme, pyrimidine and many other metabolites. Furthermore, these organelles have a role in the regulation of cellular homeostasis involving cell signalling pathways such as the apoptotic cascade (Riedl & Salvesen, 2007). Most notably, mitochondria contain the respiratory chain that catalyzes oxidative phosphorylation (OXPHOS), the metabolic pathway that converts the energy of nutrients into ATP. Thirteen essential protein components of the respiratory chain and the components of the mitochondrial translation machinery are synthesized within the mitochondrial matrix by a separate mitochondrial genome (mtDNA). Replication and transcription of mtDNA generate topological stress in this closed, double-stranded DNA molecule. Since topoisomerases are the only enzymes capable of releasing topological stress from DNA helices, their activity is believed to be an essential cofactor of mtDNA metabolism (Wang, 2002). Several topoisomerases have a dual localisation and are targeted to the nucleus and to mitochondria. Exceptionally, vertebrate topoisomerase I does not have a dual localisation. Vertebrate evolution has split this enzyme into two genetically distinct variants: the nuclear topoisomerase I (Top1) and the mitochondrial topoisomerase I (Top1mt) responsible for the nuclear and the mitochondrial compartment, respectively. This work addresses the meaning of this splitting and the role of Top1 and Top1mt in the mtDNA metabolism and mitochondrial functions.

In this first chapter, I will first introduce mitochondria and mtDNA in some details. Following, I will briefly review DNA topoisomerases in general and then focus on topoisomerases in mitochondria. Finally, I will describe in details Top1 and Top1mt, the subject of my work.

1.1 Mitochondria

1.1.1 Mitochondrial structure

Mitochondria are enclosed by two concentric membranes. The outer membrane has a protein/phospholipid ratio similar to the eukaryotic plasma membrane and is freely permeable to small molecules and ions. In contrast, the inner mitochondrial membrane (IMM) is an extremely specialized bilayer. The IMM has an elevated protein content and is rich in cardiolipin, a special phospholipid that makes the membrane impermeable to all molecules. The IMM is extensively folded to produce structures called cristae, thus expanding its surface area and enhancing its functional features.

Mitochondria are highly dynamic organelles (Okamoto & Shaw, 2005). Their overall shape, size and organisation result from balanced fusion and fission events. Mitochondria form long tubules that continually divide and fuse, building a dynamic interconnected network. This high dynamic allows mitochondria to interact with each other, ensuring exchange and complementation of metabolites, enzymes and genetic information. A correct fusion and fission balance is essential for the cell and loss of mitochondrial fusion compromises the overall energetic function of mitochondria (Chen et al, 2005).

1.1.2 Mitochondrial import

Mitochondria contain their own genome, coding for a subset of proteins of the respiratory chain. All other mitochondrial proteins (approximately 99%) are encoded by nuclear genes and then imported into the mitochondria (Bolender et al, 2008). Nuclear encoded mitochondrial proteins are synthesized in the cytosol with a characteristic amino-terminal presequence, called mitochondrial targeting signal (MTS). The MTS forms a positively charged amphipathic α helix and targets the proteins to a channel complex called Translocase of Outer mitochondrial Membrane (TOM). The pre-protein is recognized by TOM receptors and translocated through its gate into the inter membrane space. There, the electrochemical gradient generated by the activity of the respiratory chain exerts an electrophoretic effect on the positively charged MTS, driving the preprotein across a second channel complex called

Translocase of Inner Membrane (TIM). In the mitochondrial matrix the mitochondrial processing peptidase (MPP) removes the presequence, releasing the mature forms of the protein.

1.1.3 The mitochondrial respiratory chain

The mitochondrial respiratory chain (Fig. 1.1) is a highly specialized electron transport system consisting of five protein complexes situated in the IMM. Each complex is composed of multiple subunits. Reducing factors (NADH, FADH₂) generated by the metabolism of carbohydrates, proteins and fats donate electrons to complex I (NADH dehydrogenase) and complex II (Succinate dehydrogenase). The electrons flow to complex III (cytochrome *b*_c₁-complex) and IV (cytochrome *c* oxidase) shuttled by two mobile electron carriers, ubiquinone and cytochrome *c*. Electrons finally reduce oxygen to produce water. The liberated energy is used by complex I, III and IV to pump protons out of the mitochondrial matrix, into the intermembrane space. This proton gradient is harnessed by complex V (ATP synthase) to synthesize ATP from ADP and inorganic phosphate. ATP is then released from the mitochondria in exchange with cytosolic ADP by the adenine nucleotide translocator (ANT).

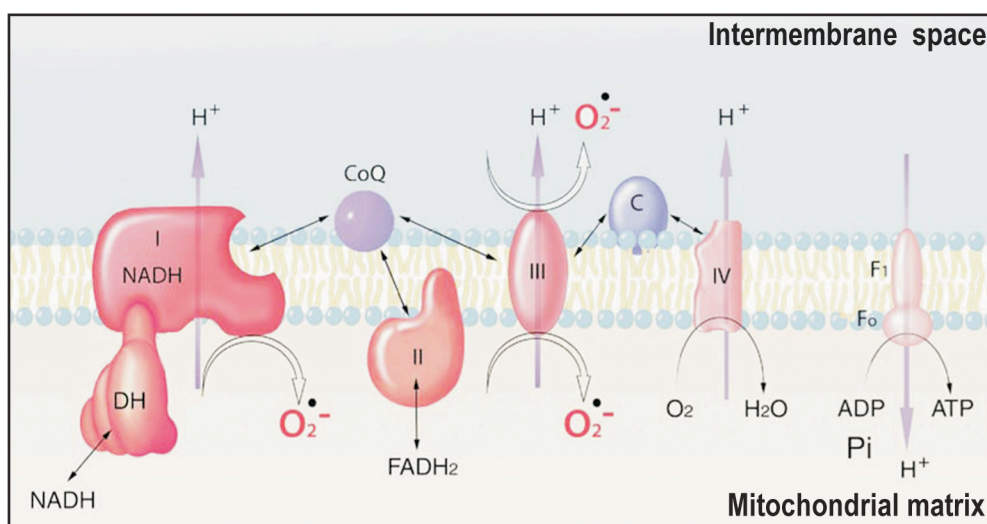


Fig. 1.1: Mitochondrial respiratory chain. Schematic representation of the five complexes of the respiratory chain. Incomplete reduction of oxygen to superoxide is shown at Complex I and III. Figure adapted from (Balaban et al, 2005).

At several sites along the respiratory chain, electrons can escape the transport system prematurely and reduce oxygen incompletely, thereby generating superoxide ($\bullet\text{O}_2^-$). Complex III and I have been identified as the two principal sites of superoxide generation in the respiratory chain (St-Pierre et al, 2002). Superoxide can then dismutate to hydrogen peroxide (H_2O_2), which can further react to form hydroxyl radicals ($\bullet\text{OH}$). All these highly reactive molecules, denoted reactive oxygen species (ROS), have a harmful potential, since they cause oxidation of membrane phospholipids, proteins and DNA. On the other hand, recent evidence indicates a prominent role of ROS as signalling molecules in several physiological pathways such as cellular growth and regulation of redox balance of the cell (Allen & Tresini, 2000). Under physiological conditions, the toxic effects of ROS can be prevented by scavenging enzymes such as superoxide dismutase (SOD), glutathione peroxidase (GSHPx) and catalase that defend the cell by converting the highly reactive ROS into water (Balaban et al, 2005).

1.1.4 MtDNA

Human mtDNA is a circular double-stranded molecule of 16,569 base pairs (bp) (Fig. 1.2). The two strands of the mtDNA molecule are historically denoted as heavy strand (H) and light strand (L) on the basis of their buoyant densities in alkaline CsCl gradients (Clayton, 1982). The mitochondrial genome comprises 0.1–2% of the total DNA in most mammalian cells and encodes two rRNAs, 22 tRNAs and 13 proteins of the respiratory chain: Seven are components of Complex I, three of Complex IV, two are subunits of Complex V and only one is part of Complex III. All other polypeptides of the OXPHOS complexes, including the entire Complex II, are encoded by nuclear genes. The 37 mitochondrial genes are extremely closely spaced on both strands of the mtDNA. The tRNA genes are fairly evenly distributed between the two strands, but the majority of mRNAs (12 of 13) and both rRNAs are products of H strand transcription. MtDNA lacks introns and the 1.1 kb displacement-loop (D-loop) control region is the only non-coding region (NCR) of substantial size. The NCR contains the origin of replication for the leading-strand synthesis (O_H) and the promoters for both mtDNA strands transcription: Light-strand promoter (LSP) and the heavy-strand promoter (HSP). H strand transcription initiates from two different sites of HSP, indicated as HSP1 and HSP2 (Montoya et al, 1982) (see below).

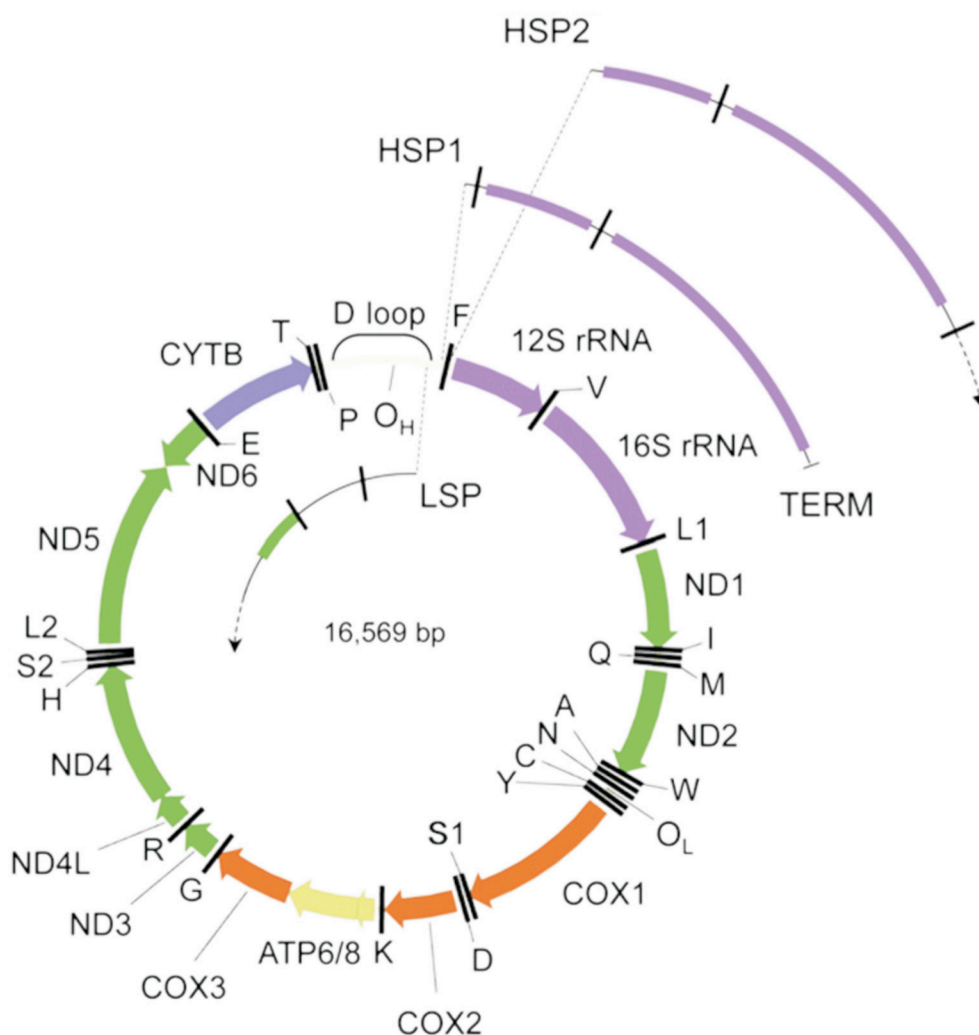


Fig. 1.2: Human mtDNA. The circular double stranded mtDNA molecule is represented with the heavy (H) and light (L) strand on the outside and inside of the circle respectively. MtDNA genes coding for complex I, III, IV and V are shown in green, blue, red and yellow, respectively. rRNAs are purple whereas black boxes denote tRNAs. The displacement loop (D-loop) at the top of the molecule represent the major noncoding portion of mtDNA. It contains the L strand promoter (LSP), the two H strand promoters (HSP1 and HSP2), and the origin of H strand synthesis (O_H). Semicircular arcs represent the primary transcripts of LSP (inside) and HSP2 and HSP1 (outside). Transcription from HSP1 preferentially terminates at a specific termination site (TERM) downstream of the 16S rRNA. Figure reproduced from (Bonawitz et al, 2006a).

1.1.4.1 MtDNA organisation

A human cell contains 10^3 - 10^4 copies of mtDNA organized in discrete structures, denoted as nucleoids. Nucleoids consist of 6-10 mtDNA molecules packaged with several proteins forming thus large mtDNA-protein complexes (Iborra et al, 2004). The most abundant protein in the nucleoids is the mitochondrial transcription factor A (TFAM). This component, originally characterized as an essential cofactor of

mtDNA transcription, has been proposed to play also a structural role in mtDNA maintenance by regulating nucleoid condensation (Kaufman et al, 2007). All essential cofactors of mtDNA transcription and replication, such as the mitochondrial DNA polymerase γ (POLG), the DNA helicase Twinkle, the mitochondrial single strand binding protein (mtSSB), mitochondrial transcription factors B1 and B2 (TFB1M and TFB2M) participate in the building of nucleoids (Holt et al, 2007). Notably, Top1mt was also identified as component of these large DNA-protein structures (Bogenhagen et al, 2008). Interestingly, both ribosomal proteins and elements of the IMM associate with nucleoids (Bogenhagen et al, 2003; Wang et al, 2007), suggesting a co-localisation of mtDNA and the transduction machinery at the matrix surface of the IMM. These observations suggest that nucleoids represent the centre of mitochondrial biogenesis, where the processes of transcription, translation and assembling of proteins in the IMM are coupled (Iborra et al, 2004) (see 1.1.4.2, MtRNA processing and translation).

1.1.4.2 MtDNA metabolism

In this section I will focus on the mitochondrial metabolism of vertebrates. Since relevant for my work, some features of yeast mtDNA metabolism will be described at the end of each section.

MtDNA transcription

Mitochondrial genes are located on both strands of mtDNA and each strand contains a single promoter region for the transcriptional initiation: LSP and HSP (Fig. 1.2). Transcription from the mitochondrial promoters produces polycistronic precursor RNAs, in which all genes coding for mitochondrial proteins or rRNAs are directly flanked by at least one tRNA gene. These polycistronic precursor RNAs are then processed excising all tRNA molecules thus releasing the individual mRNAs, rRNAs, and tRNAs (Ojala et al, 1981). HSP transcription is initiated from two specific sites, HSP1 and HSP2 (Montoya et al, 1982). Transcription from HSP1 produces a transcript, which terminates at the 3' end of the 16S rRNA gene whereas the HSP2 produces a polycistronic molecule, which corresponds to almost the entire H strand. Compared to HSP2, the HSP1 transcription unit produces 15- to 60-fold more RNA and is subjected to a transcription termination event directly downstream of the 16S rRNA (Bonawitz et al, 2006a), which is induced by specific binding of the mitochondrial transcription termination factor (mTERF) (Fernandez-Silva et al, 1997; Hyvarinen et al, 2007). The high activity of the HSP1 transcription unit ensures the

elevated level of rRNAs required for ribosome assembly.

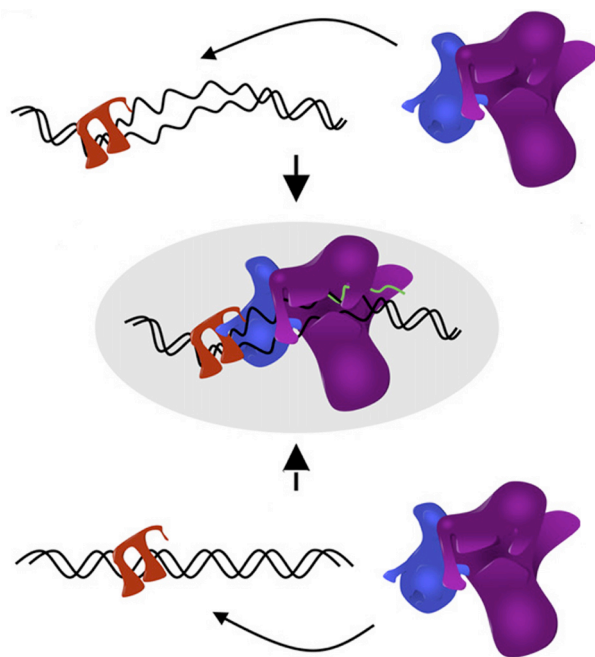


Fig. 1.3: Transcription initiation at human mtDNA promoters. The initiation of mtDNA transcription in human requires the presence of TFAM (red) and POLRMT (purple) complexed with either TFB1M or TFB2M (blue). In the first model proposed for this process (top), TFAM binds upstream of the promoter inducing structural alterations in the mtDNA. The ssDNA exposed by TFAM binding is then recognized by POLRMT in a complex with either TFB1M or TFB2M. According to a second model (bottom), POLRMT complexed with TFB2M recognizes TFAM, already bound to the promoter. Figure adapted from (Bonawitz et al, 2006a).

The mitochondrial transcription machinery is distinct from that found in the nucleus. In mammals, the combination of TFAM, the mitochondrial RNA polymerase (POLRMT) and one of the two mitochondrial transcription factor B paralogues (TFB1M and TFB2M) is sufficient and necessary for the initiation of transcription *in vitro* (Falkenberg et al, 2002). How the mitochondrial mammalian transcription machinery recognizes promoter sequences is not fully understood. TFAM is a member of the high-mobility-group (HMG) and binds specifically sequences upstream of HSP and LSP (Fisher et al, 1987). One possible role for TFAM might be to introduce specific structural alterations in mtDNA such as the unwinding of promoter regions, which can allow POLRMT to initiate transcription. Both TFB1M and TFB2M can form a heterodimeric complex with POLRMT (Falkenberg et al, 2002). Probably, these factors play a role in recruiting POLRMT to the promoters but their specific role is still unknown. Notably, TFB1M and TFB2M display sequence similarity to rRNA methyltransferases. Methyltransferases dimethylate two adjacent adenosine bases near the 3' end of the small subunit rRNA during ribosome biogenesis and are consequently involved in modulating translation and protein synthesis. Thus, both TFB1M and TFB2M are dual function proteins that support

mitochondrial transcription and also act as rRNA methyltransferases (Cotney & Shadel, 2006; Falkenberg et al, 2002). TFB2M has a less efficient rRNA methyltransferase activity than TFB1M but is a much more active transcription factor, suggesting that TFB2M has evolved as a specialized transcription factor in mammalian mitochondria. Due to its homology to rRNA methyltransferase enzymes, TFB2M may bind single strand DNA (ssDNA) (Seidel-Rogol et al, 2003). Therefore, It is possible that TFB2M recruits POLRMT to the promoter recognizing ssDNA exposed by TFAM binding (Fig. 1.3) (Bonawitz et al, 2006a). Alternatively, the direct interaction between TFB2M and TFAM may contribute to POLRMT recruitment (McCulloch & Shadel, 2003).

The transcription machinery and the promoter recognition mechanism in budding yeast are significantly different to that of mammalian mitochondria. *S. cerevisiae* mitochondrial RNA polymerase Rpo41 and a single TFB1M/TFB2M homologue Mtf1p form a heterodimer that recognizes mitochondrial promoters and initiates transcription (Cliften et al, 1997). The yeast TFAM homologue Abf2 is not required for transcription in yeast (Xu & Clayton, 1992), but instead has a role in mtDNA packaging and maintenance.

MtRNA processing and translation

MtDNA transcription and translation seem to be functionally and physically coupled. Studies in *S. cerevisiae* shown that the N-terminal domain of Rpo41 is dispensable for transcription initiation *in vivo* but is required for normal levels of mitochondrial protein synthesis (Rodeheffer & Shadel, 2003). Furthermore, other proteins involved in RNA processing and translation, interact with Rpo41 (Costanzo & Fox, 1990; Rodeheffer et al, 2001). It has been proposed that the mtRNA polymerase, through its interactions with translation factors, delivers the nascent mRNAs to the IMM, where the RNA processing and translation machinery resides. Consistent with this model, the association of mtRNAs with IMM is necessary for translation (Sanchirico et al, 1998).

Similar to yeast, mitochondrial transcription and translation seem to be coupled also in humans. Recently, the mitochondrial ribosomal protein MRPL12 has been reported to interact with POLRMT (Wang et al, 2007). Moreover, nucleoids localise at the matrix surface of the IMM together with the mitochondrial translational machinery (Liu & Spremulli, 2000). It is supposed that translation and synthesis of mtDNA genes and assembly of respiratory chain complexes are coordinated events

(Fig. 1.4). Mitochondrially encoded respiratory chain subunits are translated at the IMM close to the import channels TOM and TIM, whereas nuclear encoded subunits are translated in cytoplasm and then imported through the TOM/TIM channels into the mitochondrial matrix. There, mitochondrial and nuclear encoded subunits are joined and inserted in the IMM (Iborra et al, 2004).

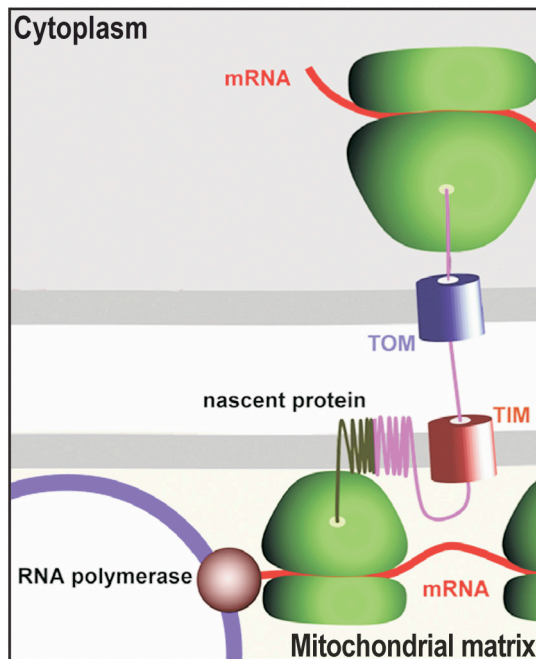


Fig. 1.4: Functional and physical coupling of transcription and translation in mitochondria. Model for the coordinated translation, synthesis and assembly of proteins in mitochondria. MtDNA encoded proteins are translated at the IMM close to TOM and TIM channels. Nuclear encoded mitochondrial proteins are imported through the TOM/TIM channel and directly assembled with the mitochondrially encoded subunits. Figure adapted from (Iborra et al, 2004).

mtDNA replication

MtDNA replication involves two unidirectional, independent origins of replication. The synthesis of the leading-strand starts at the H-strand replication origin (O_H), which is located in the NCR downstream of LSP. Differently, the L-strand replication origin (O_L) for the synthesis of lagging-strand is located approximately 1100 bp away from O_H (see fig. 1.2). MtDNA transcription and replication are intimately linked, since transcription of the LSP produces the RNA primers required for synthesis initiation at O_H (Clayton, 1991). POLRMT acts as leading and lagging-strand primase (Wanrooij et al, 2008). The enzyme efficiently transcribes long regions of dsDNA but becomes less processive on ssDNA, producing short RNA primers. POLG can then use these primers to initiate DNA replication. DNA synthesis from O_H proceeds unidirectional, thereby displacing the parental H-strand, and frequently terminates 700 bp downstream of O_H , giving rise to the 7S DNA. The termination of replication at this point produces a short triple-stranded region called D-loop (Clayton, 1991).

Two main models of mtDNA replication have been proposed (Fig. 1.5). According to the strand-displacement model (also denoted “strand-asynchronous”), mtDNA replication occurs by asynchronous synthesis of each strand: Leading-strand synthesis starts at O_H to reach O_L . O_L is then activated and lagging-strand DNA synthesis initiates in the opposite direction (Clayton, 1991). More recently, two dimensional neutral agarose gel electrophoresis (2DNAGE) has revealed mtDNA replication intermediates (RIs), whose structures are inconsistent with the asymmetric strand-displacement model. This new finding led to the assumption of the strand-coupled (or strand-synchronous) model for replication where leading and lagging-strand synthesis are largely coupled and progress from multiple, bidirectional replication forks (Holt et al, 2000). Most recent data show that during strand-coupled mtDNA replication, RNA is temporarily incorporated throughout the lagging strand and thus converted to DNA (Yasukawa et al, 2006). At present, there is no consensus on the mtDNA replication mechanism. RIs analysis indicates mtDNA replicates according to the strand-displacement model in cultured cells whereas in solid tissues mtDNA replication follows the strand-coupled model. It is supposed that both mechanisms operate in different physiological contexts (Yasukawa et al, 2005).

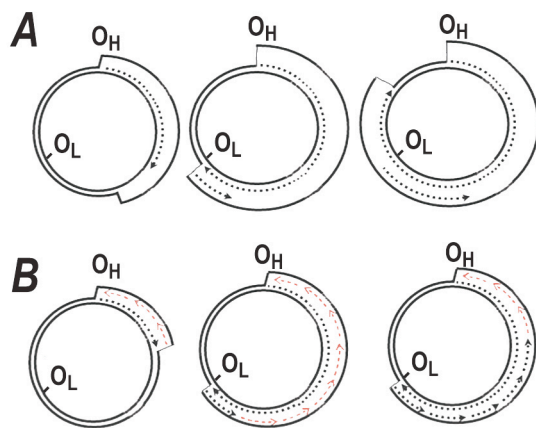


Fig. 1.5: Two models for mtDNA replication. **A)** Strand-displacement model: leading-strand synthesis starts at O_H displacing the L strand until O_L is reached. L remains single stranded until synthesis of the nascent H strand exposes O_L . O_L is then activated and lagging-strand DNA synthesis begins in the opposite direction (Clayton, 1991). **B)** Strand-coupled model: leading and lagging-strand synthesis are largely coupled. RNA intermediates (red dashed lines) are incorporated throughout the lagging strand and are then converted to DNA. Figure adapted from (Krishnan et al, 2008).

The minimal mtDNA replisome consists of POLG, the mitochondrial helicase Twinkle and mtSSB (Korhonen et al, 2004). In all vertebrates POLG is composed of two subunits α and β (POLGA and POLGB, respectively) that form a heterotrimer (POLGAB2) in mammalian cells (Fan et al, 2006). POLGB increases the processivity of the catalytic subunit POLGA and seems to play a role in initiating mtDNA

replication by substrate binding (Kaguni, 2004). POLG works together with Twinkle, which catalyzes the unwinding of DNA duplex ahead of the replication fork. The addition of mtSSB stimulates the DNA synthesis, probably enhancing the rate of DNA unwinding by Twinkle (Korhonen et al, 2003).

The replication machinery is mostly conserved between lower and higher eukaryotes. Homologs of Twinkle are present throughout the eukaryotic tree and also mtSSB could be purified from several species. In yeast, POLG lacks the subunit β and replication can proceed with high processivity in the absence of the enhancer POLGB (Lucas et al, 2004).

mtDNA repair

The cell is constantly exposed to exogenous and endogenous DNA damaging agents. Because of its proximity to the electron respiratory chain and the lack of protective histones, mtDNA seems to accumulate more damage than nuclear DNA. Initially, it was proposed that repair mechanisms in mitochondria were absent or very inefficient. It was assumed that damaged mtDNA molecules were degraded and the undamaged copies served as template for replication and transcription. By now it is demonstrated that various mtDNA lesions such as oxidative damage are repaired in mitochondria (Stuart & Brown, 2006). The major repair mechanism acting there is the base excision repair (BER). The enzymes participating in mitochondrial BER have been partially identified: DNA glycosylase OGG1 and DNA ligase III have a dual localisation and are targeted to the nucleus and mitochondria (Lakshmipathy & Campbell, 1999; Takao et al, 1998). OGG1 recognizes and removes the damaged base. The one-nucleotide gap is then filled by POLG, and DNA ligase III joins the free ends. Also mismatch and recombinational repair activities seem to be present in mammalian mitochondria (Kajander et al, 2001; Mason et al, 2003; Thyagarajan et al, 1996). However, proteins involved in this processes are not yet identified to date and the significance of these repair pathways in mitochondria remains uncertain.

1.1.5 Mitochondrial dysfunctions

MtDNA as well as nuclear DNA defects can lead to loss of mitochondrial functionality. These mitochondrial dysfunctions cause a wide spectrum of human disorders and have been supposed to play a role also in ageing and age-associated degenerative diseases. In this section, I will introduce the free radical theory of ageing and mitochondrial diseases in some details. Among the mitochondrial disorders, I will focus only on mtDNA-related disorders omitting those mediated by

nuclear DNA defects.

1.1.5.1 Mitochondria and ageing

The “free radical theory of ageing” of Harman proposes that the deleterious effect of ROS is responsible for ageing (Harman, 1972). Consistent with this theory, OXPHOS leads to ROS production that damages mtDNA. Mutated mtDNA produces defective respiratory chain subunits, causing respiratory chain dysfunctions and augmented ROS. Through this vicious cycle, mtDNA mutations would increase exponentially with time, resulting in ageing and degenerative diseases (Fig. 1.6).

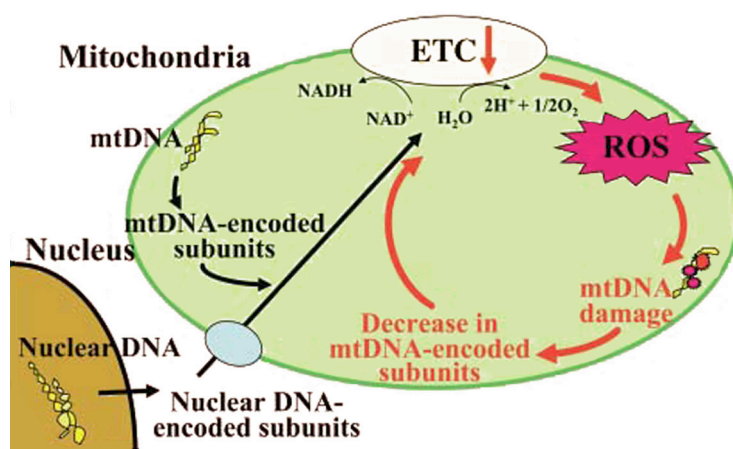


Fig. 1.6: Vicious cycle between ROS production and mtDNA damage. The activity of the respiratory chain produces ROS that damage mtDNA. Mutated mtDNA produces in turn defective proteins, impairing the respiratory chain. The impaired respiratory chain increases ROS production, closing the vicious cycle. Figure adapted from (Tsutsui et al, 2008).

Consistent with Harman's theory, increased mtDNA deletions and point mutations have been found in aged tissues of humans and other animals (reviewed in (Trifunovic & Larsson, 2008)). The direct causative link between mtDNA instability and ageing was demonstrated recently in mice with a mutated POLG (Trifunovic et al, 2004). POLGA of the mutator mice was engineered to have a defect in its proofreading function. As a consequence, homozygous POLGA mutated mice (POLGA^{mut/mut}) accumulate high levels of mtDNA point mutations and deletions, resulting in development of premature ageing phenotype and reduced lifespan. Despite this, whether mtDNA mutations present in normal ageing are sufficient to cause ageing remains questioned. Heterozygous POLGA^{mut/+} mice show 30 times more mtDNA point mutation than old wild-type animals without features of premature ageing (Vermulst et al, 2007). Recently, a correlation has been shown between premature ageing phenotype and accumulation of mtDNA deletions in brain and heart tissues of POLGA^{mut/mut} mice, indicating that mtDNA deletions rather

than point mutations are mainly responsible for the ageing phenotype (Vermulst et al, 2008).

The free radical theory of ageing assumes that increase in ROS levels triggers mtDNA instability. MtDNA is believed to be particularly vulnerable to oxidative damage, because of its close proximity to the electron transport chain and the lack of protective histones. Several studies correlate enhanced oxidative stress with mtDNA instability and degenerative dysfunctions, supporting partially the theory of Harman: In mice with insufficient antioxidant defences, the high oxidative stress results in an increased mtDNA mutation rate, degenerative dysfunctions, oversensitivity to oxidative stress and enhanced incidence of cancer (Esposito et al, 1999; St-Pierre et al, 2006; Van Remmen et al, 2003; Van Remmen et al, 2004). These studies clearly demonstrate the toxic potential of ROS, thus confirming their prominent role in the damage of cellular components and degenerative processes. However, the link between oxidative stress and ageing is questioned. A correlation between ROS and maximal lifespan in various species is demonstrated (Perez-Campo et al, 1998), but these studies do not clarify whether ROS production is cause or consequence of the ageing process. Many groups provided disagreeing results about the causal correlation between ROS production and life span in several animal models. Some studies seem to contradict the free radical theory of ageing because they showed that increased ROS levels do not influence the lifespan of mice or flies (Huang et al, 2000; Miwa et al, 2004; Van Remmen et al, 2003). Contrary, a recent study shows that an enhanced activity of catalase leads to an increased lifespan in mice, which supports Harman's theory (Schriner et al, 2005).

Especially dubious is the role of oxidative stress in mtDNA mutagenesis during ageing. It is known that ROS can induce mtDNA mutagenic lesions (Druzhyina et al, 2008). Moreover, it has been shown that impairment of the OXPHOS in mice leads to increased ROS levels and mtDNA instability (Esposito et al, 1999). On the other hand, recent observations moderate the role of oxidative stress in the induction of mtDNA mutation: The POLG mutator mice show a high mtDNA mutation rate associated with premature ageing but have normal amounts of ROS (Trifunovic et al, 2005). Furthermore, in mice lacking the major DNA-repair system in mitochondria, the increased mtDNA oxidative damage does not affect mitochondrial functions (Stuart et al, 2005). These findings support the idea, that oxidative stress is not the major trigger of mtDNA mutagenesis.

1.1.5.2 Mitochondria and diseases

The mtDNA encodes 13 subunits of the respiratory chain complexes and the components of the mitochondrial translation machinery (tRNAs and rRNAs) necessary for the synthesis of these proteins. Thus, mutations of mtDNA can result in a defective respiratory chain and ultimately in a faulty OXPHOS. Both qualitative and quantitative defects of mtDNA are a frequent cause of human diseases (Schapira, 2006). Large mtDNA deletions correlate, for example, with Pearson syndrome, Kearns-Sayre syndrome and progressive external ophthalmoplegia (PEO). MtDNA point mutations cause mitochondrial encephalomyopathy (MELAS), leber's hereditary optic neuropathy (LOHN) and the mitochondrial myopathy. MtDNA depletion correlates with Alpers syndrome. Although mitochondrial dysfunctions can affect theoretically each cell, the symptoms of almost all mitochondrial diseases affect neurological, cardiac, endocrine and ophthalmological features. This is due to the fact that tissues and organs heavily dependent upon OXPHOS are the predilection sites to fault. Furthermore, among the many mtDNA copies in the cell, a minimal admixture of mutated mtDNA is required to cause mitochondrial dysfunctions and the threshold of this varies from tissue to tissue and from disease to disease (Larsson & Clayton, 1995; Rossignol et al, 1999).

The mitochondrial genome cannot be manipulated by standard molecular biology techniques. Because of the inaccessibility and the frequent polymorphic nucleotide changes of mtDNA, engineering and study of specific mutated mtDNA genes is impossible. Cells lacking mtDNA (ρ^0 cells) represent a highly valuable tool to study mitochondrial pathophysiology or processes involving this organelle (King & Attardi, 1989), since they can be fused with enucleated cells to generate "cybrid" cells. Cybrids contain a uniform nuclear genetic background and exogenous mtDNA, which facilitates the analysis of the functional consequences of known mtDNA mutations. MtDNA can be artificially depleted using a low dosage of ethidium bromide (EtBr). This DNA intercalating agent is positively charged and concentrates within the negatively charged mitochondrial matrix. There it interferes with mtDNA metabolism resulting in a failure of mtDNA synthesis. MtDNA depletion results in respiratory chain failure in ρ^0 cells; therefore, ρ^0 cells use glycolysis as their only source of ATP. Furthermore ρ^0 cells are unable to synthesize pyrimidine because one step in the *de novo* synthesis of pyrimidine is carried out by the mitochondrial enzyme dihydroorotate dehydrogenase, whose function depends on a functioning respiratory chain. Thus, ρ^0 cells need the supplementation of uridine for growth, a

precursor for the synthesis of thymidine and cytidine (King & Attardi, 1989).

1.1.5.3 Molecular basis of mitochondrial dysfunctions

As described above, defects of mtDNA maintenance often cause disease. A defective replication has been assumed to be responsible for the generation of mtDNA deletions (Krishnan et al, 2008). In human and mouse, dominant mutations of POLG and Twinkle cause multiple mtDNA deletions (Tyynismaa et al, 2005; Wanrooij et al, 2004), presumably resulting from the stalling of mtDNA replication (Wanrooij et al, 2007). In cell culture, expression of dominant negative POLG and Twinkle induces mtDNA depletion (Jazayeri et al, 2003; Wanrooij et al, 2007). The same outcome is inflicted by knock down of Twinkle (Tyynismaa et al, 2004).

TFAM play also a key role in mtDNA maintenance. This factor has a dual function: It is involved in the mtDNA transcription and in the architectural organisation of nucleoids (Kanki et al, 2004; Kaufman et al, 2007; Larsson et al, 1998). In mice, TFAM knock out leads to mtDNA depletion due to the lack of the RNA primers necessary for mtDNA replication (Larsson et al, 1998). Paradoxically, TFAM overexpression also depletes mtDNA in cultured cells, affecting the condensation rate of nucleoids (Pohjoismaki et al, 2006).

Not only defects in maintenance of mtDNA (in terms of deletion, depletion and mutation) but also a deregulated mtDNA transcription can lead to mitochondrial dysfunctions (Park et al, 2007). Recently it has been shown in mice that knocking out MTERF3, a specific repressor for the transcription initiation, increases mtDNA transcription initiation. The enhanced transcription paradoxically decreases critical tRNA genes distal to promoter leading to a defective protein synthesis in mitochondria and, ultimately, to mitochondrial dysfunctions (Park et al, 2007).

In summary, it is clear that a high reliability and a stringent regulation of mtDNA metabolism are necessary to ensure the correct maintenance of mtDNA. Many proteins (such as Top1mt (Zhang et al, 2001)) have been shown to associate with nucleoids but their specific functions remain uncertain. Decoding of the specific role of each of these factors is necessary to understand the mechanism of mtDNA organisation, replication, transcription and inheritance. This set of information is needed to clarify the basis of mitochondrial diseases and to develop effective therapies for them. One group of enzymes with a putative role in the mtDNA metabolism are DNA topoisomerases, which are the topic of the second part of the introduction.

1.2 DNA topoisomerases

In the cell DNA is kept compact in supercoiled, knotted and catenated forms. The compact shape of DNA is continually changed to optimize essential functions such as replication and transcription. On the other hand, DNA metabolic processes themselves modify the topological state of DNA (Fig. 1.7). Transcription generates positive supercoils (overwinding) ahead and negative supercoils (underwinding) behind the translocating RNA polymerase (Fig. 1.7.A). Fork movement during DNA replication generates topological changes in both the unreplicated region ahead of the fork and the replicated region behind it (Fig. 1.7.B). Moreover, recombination and converging replication forks generate four-way branched DNA intermediates (holliday junctions), in which the parental strands are intertwined (Fig. 1.7.C).

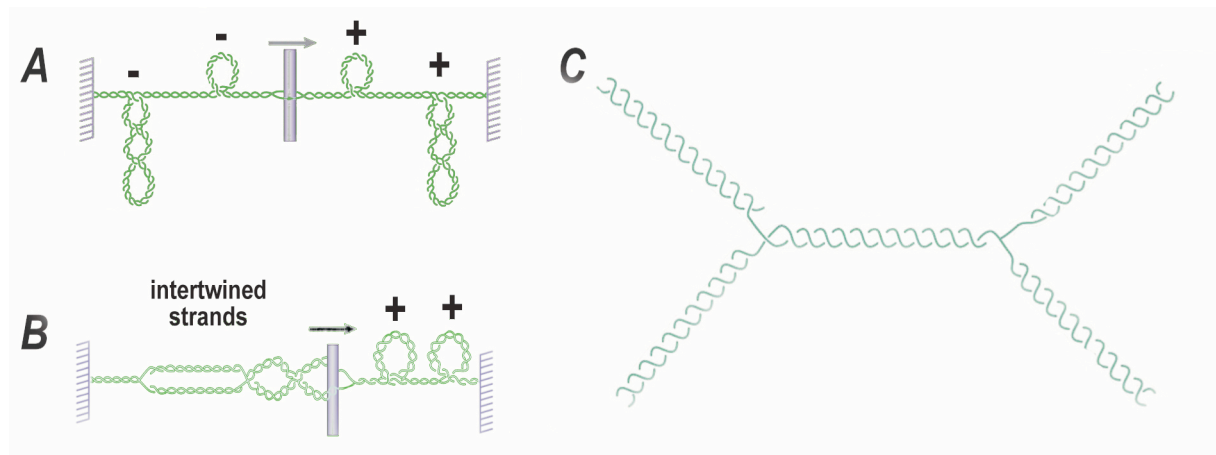


Fig. 1.7: DNA metabolism generates topological problems. **A) and B)** Problems arising during transcription and replication, respectively. The transcription and replication machinery (rod) are not allowed to rotate in the cellular milieu. Progression of the replication fork generates positive supercoils ahead the transcription machinery and negative supercoils behind it (A). Progression of the replication fork built up positive supercoils ahead the fork. When the replication machinery is free to rotate around the helical axis of unreplicated DNA, this positive supercoils can be redistributed into the region behind the fork, intertwining the new replicated helices (B). In **C)** is illustrated a four-way branched DNA intermediate. This structure can rise from the converging of two replication forks and also from the pairing of two gapped DNA molecules to form a recombination intermediate.

DNA topoisomerases are ubiquitous enzymes able to change the degree of DNA supercoiling. Their activity is required for the resolution of all topological problems generated during DNA metabolism and for the tuning of topological state of the DNA (Wang, 2002). Topoisomerases act by cleaving DNA and passing a second strand (type I subfamily) or duplex (type II subfamily) through the break. Cleavage of DNA by all topoisomerases is accompanied by the formation of a transient

phosphodiester bond between a tyrosine of the protein and one end of the broken strand, generating a topoisomerase-DNA complex denoted “cleavable complex” (Fig. 1.8). The DNA topology is modified during the lifetime of this covalent intermediate. Then, DNA is religated and the enzyme is released. Since the catalytical cycle of topoisomerases involves DNA breaks, these enzymes can potentially endanger the cell. Under physiological conditions, the half-life of the cleavable complex is very short. However, drugs and DNA modifications can prevent the religation of the DNA breaks and stabilize the cleavable complex. Such topoisomerase-DNA complexes present a physical barrier to replication and transcription, which could lead to cell death. For this reason, topoisomerases are targets of several anticancer drugs and play a prominent role in current cancer therapy.

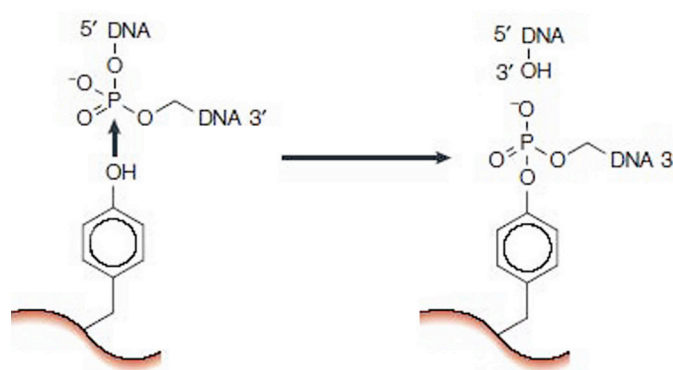


Fig. 1.8: DNA cleavage of mediated by topoisomerases. Transesterification between a topoisomerase tyrosil group and a DNA phosphate group leads to the breakage of the DNA backbone and formation of a covalent enzyme–DNA intermediate (covalent complex). In type IA or type II topoisomerases the protein is covalently bound to the DNA 5′phosphate whereas members of the type IB subfamily are attached to the 3′phosphate. Figure reproduced from (Wang, 2002).

1.2.1 Classification and cellular functions

Topoisomerases are classified into type I and type II on the basis of the number of strands cut during one catalytic cycle. Several different topoisomerases are present in all organisms from archea to human (Champoux, 2001). The principal characteristics of the different type I and type II topoisomerases and the most prominent members are summarized in table 1.1. In the following, I will briefly describe the various topoisomerases present in different organisms, thereby paying the most attention to eukaryotes.

Type	Structure	Substrate	Catalysis	Members
IA	monomers	(-) supercoils ss DNA	Single strand break (Link to 5' end)	<ul style="list-style-type: none"> • Eubacteria: topoisomerase I and III • Yeast: topoisomerase III (Top3) • Higher eukaryotes: Topoisomerase IIIα and IIIβ (Top3α and Top3β)
IB	monomers	(-)/(+) supercoils ds DNA	Single strand break (Link to 3' end)	<ul style="list-style-type: none"> • Eukaryotes: topoisomerase I (Top1) • Vertebrates: mitochondrial topoisomerase I (Top1mt)
IIA	dimers	(-)/(+) supercoils ds DNA	Double strand break (Link to 5' end)	<ul style="list-style-type: none"> • Eubacteria: DNA gyrase and topoisomerase IV • Yeast: topoisomerase II (Top2) • Higher eukaryotes: Topoisomerase IIα and IIβ (Top2α and Top2β)
IIB	tetramer	(-)/(+) supercoils ds DNA	Double strand break (Link to 5' end)	<ul style="list-style-type: none"> • <i>S. shibatae</i> topoisomerase VI

Table 1.1

1.2.1.1 Type I topoisomerases

Type I enzymes are monomers and catalyze the formation of single strand breaks of the DNA molecule in an ATP independent manner. Their reactions are driven by the conformational energy of DNA. Type I topoisomerases are further subclassified as either type IA if the protein link is to the 5' phosphate of DNA backbone or type IB if the protein is attached to the 3' phosphate (Fig. 1.8).

Type IA topoisomerases act on ssDNA substrate and remove negative, but not positive, supercoils. DNA topoisomerase III is the eukaryotic type IA enzyme. Yeasts possess only one DNA topoisomerase III (Top3), whereas higher eukaryotes possess two distinct isoforms of this enzyme: α and β (Top3 α and Top3 β), whose specific role is unclear. It is known that, in the nucleus, Top3, Top3 α and Top3 β interact with proteins of the RecQ helicase family (Ahmad & Stewart, 2005; Shimamoto et al, 2000). Currently a picture is forming, where Top3 is ascribed an essential role in recombination and maintenance of genomic stability (Mankouri & Hickson, 2006).

Type IB topoisomerases act on dsDNA substrates and can relax both positive and negative supercoils. With the only exception of topoisomerase V of *Methanopyrus kandleri* (Slesarev et al, 1993), this subfamily of topoisomerases is absent in prokaryotic cells. On the contrary, all eukaryotes contain topoisomerase I (Top1) in the nuclear compartment. It plays a major role in supporting fork movement during replication and in relaxing both negative and positive supercoils associated with transcription. In yeasts, Top1 is dispensable for growth because its activity can be complemented by type II topoisomerase (Thrash et al, 1985; Wallis et al, 1989). By contrast, in higher eukaryotes Top1 is required for viability in both flies and mice (Lee et al, 1993; Morham et al, 1996). All vertebrates contain an additional type IB topoisomerase (Top1mt) specifically developed for the mitochondrial compartment (Zhang et al, 2001). The characteristics of human Top1 and Top1mt are described in further detail in section 1.2.3 and 1.2.4.

1.2.1.2 Type II topoisomerases

Type II topoisomerases are dimers. They perform double-strand breaks in the DNA involving covalent attachment of each subunit of the dimer to the 5' end of the DNA backbone. A conformational change of the enzyme creates an opening in the cleaved DNA-duplex (gate) and a second DNA helix is passed through this gate. ATP is required for the action of Type II enzymes. Topoisomerases II are the only enzymes able to remove catenanes created during replication and are thus essential for chromosome segregation during mitosis. The discovery of a special type II topoisomerase in the archaeon *Sulfolobus shibatae* prompted the division of type II topoisomerases into type IIA and type IIB, where only *S. shibatae* topoisomerase VI belongs to type IIB topoisomerases.

Yeast possesses a single type IIA DNA topoisomerase II (Top2), which is able to relax positive and negative supercoils. By contrast, vertebrates contain two type IIA isoforms termed topoisomerases II α and II β (Top2 α and Top2 β) with similar structure and biochemical activity, but different biological functions. Top2 α is essential for cell-division (Carpenter & Porter, 2004; Grue et al, 1998; Linka et al, 2007) whereas Top2 β is important for proper development of motor and sensory neurons (Lyu & Wang, 2003; Yang et al, 2000). The latter probably reflects a role of Top2 β in regulation of gene transcription (Ju et al, 2006). Consistent with specific roles for Top2 α in proliferating cells and Top2 β in non-dividing cells, Top2 β is constitutively expressed in all cells, whereas Top2 α is expressed only in proliferating

cells (Heck et al, 1988; Kimura et al, 1994; Woessner et al, 1991). Moreover, only Top2 α associates with mitotic chromosomes (Christensen et al, 2002b; Linka et al, 2007; Meyer et al, 1997).

1.2.2. Mitochondrial topoisomerases

As described above, all transactions of nuclear DNA require the activity of one or more topoisomerases. Most eukaryotic cells possess in addition to the nuclear genome, an extra genome in the mitochondria. In line with the intimate relation between topoisomerases and DNA found in the nuclear compartment, all three topoisomerase subfamilies are also found in the mitochondrial matrix. In this section, I will describe the various topoisomerases present in the mitochondrial matrix, beginning with the situation in vertebrate organisms.

1.2.2.1 Vertebrates

In vertebrates all three topoisomerase subfamilies present in the cell nucleus (IA, IB, and IIA) are also represented in mitochondria by at least one gene product each. An overview of nuclear and mitochondrial topoisomerases and their respective genes is listed in table 1.2.

Type IA topoisomerases are represented in the mitochondrial matrix by Top3 α , whereas the closely related Top3 β isoform seems to be a nuclear entity absent in mitochondria (Wang et al, 2002). Nuclear and mitochondrial Top3 α are encoded by the same TOP3 α gene owing two alternative start codons within its ORF. Translation initiating at either start codon generates a different peptides. The longer peptide contains a MTS that facilitates targeting of Top3 α in mitochondria (Wang, 2002). The precise role of Top3 α in mitochondria is still to be elucidated. In the nucleus type IA topoisomerases are most likely involved in resolution of single-stranded intertwinings occurring, for example, in recombinational repair (Cheok et al, 2005). However, the occurrence of recombinational repair in mitochondria remains uncertain. It has been suggested that mitochondrial Top3 α may participate in the resolution of mtDNA rings in their final stage of replication, permitting the removal of the last few parental strand intertwinings (Wang et al, 2002).

Top2 β is, by now, the only representative of the type IIA family in vertebrate mitochondria. A truncated form of Top2 β with a molecular mass of 150 kDa, was isolated from bovine heart mitochondria (Low et al, 2003). This enzyme likely derives from post-translational proteolysis of the nuclear Top2 β (with a molecular mass of

180 kDa): The removal of the C-terminal region eliminates the NLS and possibly uncovers a MTS. However, this remains arguable because the putative MTS is also one of the dimerization domains of the enzyme. Since type II topoisomerases can perform DNA double strand breaks, Top2 β activity may serve to decatenate newly replicated mtDNA circles in mitochondria at the end of a cycle of mtDNA synthesis. Thus, mitochondrial type IA and IIA topoisomerases originate from post-transcriptional modifications of their nuclear counterpart. In contrast, vertebrates do not target Top1 to mitochondria but have evolved a separate type IB topoisomerase (Top1mt) for the mitochondrial compartment (Zhang et al, 2001). Top1mt is described in detail in section 1.2.4.

Nucleus ¹⁾	Gene ²⁾	Mitochondria ³⁾
Top3 α ←	TOP3A	→ Top3 α ⁴⁾
Top3 β ←	TOP3B	
Top1 ←	TOP1	
	TOP1mt	→ Top1mt ⁵⁾
Top2 α ←	TOP2A	
Top2 β ←	TOP2B	→ Top2 β (?) ⁶⁾

Table 1.2: Overview of nuclear¹⁾ and mitochondrial³⁾ topoisomerases and their coding genes²⁾ in vertebrates. TOP3A and TOP2B code for both, nuclear and mitochondrial variants of the enzyme. TOP3B and TOP2A are, so far, not found in the mitochondrion. TOP1mt codes for the only topoisomerase, which is specific for the mitochondria. On the contrary, its nuclear counterpart Top1 is coded by a separate gene called TOP1. References: ⁴⁾ (Wang et al, 2002) ⁵⁾ (Zhang et al, 2001) ⁶⁾ (Low et al, 2003).

1.2.2.2. Non-vertebrate eukaryotes

Most information about mitochondrial topoisomerases in non-vertebrates are based on analysis of their amino acid sequences and on the prediction of their mitochondrial localisation in table 1.3.

Top3 α of *D. melanogaster* and Top3 of *S. cerevisiae* or *S. pombe* reveal a high probability to be imported into mitochondria (Plank et al, 2005; Wang et al, 2002). Thus, type IA topoisomerases are likely targeted to non-vertebrate mitochondria in a manner similar to that of vertebrate eukaryotes.

Sequence analyses of type IB topoisomerase provide heterogeneous results. Top1 of *S. pombe* has been predicted to localise to both the nucleus and the mitochondria

(Wang et al, 2002). Thus, TOP1 gene probably codes for both mitochondrial and nuclear activities in fission yeast. On the contrary, Top1 does not appear to contain a MTS in budding yeast *S. cerevisiae*. However, a polypeptide with Top1 activity and reactive to Top1 antibodies is reported in isolated *S. cerevisiae* mitochondria suggesting that Top1 targeting in budding yeast is due to post-translational processing of Top1 (Tua et al, 1997; Wang et al, 1995). The unicellular parasitic protozoans possess a single mitochondrion containing a distinctive DNA called kinetoplast DNA (kDNA). The kDNA is a complex structure with several thousands topologically interlocked DNA circles, which also serves structural purposes. Consistent with the complexity of kDNA, protozoans possess a special set of topoisomerases: Top1 enzymes are heterodimers coded by two different TOP1 genes (Bodley et al, 2003; Das et al, 2004). However none of these genes codes for an exclusively mitochondria targeted protein, meaning that in protozoans also a single Top1 enzyme targets both the mitochondrial and nuclear compartment (Bakshi & Shapiro, 2004). However, these organisms possess a specific mitochondria targeted type II topoisomerase encoded by a separate gene (TOP2mt). This arrangement is unique among lower eukaryotes and probably related to the multiply catenated structure of the kDNA.

Nucleus ¹⁾	Gene ²⁾	Mitochondria ³⁾
Top3 ←	TOP3 <i>S. Cerevisiae</i> <i>S. Pombe</i>	→ Top3 ⁴⁾
Top3α ←	TOP3A <i>D. melanogaster</i>	→ Top3α ⁴⁾
Top1 ←	TOP1 <i>S. Cerevisiae</i>	? Top1 ^{4) 5)}
Top1 ←	<i>S. Pombe</i>	→ Top1 ⁴⁾
Top2 ←	TOP2	
	TOP2mt <i>Trypanosoma</i> <i>Chrithidia</i> <i>Leishmania</i>	→ Top2mt ⁶⁾

Table 1.3: Overview of nuclear¹⁾ and mitochondrial³⁾ topoisomerases and their coding genes²⁾ in non-vertebrates. *In silico* analysis of yeast Top3, *D. melanogaster* Top3α and *S. pombe* Top1 predict a localisation of these enzymes in both nucleus and mitochondria. Although Top1 activity was reported in *S. cerevisiae* mitochondria (Tua et al, 1997; Wang et al, 1995), *S. cerevisiae* Top1 does not appear to contain MTS. Top2mt of protozoan parasites is the only representative of a mitochondrial specific topoisomerase in lower eukaryotes. References: ⁴⁾ (Wang et al, 2002); ⁵⁾ (Tua et al, 1997; Wang et al, 1995); ⁶⁾ (Kulikowicz & Shapiro, 2006)

1.2.3. Human nuclear topoisomerase I (Top1)

1.2.3.1 Structure

Human Top1 is encoded by the TOP1 gene located in chromosome region 20q12-13.2 (Juan et al, 1988). The 91 kDa protein consists of 765 amino acids. On the basis of its crystal structure, Top1 can be divided into four distinct domains (Redinbo et al, 1998): the N-terminal domain (NTD, a.a. 1–214), the core domain (a.a. 215–635), the linker (a.a. 636–698), and the C-terminal domain (CTD, a.a. 699–765) which contains at position 723 the tyrosine of the active site (Tyr⁷²³) (Fig. 1.10.A.). Top1 NTD is encoded by the first 8 exons of TOP1, whereas the entire catalytic domain (core, linker and C-terminal domain) is encoded by the highly conserved last 13 exons (see below). The NTD is poorly conserved through evolution; it contains four Nuclear Localisation Signals (NLS) and is therefore implicated in the nuclear localisation of Top1 (Mo et al, 2000a). This domain is not strictly required for the catalytic function *in vitro* (Stewart et al, 1996) but it seems to affect the enzymatic properties of Top1 *in vivo* (Christensen et al, 2003; Frohlich et al, 2007). The highly conserved core domain constitutes the principal DNA binding region of the enzyme and contains four of the five amino acids of the active site: Arg⁴⁸⁸, Lys⁵³², Arg⁵⁹⁰ and His⁶³². These catalytic residues position DNA during nucleophilic attack by Tyr⁷²³ (Cheng et al, 1998; Jensen & Svejstrup, 1996; Krogh & Shuman, 2000; Levin et al, 1993; Megonigal et al, 1997). The linker domain connects core and the CTD, which contains the catalytic active Tyr⁷²³. The linker is not required for relaxation activity *in vitro* but its loss leads to a 20-fold reduced affinity of Top1 for DNA (Stewart et al, 1997).

The structure of Top1 in covalent and non-covalent complexes with DNA was reported in several crystallographic studies (Leshner et al, 2002; Redinbo et al, 1998; Stewart et al, 1998). Because of its very high flexibility and disorganisation, the entire NTD of Top1 is missing in all these structures. The most complete crystal structure of Top1 comprises residues 201-765 and shows a bi-lobed protein that clamps completely around DNA (Fig. 1.10.B and C). The core domain of the enzyme can be further divided into subdomains I, II and III. Subdomains I (residues 215-232 and 320-433) and II (residues 233-319) fold tightly together forming the top half or “cap” of the enzyme. The cap is characterized by two long “nose-cone” α helices (α 5 of subdomain II and α 6 of subdomain I) that come together in a “V” away from the body of the enzyme. Subdomain III (residue 434-635) together with the CTD, forms the lower lobe of Top1; it extends from the cap of the enzyme downward bearing two

long α helices ($\alpha 8$ and $\alpha 9$). Most likely these function as the hinge that allows the clamp to close or open around DNA. Subdomains III and I interact directly across the hinge via two “lips” (residues 367-369 of subdomain I and residues 497-499 of subdomain III). These lips converge to bring the cap close to the lower lobe. The CTD is connected to core subdomain III through the linker, a flexible coiled-coil structure that protrudes from the base of the enzyme. The CTD is positioned such that the active site tyrosine is embedded within the base of the protein near the surface of the central cavity created by the tight clamping of the enzyme around duplex DNA.

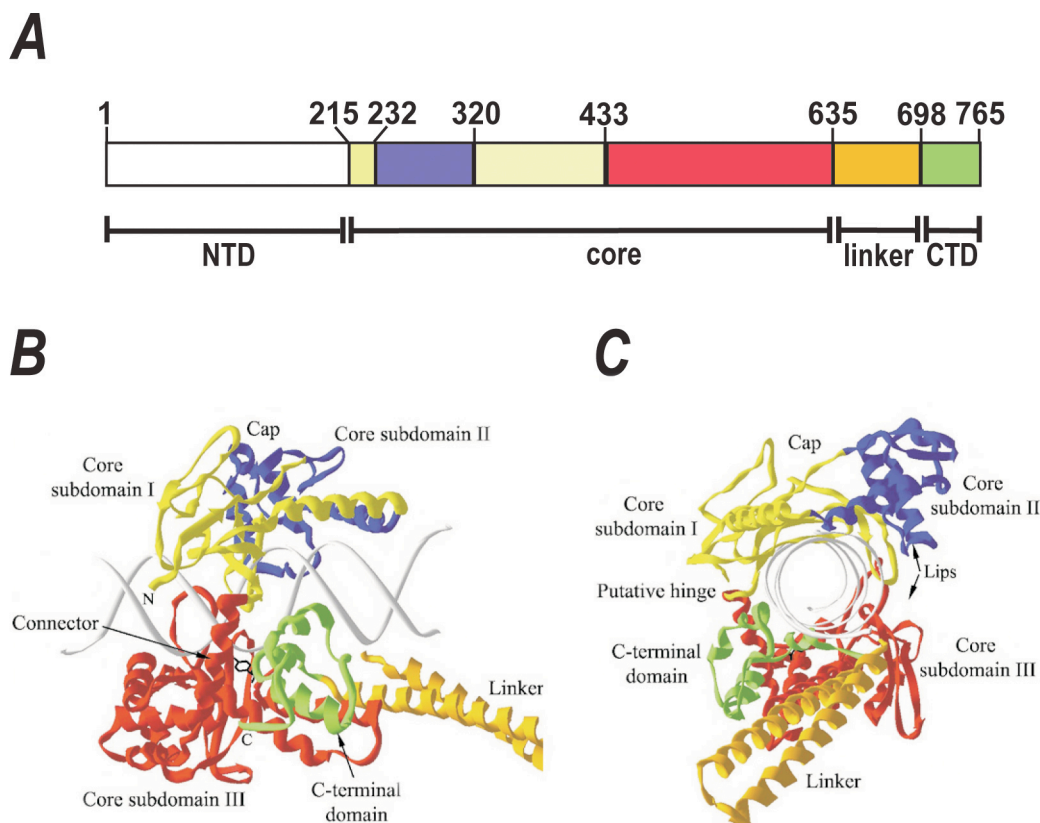


Fig. 1.9: Structure of human topoisomerase I. **A)** Top1 can be divided into four domains: the N-terminal domain (NTD, a.a.1-124, open box), the core domain (a.a. 215–635), the linker (a.a. 636–698, orange), and the C-terminal domain (CTD, a.a. 699–765, green). The core domain can be further divided into subdomain I (a.a. 215-232 and a.a. 320-433, yellow), subdomain II (a.a.233-319, blue) and subdomain III (a.a. 434–633, red). **B)** and **C)** Crystal structure of Top1 in complex with DNA: views of the protein from the side (**B**) or looking down the axis of DNA (**C**). Top1 various domains are labelled as in **A**). Core subdomains I and II forms the CAP of the enzyme whereas core subdomain III and CTD form the base lobe. The lip regions where the protein opens during DNA binding and release, are marked by arrows, and the hinge region is labelled ‘putative hinge’. Figure adapted from (Champoux, 2001).

Top1 engages in an intimate interaction with DNA substrate, wrapping completely around the DNA before it is cleaved. The core domain is responsible for most molecular interactions between Top1 and DNA: Residues 410 to 429 from subdomain I and the lips region are in close contact with the DNA. The most attractive model for DNA relaxation by Top1 proposes that relaxation proceeds by a “controlled rotation” mechanism where, after cleavage, the tension in the DNA drives its rotation (Stewart et al, 1998). Rotation occurs in the closed clamp conformation and the rate of rotation is not severely impeded when the enzyme is locked in this closed conformation (Carey et al, 2003).

1.2.3.2 Cellular roles

Top1 is constitutively expressed throughout the cell cycle (Baker et al, 1995) and is the most likely candidate to resolve the topological problems during the transcription process. Plasmids carrying actively transcribed genes were found to be negatively supercoiled when isolated from yeast lacking Top1 (Brill & Sternglanz, 1988). Furthermore, localization studies show a colocalisation of Top1 with transcribed regions (Shaiu & Hsieh, 1998). Top1 is also involved in resolving topological problems generated by the movement of DNA replication forks: The enzyme copurifies with a large replication complex from mammalian cells (Lebel et al, 1999).

In interphase nuclei, Top1 accumulates in the nucleoli, which are nuclear structures involved in the ribosome biogenesis (Christensen et al, 2004). According to the high transcription activity that occurs on rDNA (Hannan et al, 1998), it is suggested that Top1 enrichment in the nucleolar compartment is due to its role in rDNA transcription. In fact, Top1 colocalises with RNA polymerase I in the nucleolus (Christensen et al, 2004). In mitotic cells, Top1 is closely associated with chromosomes in a manner independent of its catalytical activity (Mo et al, 2000b), suggesting a role also in the structural organization of chromosome.

1.2.4. Mitochondrial topoisomerase I (Top1mt)

Mammalian mitochondrial topoisomerase I activity was identified about 20 years ago (Castora & Kelly, 1986; Fairfield et al, 1985) but the corresponding peptide Top1mt was purified and characterized only seven years ago (Zhang et al, 2001). Crucial for this purpose was the discovery of the TOP1mt gene and its mapping on human chromosome 8q24. TOP1mt was found in all available vertebrate genomes (*H.*

sapiens, *R. norvegicus*, *M. musculus*, *G. gallus*, *D. rerio*) (Zhang et al, 2004). The gene consists of 14 exons. The size of the last 13 exons is identical to all known TOP1mt genes and is conserved also in all vertebrate TOP1 genes, so that this 13-exon motif is also denoted 13-exon Top1 signature (Zhang et al, 2004). Notably, non-vertebrate eukaryotes do not possess TOP1mt and TOP1 lacks the 13-exon motive. TOP1mt probably derives from the evolutionary duplication of a single gene in a common ancestor for vertebrates and chordates.

Human Top1mt is a 601-amino acids polypeptide with a molecular mass of 70 kDa (Zhang & Pommier, 2008). The alignment of the amino acid sequences encoded by the 13-exon signature of Top1mt and Top1 reveals a high degree of conservation between the two enzymes (see appendix). Although the crystal structure of Top1mt is not yet known, Top1mt can be divided into four domains based on its similarity with Top1 (see fig. 4.3.1): The first 50 amino acids form the NTD and contain the MTS of the enzyme. This NTD is encoded by the first exon of TOP1mt. It is poorly conserved among the TOP1mt genes of several vertebrates and has no similarity to Top1. Amino acids 51-601, corresponding to amino acids 215-765 of Top1, encode for the catalytical domain of Top1mt, consisting of core, linker and C-terminal domains. This domain is highly conserved between Top1mt and Top1 and all the catalytic residues, including the tyrosine of the active site (Tyr⁵⁵⁹), are conserved in mitochondrial and nuclear variants.

The purification of recombinant Top1mt allowed characterizing the properties of the enzyme (Zhang et al, 2001). Like nuclear Top1, Top1mt is a type IB enzyme since it forms a covalent bond to the 3' end of the broken DNA, following incubation with a double-stranded oligonucleotide substrate. The comparison between the mitochondrial and nuclear Top1 enzymes showed only slight biochemical differences. Top1mt requires alkaline pH (around 8) and divalent cations (Ca²⁺ or Mg²⁺) for optimal catalytic activity, whereas nuclear Top1 is active in the absence of divalent cations, and most active at neutral pH, consistent with the basic and neutral pH present in the mitochondrial and nuclear compartments, respectively.

Top1mt expression is variable amongst several tissues: It is highest in skeletal muscle, heart, and brain, matching the requirement for high mitochondrial activity in these organs (Zhang et al, 2001). The expression of Top1mt is negatively regulated by the transcription factor E2F1: Knocking down E2F1 in HeLa cells leads to an increase in Top1mt mRNA levels (Goto et al, 2006), which suggests that E2F1 can act as a repressor of Top1mt transcription. Another factor that could play a role in the regulation of Top1mt expression is the alternative splicing of the TOP1mt transcript.

Two Top1mt mRNA splice variants are known. Since the translation of both alternatively spliced transcripts give rise to inactive proteins, alternative splicing could play a limiting role for Top1mt expression (Zhang et al, 2007).

Top1mt activity seems to be critical in vertebrates, since its expression relies on a specific gene. Based on the high homology with its nuclear counterpart, it could be supposed that Top1mt is required in mitochondria to resolve topological problems occurring during mtDNA replication and transcription. However, the specific role of Top1mt is not clear. Recently, it has been demonstrated that Top1mt associates with mtDNA (Zhang & Pommier, 2008). Mapping of Top1mt cleavage sites on mtDNA reveals few detectable sites clustered within a 150 bp region downstream of the D-loop, the regulatory region of mtDNA (Fig. 1.10). In animal mtDNA replication, most nascent strands from the heavy-strand origin (O_H) are prematurely terminated around position 16100, generating 7S DNA. The formation of the D-loop has been attributed to the pausing of POLG. The role of such replication pauses in the mtDNA homeostasis is unclear but seems to be critical to the entire replication process. Inhibition of Top1mt reduces 7S DNA, indicating a role of the enzyme in the D-loop homeostasis and probably in the transcription and/or replication process.

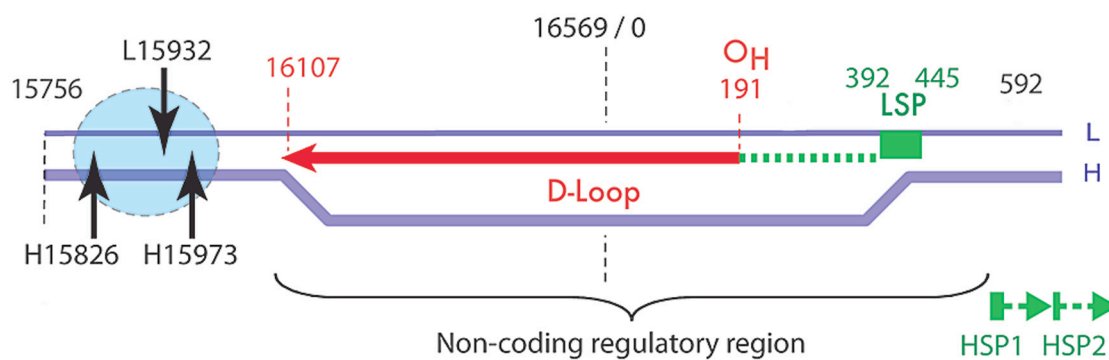


Fig. 1.10: Mapping of Top1mt cleavage sites. Schematic of the non-coding regulatory region of human mtDNA. In green are depicted the two H-strand promoters (HSP1 and HSP2) and the L-strand promoter (LSP), which also serves as the RNA primer for H-strand synthesis. During replication, most nascent strands from the H-strand origin (O_H) are prematurely terminated at site 16107. This pausing event generates the 7S DNA (red arrow) giving rise to the D-loop. Top1mt cleavage sites are clustered (blue circle) directly downstream from the replication pausing site (sites 15826 and 15973 on the H-strand and 15932 on the L-strand), suggesting a role of Top1mt in the D-loop homeostasis. Figure adapted from (Zhang & Pommier, 2008).

1.3 Aims of study

As mentioned previously, topoisomerase activity is believed to be an essential cofactor of mtDNA replication and transcription. In accordance with this, all three topoisomerase subfamilies present in the vertebrate cell nucleus (IA, IB, and IIA) are also represented in mitochondria by at least one gene product each. The mitochondrial representative of the IA family (Top3 α) and IIA family (Top2 β) are created by alternative posttranscriptional pathways of the same genes that encodes their nuclear variant. In contrast, the mitochondria-targeted (Top1mt) and the nuclear-targeted type IB topoisomerase (Top1) are encoded by two separate genes. Splitting of the topoisomerase I gene into Top1 and Top1mt is highly conserved in all vertebrates suggesting a certain importance of Top1mt activity in vertebrate mitochondria. Presumably, similar to Top1 in the nuclear compartment, Top1mt promotes and assists the metabolism of the mitochondrial genome. However, it is also possible that topoisomerase I activity endangers mtDNA and that the separate encoding of Top1mt serves regulatory purposes and is necessary to preserve mitochondrial genome. In the first part of this work, I set out to test this hypothesis investigating:

1) The consequence of a deregulated heterologous over-expression of Top1mt on mtDNA metabolism

Furthermore, Top1 and Top1mt show a high degree of sequence homology and a nearly identical biochemical activity. Therefore, the relevance of the topoisomerase 1 splitting into Top1 and Top1mt is still unknown. In the second and third part of this work, I set out to clarify the meaning of this splitting investigating:

2) The effects of an artificial targeting of Top1 to mitochondria on mtDNA stability

3) Evolutionary changes in Top1mt enabling safe handling of mtDNA

2. Materials

2.1 Available plasmids

2.1.1 Expression vectors

For the expression of mitochondria-targeted Top1mt and Top1, bicistronic expression vectors for mammalian cells were constructed from the plasmid pMC-2PS-delta HindIII-P (see appendix 8.1.A) (Mielke et al, 2000), in which the puromycin resistance gene (pyromycin-N-acetyltransferase, *pac*) constitutes the second cistron, followed by the simian virus 40 (SV40) polyadenylation signal. In front, *pac* is linked by an IRES element (Internal Ribosomal Entry Site) to a multiple cloning site (MCS), for the insertion of the gene of interest. A cytomegalovirus promoter (CMV) fused to the myeloproliferative sarcomavirus (MPSV) LTR enhancer repeat ensures a high transcription level of the bicistronic message in various mammalian cells and the transcriptional linkage ensures a fixed simultaneous expression of *pac* and a gene of interest. To enable the constitutive expression of YFP-tagged proteins, the plasmid pMC-YFP-P-N was used (see appendix 8.1.B), in which the MCS in the first cistron is fused to a yellow fluorescent protein (YFP).

2.1.2 Viral vector

Viral vectors are tools commonly used to deliver genetic material into the cell. In this work the lentiviral (HIV based) vector pCL1P3 (see appendix 8.1.C) was used, as gene delivery vehicles. pCL1P3 was kindly supplied by Prof. Hanenberg, Dep. of Pediatric Oncology, Haematology & Immunology Children's Hospital, Heinrich Heine University Düsseldorf.

2.1.3 cDNAs

The generation of mitochondria-targeted Top1mt and Top1 constructs was enabled by the manipulation of available constructs carrying the coding sequences of Top1, Top1^{Y723F}, Top1¹⁹¹⁻⁷⁶⁵, Top1^{191-765, Y723F}, Top1²¹⁰⁻⁷⁶⁵ (Christensen et al, 2002a). The coding sequence of Top1mt was provided by the plasmid pEGFP-Top1mt (Zhang et al, 2001) kindly gifted by H. Zhang.

2.1.4 cDNAs used as PCR standards or Northern and Southern blot probes

Several plasmids containing DNA sequences of nuclear and mitochondrial genes were used as standard for quantitative PCRs (qPCR and q-RT-PCR) and for the generation of probes for Northern and Southern blot (Table 2.1). All desired DNA sequences are inserted in the pCR2.1-TOPO vector (Invitrogen) using TOPO TA Cloning Kit (see 2.9).

Plasmid name	Inserted sequence
pCR2.1-18S	533-963 (NR_003286)
pCR2.1-12S-16S	873-2340 mtDNA (NC_001807)
pCR2.1-SDHB	341-556 (NM_00300)
pCR2.1-COXI	5916-6182 mtDNA
pCR2.1-tRNAY-COXI-tRNAS	5677-7514 mtDNA
pCR2.1-COXI probe	5970-6478 mtDNA
pCR2.1-12S probe	652-1156 mtDNA

Table 2.1

pCR2.1-18S, pCR2.1-SDHB and pCR2.1-COXI were supplied by Verena Schildgen. pCR2.1-COXI probe and pCR2.1-12S probe were provided by Stefanie Goffart.

2.2 Microbiology

2.2.1 E.coli strains

DH5 α	Genotype: supE44 Δ lacU169 (Φ 80lacZ Δ M15) hsdR17 recA1 endA1 gyrA96 thi-1 relA1 (Hanahan, 1983)
SURE (Stop Unwanted Rearrangement Events)	Genotype: e14(McrA ⁻) Δ (mcrCB-hsdSMR-mrr)171 endA1 supE44 thi-1 gyrA96 relA1 lac recB recJ sbcC umuC:Tn5 (Kan ^r) uvrC [F'proAB lacI ^q Z Δ M15 Tn10 (Tet ^r)], Stratagene, La Jolla, USA

2.2.2 Bacterial growth media

LB-agar	LB-Medium (see below), 15 g/l agar
LB-medium (1 l)	10 g Trypton, 5 g yeast extract, 10 g NaCl, pH 7,5 (NaOH)
TB-medium (1 l)	12 g Trypton, 24 g yeast extract, 4 ml Glycerol, were dissolved in 900 ml H ₂ O and sterilized. 100 ml of sterile phosphate-buffer (0.17 M KH ₂ PO ₄ , 0.72 M K ₂ HPO ₄) were added after autoclaving
SOB-medium (1 l)	20 g Trypton, 5 g yeast extract, 0.5 g NaCl, 0.184 g KCl were dissolved in 1 l H ₂ O, adjusted at pH 7.0 (NaOH) and sterilized. Just before use 5 ml of 2 M MgCl ₂ and 20 ml of 1 M MgSO ₄ were added.

If necessary 50 µg/ml ampicillin were added as selection to the media.

2.3 Cell culture

2.3.1 Cell lines

HT-1080	Human fibrosarcoma cell line established from the biopsy from a 35-year-old man (Rasheed et al, 1974). DSMZ, # DSM ACC 315, Braunschweig, Germany.
143B-ρ ⁰	Human osteosarcoma cell line lacking mtDNA (King & Attardi, 1989). These cells were kindly supplied by Prof. Rudolf J. Wiesner, Institute of Vegetative Physiology, University of Köln

2.3.2 Supplements & Antibiotics

When not otherwise specified, listed products are provided by Gibco/Invitrogen, Carlsbad, USA:

Dulbecco's Modified Eagle's Medium (DMEM) high glucose

Dulbecco's Modified Eagle's Medium (DMEM) no glucose

CO₂ Independent Medium (without L-Glutamine)

D-PBS (Ca²⁺, Mg²⁺ free),

Materials

Foetal Bovine Serum (FCS)

Penicillin (10.000 U/ml) & Streptomycin (100 µg/ml) solution

Trypsin-EDTA solution

Sodium Pyruvate MEM 100 mM

GlutaMAX-I Supplement, 200 mM

Puromycin

Sigma, St. Louis, USA

Uridine

Sigma, St. Louis, USA

2.3.3 Media

Growth medium DMEM high glucose, 10% FCS, 100 units/ml penicillin, 100 µg/ml streptomycin

Selection medium DMEM high glucose, 10% FCS, 100 units/ml penicillin, 100 µg/ml streptomycin, 0.6 µg/ml puromycin

CO₂-independent medium CO₂-independent medium, 10% FCS, 100 units/ml penicillin, 100 µg/ml streptomycin, 1% GlutaMAX-I

Respiration medium DMEM no glucose, 10% FCS, 100 units/ml penicillin, 100µg/ml streptomycin, 1% sodium pyruvate, 1% GlutaMAX-I

2.4 Buffers and Stock Solutions

6X Agarose loading buffer 15 % Ficoll type 400, 40 mM Tris-HCl pH 8.5, 40 mM Glacial acetic acid, 2 mM EDTA, 0.25 % Bromphenol blue

50X TAE buffer 2 M Tris-HCl pH 8.5, 2 M Acetic acid, 0.1 M EDTA

10X TGS buffer 2.5 M Tris, 1.92 M Glycin, 0.1% SDS

20X NuPAGE MOPS SDS supplied by invitrogen, Carlsbad, USA

Running Buffer

10X D-PBS (Phosphate-Buffered Saline) 1.4 M NaCl, 27 mM KCl, 100 mM Na₂HPO₄ 2H₂O, 18 mM KH₂PO₄

10X TBE buffer 0.89 M Tris, 0.89 mM Boric acid, 20 mM EDTA

0.25% bromphenol blue, 4 mM EDTA, 0.9 M formaldehyde,

5X RNA loading buffer	20% glycerol, 30.1% formamide, 4XMOPS running buffer
10X MOPS running buffer	200 mM MOPS, 50 mM sodium acetate, 10 mM EDTA
20X SSC	0.25 M tri-Sodium citrate, 3 M NaCl
HBSS (Hanks Balanced Salt Solution)	5.4 mM KCl, 0.3 mM Na ₂ HPO ₄ , 0.4 mM KH ₂ PO ₄ , 4.2 mM NaHCO ₃ , 1.3 mM CaCl ₂ , 0.5 mM MgCl ₂ , 0.6 mM MgSO ₄ , 137 mM NaCl

2.5 Enzymes

Expand High Fidelity PCR system	Roche, Mannheim, Germany
Platinum SYBR Green qPCR SuperMix-UDG w/ROX	Invitrogen, Carlsbad, USA
RNase A	Qiagen, Hilden, Germany
Quick Ligation Kit	NEB, Ipswich, USA

2.6 Chemicals

Digitonin High purity	Calbiochem, Darmstadt, Germany
Antimycin A	Sigma, St. Louis, USA
2'3'-Dideoxycytidine (ddC)	Sigma, St. Louis, USA
5-Brom-4-chlor-3-indoxyl-β-D-galactopyranosid (X-gal)	Calbiochem, Darmstadt, Germany
MitoTracker Red CMXRos	Invitrogen, Carlsbad, USA
MitoSOX Red mitochondrial superoxide indicator	Invitrogen, Carlsbad, USA
Ethidium Bromide solution 1%	Roth, Karlsruhe, Germany

2.7 Antibodies

2.7.1 Primary antibodies

Target (gene ref. Num.)	Name	Clone	from	Working dilution	Source
YFP	Living Colors anti GFP	JL-8	mouse	1:4000	#632381, Clontech, Mountain View, USA
MTCO1	Anti COXI-Complex IV	1D6	mouse	1:750	#A6403, Molecular probes, Invitogen, Karlsruhe, Germany
NDUFA9	Anti a subcomplex, 9- Complex I	20C11	mouse	1:4000	#A21344, Molecular probes
ATP5A1	Anti F1 complex, a subunit-Complex V	7H10	mouse	1:4000	#A21350, Molecular probes
UQCRC2	Anti core II subunit-Complex III	13G12	mouse	1:5000	# A11143, Molecular probes
NDUFB8	Anti a subcomplex, 9- Complex I	20E9DH1 0C12	mouse	1:3000	#MS105, Mitoscience Eugene, Oregon, USA
COX4	Anti COXIV-Complex VI	10G8	mouse	1:3000	# A21347, Molecular probes
MnSOD	SOD-2	FL-222	rabbit	1:2000	#sc-30080, Santa cruz biotechnology, Heidelberg, Germany
TOP1MT	γ Top1mt		rabbit	1:1500	Kindly supplied by Zhang
TUBULIN ALPHA	Anti- α -Tubulin	B-5-1-2	mouse	1:10000	#T6074, Sigma, St. Louis, USA

2.7.2 Secondary antibodies

Name	from	Working dilution	Source
ECL Mouse IgG, HRP-Linked Whole Ab	sheep	1:40000	Amersham, Little Chalfont, England
ECL Rabbit IgG, HRP-Linked Whole Ab	donkey	1:10000	Amersham, Little Chalfont, England

2.8 Consumable items

Immobilon-P (PVDF) Transfer Membrane	Millipore, Bedford, USA
Hybond TM -N+ nylon membrane	Amersham, Little Chalfont, England
NuPAGE Novex 4-12% Bis-Tris Gel	Invitrogen, Carlsbad, USA
Gel cassette Novex, 1 mm	Invitrogen, Carlsbad, USA
BD vacutainer tubes for Lactate-quantification (REF 368920)	BD bioscience, Heidelberg, Germany

2.9 Kits

TOPO TA Cloning Kit	Invitrogen, Carlsbad, USA
QIAquick Gel Extraction Kit	Qiagen, Hilden Germany
QIAGEN Plasmid Maxi Kit	Qiagen, Hilden Germany
QuantiTect SYBR Green RT-PCR Kit	Qiagen, Hilden Germany
DNeasy Mini Kit	Qiagen, Hilden, Germany
RNeasy Mini Kit	Qiagen, Hilden, Germany
Effectene Transfection Reagent	Qiagen, Hilden, Germany
BCA Protein Assay Reagent	Pierce, Rockford, USA
ECL Plus Western Blotting Reagents	Amersham, Little Chalfont, England
ECL Direct Labeling and Detection System	Amersham, Little Chalfont, England

2.10 Instruments

Horizontal Gel Electrophoresis Apparatus Horizon 11.14	Whatman/ Biometra, Göttingen, Germany
Vertical polyacrilamid gel electrophoresis system Novex Mini-Cell Electrophoresis	Invitrogen, Carlsbad, USA
Semi-dry blot chamber multiphor II novablot	Amersham, Little Chalfont, England

Materials

PCR Cycler Mastercycler	Eppendorf, Hamburg, Germany
Photometer Biophotometer	Eppendorf, Hamburg, Germany
PH meter Calimatic 766	Knick, Berlin, Germany
Ultrasound Homogeniser Sonopuls	Bandelin, Berlin, Germany
Dounce homogenizer	Wheaton Inc., Millville, USA
Flow cytometer FACSCalibur	BD bioscience, Heidelberg, Germany
Automated blood analyzer Modular P analyzer	Roche, Mannheim, Germany
Agilent 2100 Bioanalyzer & Agilent RNA 6000 NanoChip,	Agilent Technologies, SantaClara, USA
Luminscent image analyzer LAS-4000	Fujifilm, Tokyo, Japan
Epifluorescent inverse microscope Axiovert 100	Carl Zeiss, Göttingen, Germany
Delta TC3 Culture Dish System	Bioprotechs Inc., Butler, USA
Digital Camera Spot-RT SE Monochrom	Diagnostic Instruments, Sterling Heights, USA
Confocal Laser Scanning Microscope LSM 510 Meta	Carl Zeiss, Göttingen, Germany
Centrifuge Centrikon H-401	Kontron, Heraeus, Hanau, Germany
Centrifuge 5417R	Eppendorf, Hamburg, Germany
Centrifuge Rotixa / P	Hettich, Tuttlingen, Germany

3. Methods

3.1 Cloning

3.1.1 Plasmids construction

3.1.1.1 Basic construct

To enable mitochondrial targeting of YFP fusion proteins, we generated the vector pMC-MTS-YFP-N (see appendix 8.1.D) by modifying pMC-YFP-P-N (see 2.1.1). YFP of pMC-YFP-P-N was extended in frame at the 5' end with the sequence encoding the MTS (Mitochondrial Targeting Signal) from subunit VIII of COX (Rizzuto et al, 1995), generating pMC-MTS-YFP-P.

3.1.1.2 Mitochondria-targeted YFP chimera

The coding sequences of human Top1 (RefSeq NM_003286) and human Top1mt (RefSeq NM_052963) were fused behind YFP in the vector pMC-MTS-YFP-N. Thus, the first cistron of the transcribed messenger encodes the mitochondrial addressed Top1mt or Top1 YFP chimeras and the second cistron the puromycin resistance gene.

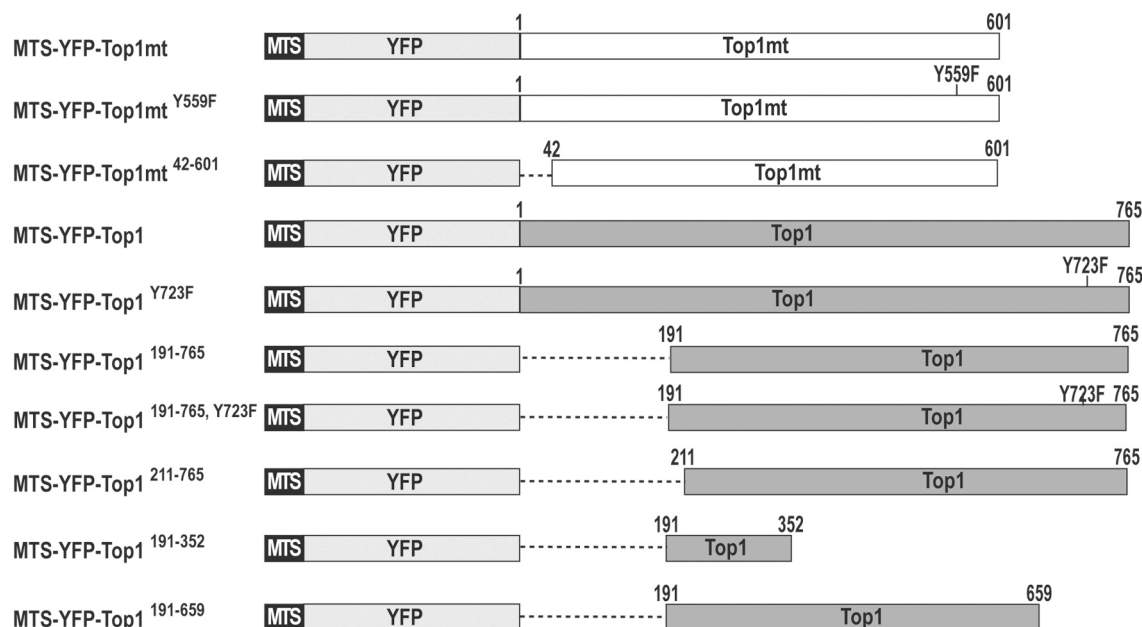


Fig. 3.1. Mitochondria-targeted YFP chimeric proteins. Several variants of Top1mt (white) and Top1 (dark grey) were fused in frame with YFP (grey). The import into the mitochondrial matrix of these constructs was ensured by the N-terminal MTS (black)

Methods

YFP was fused to the N-terminus of Top1mt and Top1, because previous experiences suggested that at these positions YFP would less likely disrupt enzymatic functions. The mitochondria targeted YFP chimeras studied in this work are shown in the figure 3.1.

MTS-YFP-Top1mt, MTS-YFP-Top1mt⁴²⁻⁶⁰¹, MTS-YFP-Top1¹⁹¹⁻³⁵¹, MTS-YFP-Top1¹⁹¹⁻⁶⁵⁹ were generated from cDNAs of Top1mt (Zhang et al, 2001) and Top1 (Christensen et al, 2002a) by linker PCR, using the primers listed in table 3.1.

Construct	Primer	Sequence
pMC-MTS-YFP-Top1mt-P	1) 5'- <u>MluI</u> -Top1mt ¹⁻²¹	5'-GGGCGGACGCGTATGCGCGTGG TGGGCTGCTG-3'
	2) 3'-Top1mt ¹⁷⁸⁴⁻¹⁸⁰⁶ - <u>SpeI</u>	5'-GGGCGGACTAGTTTAGAATTCAA AGTC TTCTCCTG-3'
pMC-MTS-YFP-Top1mt ⁴²⁻⁶⁰¹ -P	3) 5'- <u>MluI</u> -Top1mt ¹²⁴⁻¹⁴⁵	5'-GGGCGGACGCGTTGGGAGAA GGAGAAGCACGAAG-3'
	2) 3'-Top1mt ¹⁷⁸⁴⁻¹⁸⁰⁶ - <u>SpeI</u>	See above
pMC-MTS-YFP-Top1 ¹⁹¹⁻³⁵¹ -P	4) 5'- <u>MluI</u> -Top1 ⁵⁷¹⁻⁵⁹⁵	5'-GGGCGGACGCGTAAGAAAAAGAAGCCG AAGAAAGAAG-3'
	5) 3'-Top1 ¹⁰³⁵⁻¹⁰⁵³ - <u>ApaI</u>	5'-GGGCGGGGGCCCCTAAGCAAT CCTCTTTTGTGG-3'
pMC-MTS-YFP-Top1 ¹⁹¹⁻⁶⁵⁹ -P	4) 5'- <u>MluI</u> -Top1 ⁵⁷¹⁻⁵⁹⁵	See above
	6) 3'-Top1 ¹⁹⁵⁸⁻¹⁹⁷⁸ - <u>ApaI</u>	5'-GGGCGGGGGCCCCTATGCTAG CTGTTCTTCTTGG-3'
pMC-MTS-YFP-Top1mt ^{Y559F} -P	7) 5'-Top1mt ⁹¹²⁻⁹³²	5'-GGAAATGAAGACGAGACAGC-3'
	8) 3'-Top1mt ¹⁶⁵⁶⁻¹⁷⁰¹ -mut	5'-GGCAATGCTGATCCTGGGGTCC AGAAGTTGAGCTTGGACGTGCCC-3'
	9) 5'-Top1mt ¹⁶⁵⁶⁻¹⁷⁰¹ -mut	5'-GGGCACGTCCAAGCTCAACTTCCT GGACCCCAGGATCAGCATTGCC-3'
	10) 3'-pMC-2-3	5'-CAAGGGTACCGCAATACCGG AG-3'

Table 3.1

Linker-primers place restriction sites (underlined) at the ends of the PCR products, facilitating their later insertion into pMC-MTS-YFP-N using MluI/SpeI for Top1mt or MluI/ApaI for Top1. To generate MTS-YFP-Top1mt^{Y559F}, the tyrosine (Y) at position 559 of Top1mt was mutated into Phenylalanine (F) by overlap-extension PCR ((Horton et al, 1989), see 3.1.1.7). Top1mt cDNA was amplified in two separate PCRs (primers 7+8 and 9+10) using primers carrying the intended mutation. Products of PCR 1 and 2 were then amplified in a third PCR (primers 7+10). The mutated PCR product was sub-cloned in pMC-MTS-YFP-Top1mt-P using SpeI/BstXI, generating pMC-MTS-YFP-Top1mt^{Y559F}-P. MTS-YFP-Top1, MTS-YFP-

Top1^{Y723F}, MTS-YFP-Top1¹⁹¹⁻⁷⁶⁵, MTS-YFP-Top1^{191-765, Y723F}, MTS-YFP-Top1²¹¹⁻⁷⁶⁵ were sub-cloned from ready available plasmids carrying cDNAs of Top1, Top1^{Y723F}, Top1¹⁹¹⁻⁷⁶⁵, Top1^{191-765, Y723F}, Top1²¹⁰⁻⁷⁶⁵ (see 2.1.3). The mentioned coding sequences were cloned in pMC-MTS-YFP-N generating the respective mitochondria-targeted YFP chimeras.

3.1.1.3 Nuclear targeted chimera

To target the mitochondrial variant of topoisomerase I to the nucleus, the constructs pMC-YFP-NLS-Top1mt-P was generated (Fig. 3.2). Top1mt was supplemented at the N-terminus with the SV40 NLS sequence (PKKKRKV), using linker PCR. Top1mt was amplified respectively with the primers 11+2 (Table 3.2), and then inserted in pMC-YFP-P-N (see 2.1.1) using MluI/SpeI digestion.



Fig. 3.2. Nuclear targeting of Top1mt. To allow the targeting of Top1mt (white) to the nuclear compartment, the protein was fused in frame with YFP (grey) and the SV40 NLS sequence (Black).

Construct	Primer	Sequence
pMC -EYFP- NLS-Top1mt-P	1) 5'-MluI-SV40NLS- Top1mt ¹⁻²¹	5'-GGGCGGACGCGTCCTCCTAAGA AGAAAAGGAAGGTGCCCCCATGCG CGTGGTGCGGCTGCTG-3'
	2) 3'-Top1mt ¹⁷⁸⁴⁻¹⁸⁰⁶ -SpeI	See Table 3.1

Table 3.2

3.1.1.4 Untagged Top1mt

To assay the deregulated expression of untagged Top1mt, the construct pMC-Top1mt-P was designed. In this case, the N-terminus of Top1mt is fused neither to YFP nor to the artificial MTS. Top1mt sequence was amplified with the linker-primers 12+13 (Table 3.3) and the PCR product was then inserted in the pMC-2PS-delta HindIII-P vector (see 2.1.1) using NotI/HindIII.

Construct	Primer	Sequence
pMC- Top1mt-P	12) 5`- <u>NotI</u> -Top1mt ¹⁻²¹	5'- GGGCGGGCGGCCCGCCACCATGCGCG TGGTGCGGCTGCTG-3'
	13) 3`-Top1mt ¹⁷⁸⁴⁻¹⁸⁰⁶ - <u>HindIII</u>	5'-GGGCGGAAGCTTTAGAAATCAA AGTCTTCTCCTG-3'

Table 3.3

3.1.1.5 Viral constructs

Recombinant lentiviral vectors were generated from the HIV-vector pCL1P3 (see 2.1.2, appendix 8.1.C).

The entire bicistronic expression units of pMC-MTS-YFP-P, pMC-MTS-YFP-Top1-P and pMC-MTS-YFP-Top1^{Y723F}-P were sub-cloned in pCL1P3 (ClaI/SplI), generating pCL1P3-MTS-YFP, pCL1P3-MTS-YFP-Top1 and pCL1P3-MTS-YFP-Top1^{Y723F}.

3.1.1.6 Swap constructs

To investigate the differences between Top1mt and Top1, several Top1mt/Top1 hybrid proteins were designed on the basis of their protein alignments. Top1mt/Top1 protein sequences were swapped at diverse specific sites, using overlap extension PCR (see 3.1.1.7) Generated Top1 /Top1mt-hybrids were then sub-cloned into an appropriate vector, thereby generating MTS-YFP fused hybrid-protein (Fig 3.3).

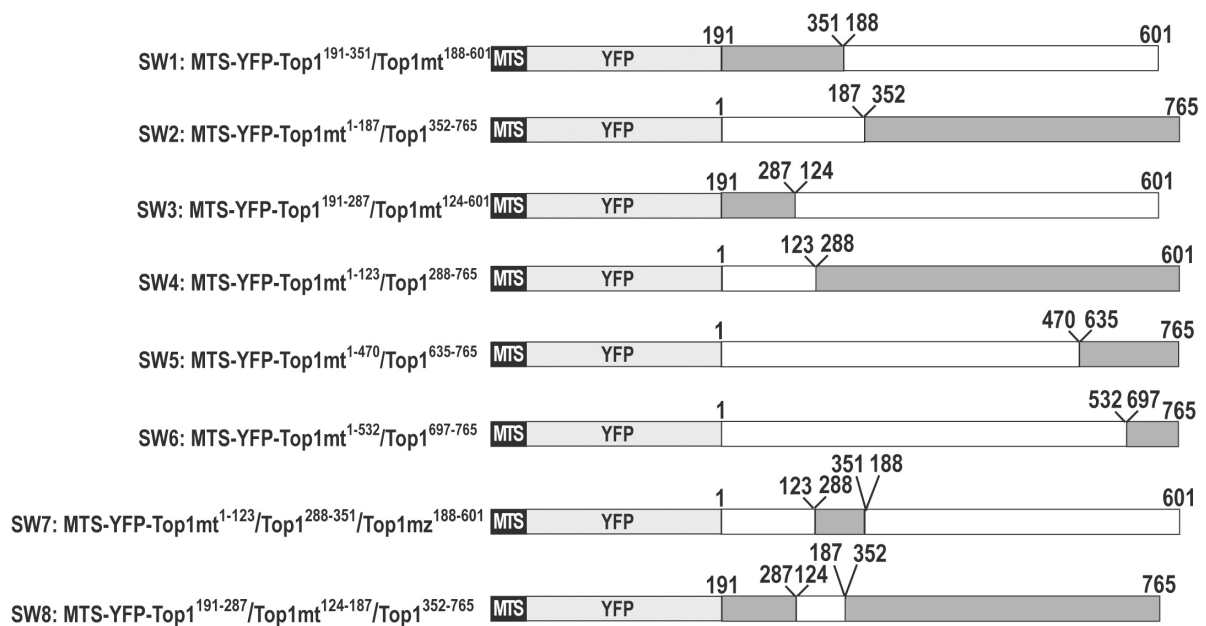


Fig. 3.2. Swap constructs. Top1mt (white) /Top1 (dark grey) hybrid proteins were fused in frame with MTS-YFP.

Into pMC-MTS-YFP-Top1mt were cloned Top1¹⁹¹⁻³⁵¹/Top1mt¹⁸⁸⁻⁶⁰¹ (MluI/AflIII), Top1mt¹⁻⁵³²/Top1⁶⁹⁷⁻⁷⁶⁵ (EcoNI/SpeI), and Top1mt¹⁻⁴⁷⁰/Top1⁶³⁵⁻⁷⁶⁵ (EcoNI/ SpeI). Top1mt¹⁻¹⁸⁷/Top1³⁵²⁻⁷⁶⁵ was inserted into pMC-MTS-YFP-Top1¹⁹¹⁻⁷⁶⁵ (MluI/XcmI). Afterwards Top1¹⁹¹⁻²⁸⁷/Top1mt¹²⁴⁻⁶⁰¹ was inserted into pMC-MTS-YFP- Top1¹⁹¹⁻³⁵¹/Top1mt¹⁸⁸⁻⁶⁰¹ (Eco47III/EcoNI) and Top1mt¹⁻¹²³/Top1²⁸⁸⁻⁷⁶⁵ was inserted into pMC-MTS-YFP- Top1mt¹⁻¹⁸⁷/Top1³⁵²⁻⁷⁶⁵ (PvuII/XcmI). Top1mt¹⁻¹²⁴/Top1²⁸⁸⁻³⁵²/Top1mt¹⁸⁸⁻⁶⁰¹ was cloned in pMC-MTS-YFP-Top1¹⁹¹⁻³⁵¹/Top1mt¹⁸⁸⁻⁶⁰¹. pMC-MTS-YFP-Top1¹⁹¹⁻²⁸⁷/Top1mt¹²⁴⁻¹⁸⁷/Top1³⁵²⁻⁷⁶⁵ was sub-cloned in pMC-MTS-YFP-Top1mt¹⁻¹⁸⁷/Top1³⁵²⁻⁷⁶⁵ (MluI/BstEII).

Primer	Sequence
14) 5`-YFP ⁶⁷⁷⁻⁶⁹⁶	5'-GATCACTCTCGGCATGGAC-3'
10) 3`-pMC2-3	5'-CAAGGGTACCGCAATACCGGAG-3'
15) 3`-SpeI-Top1 ²²⁷⁴⁻²²⁹⁸	5'-GGGCGGACTAGTCTAAACTCATAGTCTTCATCAGCC-3'
16) 3`-SW1	5'-GCCACGGAACAAGCCAGGCGGCTCAATCTTGAAGTT/ AGCAATCCTCTCTTTGTGGTTATCCATAATAC-3'
17) 5`-SW1	5'-GTATTATGGATAACCACAAAGAGAGGATTGCT/ AACTTCAAGATTGAGCCGCCTGGCTTGTTCGTGGC-3'
18) 3`-SW2	5'-GCCGCGGCCACGGAAAAGTCCAGGAGGCTCTATCTTGAAGTT/ GCCTATTTTTCTTGGTGACCATCTAAAATAC-3'
19) 5`-SW2	5'-GTATTTTAGATGGTCACCAAGAAAAAATAGGC/ AACTTCAAGATAGAGCCTCCTGGACTTTTCCGTGGCCGCGGC-3'
20) 3`-SW3	5'-GGCTCTTGATGACTTCCCTCTTCCACCGC/ CATTTCCTTCTCCAGTCTTTAAAGAAATTTTTCT-3'
21) 5`-SW3	5'-GGAAAAATTTCTTTAAAGACTGGAGAAAGGAAATG/ GCGGTGGAAGAGAGGGAAAGTCATCAAGAGCC-3'
22) 3`-SW4	5'-GGTGATAATATTCTTCTTTCATTAGT/CATTCC TTTCGCCAGTCATTGAAGAAGTTCTTCCGAAAACC-3'
23) 5`-SW4	5'-GGTTTTCCGGAAGAAGTCTTCAATGACTGGCGAAAGGAAATG /ACTAATGAAGAGAAGAATATTATCACC-3'
24) 3`-SW5	5'-CATAGACTTCTCAAAAGTTTTTGGTGGTGC/ TCGCTGATGGTTGCAGAGAATGGCCACG-3'
25) 5`-SW5	5'-CGTGGCCATTCTCTGCAACCATCAGCGA/ GCACCACAAAAACTTTTGAGAAGTCTATG-3'
26) 3`-SW6	5'-GGTCTGTGGCTTGAAGTCCAGCTTCATCAACTG/ CTCCTGCAGCTTCTCCAGGAGCCGCCTCTTC-3'
27) 5`-SW6	5'-GAAGAGGCGGCTCCTGGAGAAGCTGCAGGAG/ CAGTTGATGAAGCTGGAAGTTCAAGCCACAGACC-3'

Table 3.4

Construct	Primers		Template
SW1	PCR 1	17+10	MTS-YFP-Top1mt
	PCR 2	14+16	MTS-YFP-Top1
	PCR 3	14+10	Products PCR 1 & 2
SW2	PCR 1	19+10	MTS-YFP-Top1
	PCR 2	14+18	MTS-YFP-Top1mt
	PCR 3	14+10	Products PCR 1 & 2
SW3	PCR 1	21+10	MTS-YFP-Top1mt
	PCR 2	14+20	MTS-YFP-Top1
	PCR 3	14+10	Products PCR 1 & 2
SW4	PCR 1	23+10	MTS-YFP-Top1
	PCR 2	14+22	MTS-YFP-Top1mt
	PCR 3	14+10	Products PCR 1 & 2
SW5	PCR 1	25+15	MTS-YFP-Top1
	PCR 2	14+24	MTS-YFP-Top1mt
	PCR 3	14+15	Products PCR 1 & 2
SW6	PCR 1	27+15	MTS-YFP-Top1
	PCR 2	14+26	MTS-YFP-Top1mt
	PCR 3	14+15	Products PCR 1 & 2
SW7	PCR 1	23+10	MTS-YFP-Top1 ¹⁹¹⁻³⁵¹ / Top1mt ¹⁸⁸⁻⁶⁰¹
	PCR 2	14+22	MTS-YFP-Top1mt
	PCR 3	14+10	Products PCR 1 & 2

Table 3.5

3.1.1.7 Overlap extension PCR

To recombine two proteins, fragments of their genes are generated in separate PCRs using primers designed so that the products ends contain complementary sequences. These PCR products overlap partially and extension of the matching sequence produces a molecule in which the original sequences are 'spliced' together (Horton et al, 1989).

Segments of Top1 and Top1mt are amplified in two separated PCRs using the primers listed in Table 3.3. The first PCR was performed using the forward primer 14 and the appropriate 3'-SW reverse primer. The second PCR was performed using the reverse primer 10 (for SW1, SW2, SW3, SW4 and SW7) or 15 (for SW5 and SW6) and the appropriate 5'-SW forward primer (Table 3.4). Plasmids MTS-YFP-Top1mt or MTS-YFP-Top1 were used as template. The PCR products of the first and second PCR were then mixed together in a third PCR performed with the primers 14 and 10 (for SW1 and SW2) or 15 (for SW5 and SW6).

First and second PCR were performed with 18 cycles, the third with 22 cycles, under the following conditions:

Denaturation	2' 96°C	
Addition of polymerase		
Denaturation	30'' 94°C	18/22 cycles
Annealing	30'' 56°C	
Elongation	2' 72°C	
Final elongation	12' 72°C	

3.1.1.8 Standard PCR

PCR was performed using the Expand high fidelity PCR Kit (Roche). To reduce non-specific amplification and increase the target yield, Hot Start PCR was used under the following conditions:

Denaturation	2' 96°C	
Addition of polymerase		
Denaturation	30'' 94°C	25 cycles
Annealing	30'' 55°C	
Elongation	1-3' * 72°C	
Final elongation	12' 72°C	

*: Depending on the length of the expected PCR product

3.1.2 Restriction nucleases digestion, gel electrophoresis and recovery of DNA from agarose gels

For the insertion in the appropriate vector, PCR products or plasmids that contain the sequence of interest were digested with the appropriate restriction nucleases for 60 min. Agrose loading buffer was added and DNA separated by electrophoresis through a 0.8-1.2% agarose gel, containing 0.5 µg/ml EtBr in 1X TAE buffer. After electrophoresis, the DNA fragments were excised and recovered from the agarose using gel extraction Kit (Qiagen), according to the manufacturer's instructions.

3.1.3 Ligation

To insert restriction fragments into vectors, Quick Ligation Kit (NEB) was used according to manufacturer's protocol. Ligation was performed in a final volume of 10-20 μ l for 10 min at RT and transferred to ice.

3.1.4 Transformation and isolation of plasmid DNA

3.1.4.1 Generation of competent E.Coli cells

E.coli were grown in 1 L SOB medium at 18°C and harvested (4000 \times g, 20 min, 4°C), when the OD₆₀₀ of the culture reached a value of 0.5-0.8. The cells were gently resuspended in 40 ml ice-cold TB buffer (10 mM Pipes, 55 mM MnCl₂, 15 mM CaCl₂, 250 mM KCl), incubated on ice for 20 min and again sedimented (4000 \times g, 20 min, 4°C). Cells were gently resuspended in 20 ml ice-cold TB buffer and DMSO was added with gentle swirling to a final concentration of 7%. After 10 min incubation on ice, cells were dispensed in 0.5 ml aliquots, frozen in liquid nitrogen and stored at -80 °C.

3.1.4.2 Transformation of E.coli

An aliquot of 0.5 ml competent cells was mixed with 2 μ l ligation reaction mixture, incubated on ice for approx. 30 min, shocked at 42°C 30" and immediately re-transferred to ice. 0.5 ml pre-warmed LB-media was added to the cells and the mixture was incubated for 1 h at 37°C with vigorous shaking (250 rpm). Hereafter transformed cells were transferred to LB-agar plates containing 50 μ g/ml ampicillin.

3.1.4.3 Plasmid preparation at a small scale (Minipreps)

Several single colonies from a selective plate were picked and inoculated in 2.5 ml TB medium containing 50 μ g/ml ampicillin and incubated overnight at 37°C with vigorous shaking (250 rpm). After approximately 14 hours, 2ml of the culture were pelleted (6800 g, 2 min, 4°C). The cell pellet was mixed with 400 μ l lysis solution (0.2 N NaOH, 1% SDS), immediately neutralized with 300 μ l 7.5 M NH₄oAC, kept for 10 min on ice, to precipitate genomic DNA and proteins, then sedimented at 14000 \times g, 10 min, 4°C. The plasmid DNA was precipitated from the supernatant with 500 μ l 2-Propanol and pelleted (14000 g, 30 min, 4°C). DNA pellet was washed with 70%

EtOH, dried and resuspended in 50 µl TE (10 mM Tris-HCl pH 8.0, 1 mM EDTA) supplemented with 50 µg/ml RNaseA. The plasmids sequence was finally confirmed by restriction digestions and sequencing.

3.1.4.4 Plasmid preparation at a large scale (Maxipreps)

A single colony from a selective plate was picked and inoculated in a primary culture of 3 ml selective TB medium (containing 50 µg/ml ampicillin) and incubated for approx. 8 h at 37°C with vigorous shaking (250 rpm). Afterwards the starter culture was diluted into 250 ml selective TB medium and grown overnight under the above-mentioned conditions. Bacterial cells were harvested by centrifugation (6000 x g, 15 min, 4°C) and the purification of plasmid DNA was performed with QIAGEN Plasmid Maxi Kit according to manufacturer's protocol. DNA concentration was determined spectrophotometric by absorption at wavelength of 260 nm.

3.1.4.5 Sequencing of plasmids

Sequencing of the constructs was performed by the BMFZ (Biologisch-Medizinisches Forschungszentrum) of the Heinrich-Heine-University Düsseldorf (Germany).

3.2 Cell culture

3.2.1 Maintenance of mammalian cells

HT1080 cells were maintained as subconfluent monolayer cultures in growth medium (see 2.3.3) at 37°C under a humidified 5% CO₂ atmosphere. For passage, cells layers were washed once with PBS, detached by a short treatment with Trypsin-EDTA solution and reseeded upon dilution (1:6).

3.2.2 Transfection and selection of HT-1080 cells

An 80% confluent monolayer culture (25 cm²) was diluted 1:4 24 hours before transfection. Cells were transfected with 1 µg DNA using "Effectene Transfection Reagent" (Qiagen) according to the manufacturer's instructions. Transient expression could be estimated under microscope after 12-24 hours with a transfection efficiency varying between 20-90 % depending on the construct used. 30 hours after transfection, cells were appropriately diluted into tissue culture dishes and stable cell

clones were selected with selection medium (see 2.3.3). Stable expressing clones were expanded and maintained in selection medium. Cell clones lacking mtDNA were selected and maintained in selection medium supplemented with 50 µg/ml uridine.

3.2.3 Viral transduction

Viral vectors were used as alternative gene delivery vehicle to overcome the limitations of the transfections methods (in our case: low liposomal transfection efficiency). Compared to the conventional transfection, viral vectors permit the quick introduction of foreign material into a large amount of cells (a process called transduction) allowing further analyses.

We used the HIV- lentiviral vectors pCL1P3-MTS-YFP, pCL1P3-MTS-YFP-Top1 and pCL1P3-MTS-YFP-Top1^{Y723F} (see 3.1.1.5) to monitor the mtDNA metabolism in the early phase of mitochondrial targeting of Top1.

3.2.3.1 Lentivirus production

To produce the lentivirus, three different plasmids were transfected into the „packaging cell line“ HEK 293T: The helper virus (CD/NL-BH), that is required for the viral infection; the packaging plasmid (VSV-gwt), that encode the virion proteins, such as the capsid and the reverse transcriptase and the viral vector (pCL1P3-MTS-YFP, pCL1P3-MTS-YFP-Top1 and pCL1P3-MTS-YFP-Top1^{Y723F}), that contains the genetic material of the virus. In the HEK 293T cells, the vector is transcribed to produce the single-stranded RNA viral genome. The presence of a so-called psi (Ψ) sequence, that marks viral RNA, is used to package the genome into the virion. 48 hours after transfection, the supernatant of HEK 293T, containing the viruses, was collected and filtered through a 0.45 µm filter to clear the viral particles of cell debris. The titers of viral stocks were measured by transducing HT1080.

3.2.3.2 HT1080 transduction

A 75 cm² culture flask of HT1080 was transfected with 2 ml of viral stock diluted 1:3 in DMEM. After 30 hours, the transduction efficiency (nearly 100%) was monitored under microscope and the cells were then selected and maintained in selection medium supplemented with 50 µg/ml uridine.

3.2.4 Cell cycle analysis

50%-60% confluent cells from a 25 cm² culture flask were harvested and washed once in D-PBS. Cells were fixed with 2 ml cold 70% ethanol (-20°C) and kept on ice for at least 30 min. Cells were washed once in D-PBS and counted. An aliquot of 1x10⁶ cells was incubated in D-PBS, 100 µg/ml RnaseA for 30 min at 37°C, washed again and then resuspended in 500 µl D-PBS contains 50 µg/ml propidiumiodid. Samples were kept 10 min on ice in the dark and then analyzed by FACS by reading on cytometer at 488 nm.

3.2.5 β-galactosidase staining

Cells were seeded on cover slips situated in six well plates. After two days cells were washed with D-PBS and fixed for 5 min in 3% formaldehyde at RT. Cells were washed and incubated at 37°C in the absence of CO₂ with fresh prepared Senescence Associated 5-Brom-4-chlor-3-indoxyl-β-D-galactopyranoside (X-gal) Stain Solution (1 mg /ml X-gal, 40 mM citric acid/sodium phosphate, pH 6.0, 5 mM potassium ferrocyanide, 5 mM potassium ferricyanide, 150 mM NaCl, 2 mM MgCl₂). Cells were incubated for 8-10 hours and then the cover slips were mounted on standard slides and examined under microscope by phase contrast.

3.3 Microscopy

3.3.1 Fluorescence microscopy

Epifluorescent images were acquired using an inverted microscope equipped with a cooled charge-coupled device camera. For observation of living cells, they were grown and inspected in CO₂-independent medium (see 2.3.3) using live-cell chambers to keep the cells at 37 °C.

3.3.2 Confocal microscopy

Confocal imaging of living cells were performed at 37 °C with a Zeiss LSM 510 inverted confocal laser scanning microscope built into a Zeiss incubator XL and a 63x/1.4 NA oil-immersion objective. Cells were grown in CO₂-independent medium and kept at 37 °C during microscopy.

For visualization of mitochondria, cells were incubated for 5 min with 10 nM MitoTracker Red CMXRos (Invitrogen) and then washed twice with D-PBS and once with fresh medium.

3.4 Proteins analysis

3.4.1 Preparation of mitoplasts

Cells from four confluent 175 cm² tissue culture flasks were harvested and washed with D-PBS. Henceforth all steps were performed on ice. The cell pellet was resuspended in 10 ml mitochondria isolation Buffer (MIB; 0.3 M sucrose, 1 mM EGTA, 5 mM Mops, 5 mM KH₂PO₄, 1 mg/ml BSA, pH 7.4) supplemented with 0.1 mg/ml digitonin, a detergent disrupting all cellular membranes except the inner mitochondrial membrane. After an incubation time of 10 min, the samples were homogenized with 20 strokes in a Dounce homogenizer and centrifuged twice at 2600 g for 7 min at 4°C to pellet unlysed cells and nuclei. The supernatant fraction, consisting of the whole cytosolic fraction, was centrifuged at 15000 g for 10 min at 4°C to pellet mitoplasts. Pelleted mitoplasts were finally resuspended in 0.2 ml MIB without digitonin, aliquoted and stored at – 80°C.

The protein content within mitoplasts fraction was determined by BCA protein assay according to manufacturer's protocol.

3.4.2 Preparation of whole cells lysates

3x10⁶ cultured cells were pelleted, washed and resuspended in 100 µl D-PBS. Cell lysis was performed by addition of 100 µl of 2-fold lysis buffer (250 mM Tris-HCl, pH 6.8, 2% Glycerol, 4% SDS, 20 mM DTT, 1.4 M Urea, 20 mM EDTA, 2 mM PMSF, 5 mM pefa block, 0.04% bromphenol blue) and homogenised by exposure to ultrasound for 15 s by power 20%. Subsequently, samples were boiled (98°C, 5 min), warm aliquots equivalent to 3 x 10⁵ cells were then loaded into the slots of SDS-polyacrylamide gels and electrophoresis was started immediately.

3.4.3 Preparation of mitoplast lysates

Mitoplast lysates were prepared by addition of an equal volume of 2-fold lysis buffer (see 3.4.2) and kept on ice. Samples were normally boiled (98°C, 5 min) and warm loaded. Exceptionally, for the analysis of respiratory chain proteins, mitoplast lysates were not heated prior to electrophoresis.

3.4.4 Polyacrylamide gel electrophoresis

3.4.4.1 Gel run

Electrophoresis was performed in 1X TGS buffer or in 1X MOPS SDS running buffer (in the case of NuPAGE Gels) at 50-150 V.

3.4.4.2 Blotting

After separation, proteins were electrophoretically transferred from the gel to a PVDF membrane by the semi-dry method. Briefly, five 3MM paper filters soaked in K-buffer (70 mM CAPS-NaOH pH 10.5, 10% MeOH) were stacked on the cathode side of the gel, whereas the PVDF membrane soaked in MeOH, one 3 MM paper filter soaked in A2-buffer (25 mM Tris-HCl pH 10.4, 20% MeOH), and two paper filters soaked in A1-buffer (300 mM Tris-HCl pH 10.4, 20 % MeOH) were stacked on the anode side of the gel. Subsequently, the stack was placed between two graphite plates and 0.8 mA/cm² were applied for 1-2,5 h (depending on the size of the protein of interest).

3.4.4.3 Western Blot

After blotting, the PVDF membrane was soaked in D-PBS (140 mM NaCl, 2.7 mM KCl, 10 mM Na₂HPO₄ 2H₂O, 1.8 mM KH₂PO₄), containing 0.05% Tween 20 and 5% Milk powder and incubated overnight at 4°C. After blocking the membrane was briefly washed with D-PBS, 0.05% Tween 20 and incubated for 1 h with the primary antibody diluted in D-PBS, 0.05% Tween 20, 1% BSA and washed four times (1 x 5 min, 3 x 10 min). The membrane was then incubated for 1 h with the secondary antibody (peroxidase conjugated) diluted in D-PBS, 0.05% Tween 20, 1% BSA. The membrane was then washed as above and the protein bands labelled by the secondary antibody were visualized by chemiluminescence using the ECL Plus system (Amersham).

3.4.5 Catalytic activity of topoisomerase I

3.4.5.1 Mitoplast protein extracts

Mitoplast were extracted for 10 min on ice in MIB containing 500 mM NaCl and 0.1% triton. Mitoplast extracts was cleared by centrifugation (15000 g, 10 min, 4°C) and the protein concentration was determined by BCA protein assay according to manufacturer's protocol.

3.4.5.2 Relaxation assay

Mitoplast extracts (170 ng) were incubated for various times at 37°C with 0.4 µg supercoliled pUC18 in a final volume of 20 µl assay buffer (120mM KCl, 50 mM Tris-HCl, pH 7.9, 10 mM MgCl₂, 0.5 mM DTT, 0.5 mM EDTA, 30 µg/ml BSA). The reaction was stopped by addition of SDS (0.5%) and subsequently digested with Proteinase K (1 mg/ml, 30 min, 50°C). Finally samples were subjected to agarose gel electrophoresis and separated overnight at 0.5 V/cm in the absence of EtBr.

3.5 MtDNA analysis

3.5.1 Quantification of mtDNA copy number and mtDNA deletions

3.5.1.1 DNA extraction

Total DNA from 5x10⁶ cells was isolated using the "DNeasy Mini kit" (Qiagen) according to the manufacturer's protocol. DNA concentration was determined using spectrophotometer by absorbtion at wavelenghts of 260 nm.

3.5.1.2 Quantitative Real-Time PCR (qPCR)

MtDNA copy number was determined according to the quantitative TaqMan-PCR method. TaqMan Real-time PCR measures the accumulation of PCR products using a dual-labelled fluorogenic probe during the exponential stages of the PCR. A fluorescent reporter and a quencher are covalently attached to the 5'- and 3'-ends of the probe. The close proximity between fluorophore and quencher inhibits fluorescence from the fluorophore. During PCR, the 5' to 3' exonuclease activity of Taq polymerase degrades the proportion of the probe that has annealed to the template. Degradation of the probe releases the fluorophore allowing fluorescence

emission of the reporter dye. Hence, fluorescence detected in the real-time PCR thermal cycler is directly proportional to the amount of DNA template present in the PCR. Template DNA was diluted to a concentration of 10 ng/ μ l in PCR water. 100 ng total DNA were subjected to amplification reactions performed as 25 μ l duplicates in a 96-well microplate with 1X Platinum SYBR Green qPCR SuperMix-UDG with ROX (Invitrogen) and forward and reverse primer. To determine the abundance of mtDNA in the sample, amplification was performed in parallel with different concentrations of standard plasmids to allow the generation of a calibration curve.

PCR setting per reaction (25 μ l)

Component	Volume	Final concentration
DNA template (10 ng/ μ l)	10 μ l	100 ng
Primer Forward	0.125 μ l	500 mM
Primer Reverse	0.125 μ l	500 mM
2X Platinum SYBR Green qPCR SuperMix-UDG with ROX	12.5 μ l	1X
H ₂ O	2.25	/

Quantification of DNA copies analysis was carried out in an ABI PRISM 7000 Sequence Detector (Applied Biosystems) under the following conditions:

Denaturation	10' 95°C	40 cycles
Denaturation	15" 94°C	
Anealing and Elongation	1' 60°C	

Quantification of mtDNA copies was carried out using the primers IS-F and IS-R, binding to unique mtDNA sequences (Table 3.4). Quantification of the common deletion (CD) and 284 deletion were performed using the primers CD-F and CD-R and D284-F and D284-R, respectively (Table 3.6). The primers amplified the sequence spanning the deletion positions. In deleted mtDNA molecules, these primers come close enough to synthesize a PCR product within the given extension time, whereas in no deleted mtDNA the distance between the primers is too long.

Primer	Sequence	Mach
IS-F	5'- TTGACTCACCCATCAACAACC -3'	mtDNA 16091-16111
IS-R	5'- AATATTCATGGTGGCTGGCAGTA -3'	mtDNA 16130-16152
CD-F	5'- ACCCCCATACTCCTTACACTATTCC-3'	mtDNA 8417-8441
CD-R	5'- AAGGTATTCCTGCTAATGCTAGGCT-3'	mtDNA 13485-13509
D284-F	5'- TACCCCCTCTAGAGCCCACT-3'	mtDNA 8291-8310
D284-R	5'-GTAGCTTTGGCGTTTGTAT-3'	mtDNA 13541-13559

Table 3.6

3.5.2 Southern Blot

3.5.2.1 DNA preparation

For Southern blotting 3 µg of total genomic DNA was digested overnight with Bgl II, Dra III, Mlu I, and Not I, restriction enzymes that not cut mtDNA. As positive control, each probe was further treated with 5 ng recombinant human Top1 overnight at 37°C. Reactions were stopped by adding 0.5% SDS and proteinase K (1 mg/ml, 37°C, 60 min). DNA was recovered by ethanol precipitation and separated in an agarose gel.

3.5.2.2. DNA separation and transfer

DNA was run on large 0.6% agarose gels overnight in 1X TBE buffer. Gel electrophoresis was carried out by 0.5 V/cm in the absence of EtBr, to separate various (relaxed, supercoiled) mtDNA forms. After separation, the gel was depurinated in 0.25 M HCl for 30 min and following denaturated in 0.4 N NaOH for 20 min at RT with gently shaking. Gel was blotted by alkaline transfer overnight onto a "Hybond-N+ nylon membrane" (Amersham) using 0.4 N NaOH. After the transfer, the membrane was dried on a sheet of filter paper and DNA was fixed by baking for 30 min at 80°C.

3.5.2.3. Probe generation

Southern hybridization was performed with probes for COXI (nts 5970-6459), inserted in the pCR2.1-TOPO vector (see 2.1.3). The relevant restriction fragment was generated by EcoRI digestion and gel-purified. Concentration of the eluted probe was estimated to be 70% of the first step.

3.5.2.4. Labelling and hybridization

Labelling of the probes and signal detection were carried out using the chemiluminescence based “ECL direct nucleic acid labelling and detection system” (Amersham) according to manufacturer’s protocol. Probes were denatured at 100°C for 5 min and cooled on ice for further 5 min. The “DNA labelling reagent” was immediately added to the cooled DNA, where positively charged peroxidase molecules form a loose attachment to the nucleic acid by charge attraction. Addition of glutaraldehyde induces chemical cross-links, so that the probe is covalently labelled with peroxidase. Once labelled, 200 ng probe was used for hybridization with target DNA immobilized on a approximately 6 cm x 11 cm membrane.

Blots were prehybridized for 1 h at 42°C with rotation in hybridization buffer containing 5% (w/v) blocking reagent and 0.5 M NaCl followed by addition of the labelled probe directly to the hybridization buffer and incubation was continued overnight. After hybridization, blots were washed (once 20 min, twice 10 min) with primary wash buffer containing urea (6 M Urea, 0.4% SDS, 0.5 x SSC) at 42°C, followed by two washes at RT with 2X SSC. Hereafter blots were subjected to detection.

3.5.3 Analysis of mitochondrial transcripts

3.5.3.1 Total RNA isolation

Total RNA from 5×10^6 cultured cells was isolated with “RNeasy Mini Kit” (Qiagen) according to the manufacturer’s protocol. RNA concentration was determined by measuring absorption at wavelength of 260 nm.

For quality assurance the RNA integrity was determined with the “Agilent 2100 Bioanalyzer” (RNA 6000 NanoChip, Agilent Technologies) with kind support from the BMFZ.

3.5.3.2 Semiquantitative analysis of mtDNA transcripts: Northern Blotting

Denaturing agarose gel electrophoresis

For the analysis of mtRNAs 2-5 µg of total RNA was diluted in RNase-free water. The samples were denatured by addition of 5X RNA loading buffer (see 2.4.) and incubated at 65°C for 5 min. Samples were briefly chilled on ice and loaded on a denaturing 1.2% agarose gel containing 0.667 % formaldehyde, 1X MOPS running buffer (see 2.4) and 50 µg/ml EtBr. Gel runs in 1X MOPS running buffer containig

2.5 M formaldehyde at 7 V/cm until the bromphenol blue dye has migrated approximately 2/3 of the way through the gel.

Transfer

Immediately after electrophoresis, gel was first soaked in RNase-free water for 10 min, then for 10 min in 10x SSC. RNA was transferred to a nitrocellulose membrane by overnight capillary transfer using 20X SSC. After the transfer, the membrane was briefly washed in 10X SSC and dried on a sheet of filter paper. RNA was fixed by baking for 30 min at 80°C.

Preparation of the probes, labelling and hybridisation were carried out as described for Southern blots (3.5.2.).

3.5.3.3 Quantitative analysis of mtDNA transcripts: Real-Time Reverse-Transcription PCR (qRT-PCR)

Quantitative measurement of mtDNA transcripts was performed with qRT-PCR using “OneStep RT-PCR Kit” (QIAGEN) that allows both reverse transcription and PCR to take place successively in a single tube.

As in the case of qPCR, qRT-PCR reactions were performed as 25 µl duplicates in a 96-well microplate. To 5 ng total RNA template was added the Mastermix, consisting of RT-PCR Master Mix, for the reverse transcription of RNA into cDNA, QuantiTect SYBR Green, for the detection of PCR product accumulation, forward and reverse primer (Table 3.7).

PCR setting per reaction (25 µl)

component	Volume	Final concentration
RNA template (500 pg/µl)	10 µl	5 ng
Primer Forward	0.125 µl	500 nM
Primer Reverse	0.125 µl	500 nM
2X QuantiTect SYBR Green	12.5 µl	1X
RT-mix	0.25 µl	0.25 µl/ reaction
H ₂ O	2 µl	/

For quantification, standard plasmids were used (see 2.1.3). Background fluorescence, e.g. from residual mtDNA, was subtracted as for each sample at least one PCR reaction was performed without the RT-PCR Master Mix. RNA levels of the transcripts were normalized to the level of 18S rRNA.

The thermal cycling conditions included a reverse transcription step of 30 min at 50°C, followed by a heating step of 10 min at 95°C for the deactivation of the reverse transcriptases and the activation of DNA polymerase. PCR amplification was performed with 40 cycles under followings conditions:

Primers T_m 58°C		Primers T_m 80°C	
Denaturation	20" 94°C	Denaturation	15" 95°C
Annealing	20" 57°C	Annealing and elongation	1' 60°C
Elongation	30" 72°C		

Oligonucleotides used as PCR-primers

Primer	Sequence	T_m (°C)
COXI F	5'-TACCTATTATTCGGCGCATGAGCTGGA	80
COXI R	5'-TGCATGGGCTGTGACGATAACGTTGTA	80
12S F	5'-GGTTGGTCAATTTTCGTGC	58
12S R	5'-GAGTTTTTTACAACCTCAGGTG	58
16 S F	5'-AGCCACCAATTAAGAAAGCG	58
16 S R	5'-GCTTATGCGGAGGAGAATG	58
Splice site before COXI F	5'-CCCCTGTCTTTAGATTTACAGTCCAATG	80
Splice site before COXI R	5'-CCGAATAATAGGTATAGTGTTCCAATGTC	80
Splice site after COXI F	5'-ACCTGGAGTGACTATATGGATGCCCC	80
Splice site after COXI R	5'-GAGGCCATGGGGTTGGCTTGAAAC	80
18S F	5'-ATTAGAGTGTTCAAAGCAGGCCCGAGC	80
18S R	5'-CGTCCCTCTTAATCATGGCCTCAGTTC	80
18S short F	5'-GTCCAAAGCAGGCCCGAG	58
18S short R	5'-CCCTCTTAATCATGGCCTC	58

Table 3.7

3.5.3.4 Quantitative analysis of nuclear transcripts for mitochondria-targeted proteins

Quantitative measurements of nuclear transcripts for mitochondrial proteins were performed with qRT-PCR as described above, using the primers listed in Table 3.8. PCR amplification of SDHB cDNA was performed under the same conditions described for mtDNA transcripts (primers T_m 80°C). PCR amplification of Top1mt cDNA was performed with 40 cycles under followings conditions:

Denaturation	15" 95°C
Annealing	1' 60°C
Elongation	1' 72°C

Primer	Sequence	T_m (°C)
SDHB F	5'-AGTTGACTCTACTTTGACCTTCCGAAG	80
SDHB R	5'-GACCTTATTGAGGTTGGTGTCAATCCT	80
Top1mt F	5'-GGAAATGAAGACGAGACAGC	60
Top1mt R	5'-GGAGGGAACAGCAGCCCAC	64

Table 3.8

3.6 Investigation of mitochondrial functions

3.6.1 Mitochondrial reactive oxygen species (ROS) production

Measuring of reactive oxygen species was carried out using MitoSOX Red reagent (invitrogen), a cell-permeant fluorogenic dye for highly selective detection of superoxide in the mitochondria. Once in the cell, MitoSOX is rapidly targeted to the mitochondria, where it is oxidized by superoxide and exhibits red fluorescence.

Cells were grown till 80% confluence and loaded with 5 μ M MitoSOX in medium for 30 min at 37°C. Cells were trypsinized, washed and resuspended in HBSS (see 2.4) containing 1% BSA at a density of 1 x10⁷ cells/ml.

Fluorescence was monitored by flow cytometry. MitoSOX was excited by laser at 488 nm and the data collected at FL2 channel. Since YFP and MitoSOX signals could

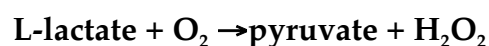
not be completely separated at the chosen FACS settings, the intensity without MitoSOX for each cell clone was measured and subtracted from signal with MitoSOX. Mitochondrial superoxide generation was increased by addition of 100 μ M Antimycin A inhibiting the complex III of the respiratory chain.

3.6.2 Mitochondrial respiration

To determine oxygen consumption rate in intact cells, cells were harvested, counted and resuspended at a density of 3.5×10^6 /ml in respiration medium. O_2 consumption rate was measured for 3.5×10^6 intact cells using a Clark oxygen electrode.

3.6.3 Lactate production

For the quantification of lactate levels 1×10^6 cells were seeded in a 25 cm² culture flask. After 48 hours the medium was removed and first cleared by centrifugation then transferred to BD vacutainer tubes for lactate-quantification, contain 5 mg Na-Fluorid and 4 mg K-Oxalat. To adjust the differences in growth rate among different cell-clones, cells were counted and lactate levels were normalized to the cells number. Lactate concentration was assayed in an automated blood analyzer. The method uses an enzymatic reaction, catalized by the lactate oxidase, to convert lactate to pyruvate:



The hydrogen peroxide produced by this reaction is then used by the enzyme peroxidase to generate a detectable colored dye



The intensity of the colour formed is then proportional to the L-lactate concentration.

3.7 Statistics

Quantitative results are represented as mean values \pm standard error of the mean of measurements carried out in duplicate or triplicate on independent cell clones expressing the same construct. Data sets were compared by an unpaired T-test and the null hypothesis was rejected on a probability level of <0.05 (i.e. $P < 0.05$ was considered significant).

4. Results

4.1 Deregulated Top1mt expression

The mtDNA is a circular duplex molecule, which needs to be transcribed, replicated, and repaired and in mitochondria topoisomerases probably support these processes. All three topoisomerase subfamilies present in the vertebrate cell nucleus (IA, IB, and IIA) are also represented in mitochondria but only Top1mt is genetically independent of its nuclear variant. The presence of an orthologous gene for Top1mt in all vertebrates indicates a certain importance of Top1mt activity. On the other hand, this could suggest the need of a strict regulation of this protein. Therefore, it is possible that unregulated expression of Top1mt can have an adverse effect on the mtDNA metabolism or stability and, consequently, on mitochondrial function.

To assess this question, Top1mt was overexpressed in human cells and the effects of such a deregulated Top1mt expression on mtDNA stability and mitochondrial functions *in vivo* was investigated.

4.1.1 Mitochondrial targeting of transgenic Top1mt variants

For studying the effects of chronic, deregulated Top1mt expression, the Top1mt gene was placed under control of the CMV-promoter (Fig 4.1.1. construct b). To monitor cellular localisation of the transgenic Top1mt, the full-length and the inactive variant of Top1mt were fused in frame to the sequence of YFP. Since the N-terminal fusion of YFP should disturb the endogenous MTS of Top1mt, the targeting of chimera-proteins was re-established by fusion with the MTS of cytochrome C oxidase-subunit VIII (Rizzuto et al, 1995), generating MTS-YFP-Top1mt and MTS-YFP-Top1mt^{Y559F}, respectively (Fig 4.1.1, constructs c and d). The latter construct served as control for a DNA binding protein that cannot cut and manipulate DNA. MTS are N-terminal signal peptides that enable the import of proteins to the mitochondria. Most mitochondrial proteins are synthesized as cytosolic precursors containing MTS. After the import into the mitochondrial matrix, the presequences are cleaved off by a protease called mitochondrial-processing peptidase (MPP). In the tracking system described above, YFP is positioned in front of the endogenous MTS of Top1mt.

Therefore, the fluorescent tag could be cleaved away by MPP after import of the chimera into the mitochondria, generating wild type Top1mt. To bypass this potential problem I created an additional chimera, in which Top1mt lacks the first 41 amino acids and, hence, its own MTS and the predicted cleavage site for MPP (MTS-YFP-Top1mt⁴²⁻⁶⁰¹, fig 4.1.1. construct e). The basic vector MTS-YFP, encoding for mitochondria-targeted YFP alone served as control for a non-DNA-binding protein (Fig 4.1.1. construct a).

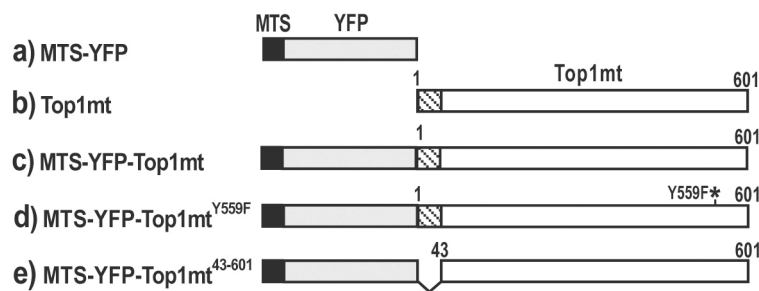


Figure 4.1.1. Mitochondrial targeting of Top1mt variants. Schematic of the constructs studied in this section. Mitochondrial targeting of construct a, c, d and e relied on the MTS of cytochrome C oxidase subunit VIII (black), whereas the endogenous MTS of Top1mt (striped box) ensures the mitochondrial localization of construct b.

Transfection of human HT-1080 cells with these constructs and subsequent puromycin selection resulted in the rise of clones, showing gross morphology and growth rates similar to the parental cell lines. For each construct 30 cell clones were isolated and expanded.

Cell clones expressing untagged Top1mt were first screened for increased Top1mt mRNA levels, using qRT-PCR. Positives clones showed 10-50-fold more Top1mt messenger than untransfected cells. Clones, expressing YFP-tagged Top1mt variants, were first screened using fluorescent microscopy and only the clones showing the expected mitochondrial YFP-fluorescence were further investigated. To verify the integrity of the expressed proteins cells lysates of selected clones were subjected to western blotting (Fig.4.1.2.). The blot of cells overexpressing Top1mt was probed with Top1mt antibody detecting the presence of overexpressed Top1mt at expected size in several clones (Fig.4.1.2.A). Blots of clones expressing YFP-tagged Top1mt variants were probed with YFP antibody (Fig. 4.1.2, B, C and D). In clones expressing all three constructs, I detected proteins corresponding to the chimera at the expected size and an additional band similar in size to YFP alone (~30 kDa). This additional band suggested that all YFP-tagged Top1mt variants were subjected to a certain proteolytic turnover inside the mitochondria, leading to the removal of YFP from a

fraction of the chimera. Interestingly, the additional 30 kDa band is the same in MTS-YFP-Top1mt, MTS-YFP-Top1mt^{Y559F} and MTS-YFP-Top1mt⁴²⁻⁶⁰¹ expressing clones (Fig. 4.1.2.2 compare B, C and D). Since cleavage of YFP affected also the Top1mt variant lacking its endogenous MTS and MPP recognition site (Top1mt⁴²⁻⁶⁰¹), the proteolytic product was probably not generated by MPP cleaving. Since the endogenous MTS did not enhance the removal of YFP, all further investigations were performed using full-length Top1mt variants (MTS-YFP-Top1mt and MTS-YFP-Top1mt^{Y559F}).

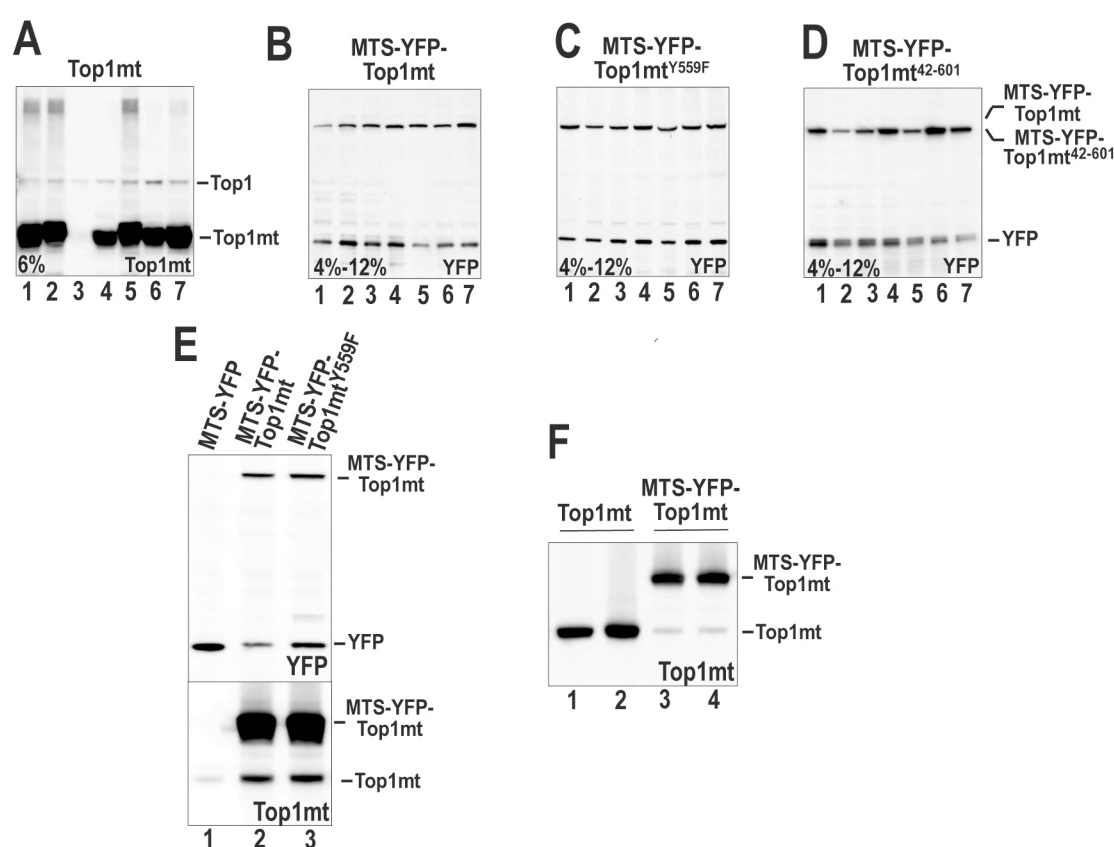


Figure 4.1.2. Generation of clones expressing transgenic Top1mt variants. Western blots analysis of lysates from whole cells (A, B, C and D) or isolated mitoplasts (E and F). Blots were probed with Top1mt antibodies (A, E lower panel and F) or antibodies against YFP (B, C, D, E upper panel). Screening of seven representative clones raised from transfection of Top1mt, MTS-YFP-Top1mt, MTS-YFP-Top1mt^{Y559F} and MTS-YFP-Top1mt⁴²⁻⁶⁰¹ were shown in A, B, C and D respectively. In E mitoplasts lysates from one representative clone expressing MTS-YFP, MTS-YFP-Top1mt and MTS-YFP-Top1mt^{Y559F} are shown. 70% less lysate was loaded in lane 1 of the YFP stained blot (top), since expression levels of MTS-YFP is higher than MTS-YFP-Top1mt and MTS-YFP-Top1mt^{Y559F}. In F expression levels of Top1mt and MTS-YFP-Top1mt are compared in two representative clones overexpressing Top1mt (lanes 1 and 2) or expressing MTS-YFP-Top1mt (lanes 3 and 4). Positions of YFP fusion proteins and untagged Top1mt are indicated on the right margin.

To assess the targeting of overexpressed Top1mt and corresponding YFP-chimera to the mitochondrial matrix and to compare their relative expression levels, I subjected isolated mitoplasts (mitochondrial matrix surrounded by inner mitochondrial membrane) to Western blotting and probed these with Top1mt and YFP antibodies (Fig. 4.1.2.2 E and F). Western blots of YFP-tagged Top1mt variants are shown in figure 4.1.2.2.E. whereas a comparison of Top1mt overexpression and MTS-YFP-Top1mt expression of two representative clones each is presented in figure 4.1.2.F. The same band pattern in extracts from whole cells and isolated mitoplasts confirmed that the removal of the YFP tag from a fraction of the chimera occur in the mitochondria (compare Fig. 4.1.2.B and C with Fig. 4.1.2.E upper blot). Levels of untagged Top1mt were elevated in clones expressing MTS-YFP-Top1mt or MTS-YFP-Top1mt^{Y559F} in comparison to clones expressing MTS-YFP (Fig.4.1.2.E bottom blot). This, together with the additional band in the YFP stained blot (Fig.4.1.2.E upper blot), indicates that the YFP tag is proteolytically removed from a fraction of both YFP-tagged Top1mt variants. However, comparison within each lane indicates that most of the expressed enzymes are YFP-fused. Thus, I could safely assume that all cell clones selected for further studies expressed the desired protein species in the mitochondrial matrix at similar levels allowing the comparison of data between cells expressing the various constructs.

Taken together, I generated cell clones heterologously expressing wild type and YFP-tagged variants of Top1mt. These clones were analyzed with respect to the influence of increased Top1mt levels on mtDNA. Moreover, fusion of Top1mt with YFP allowed me to identify its distribution in live cells. However it was critical first to determine whether the heterologously expressed proteins were catalytic active.

4.1.2 Deregulated expression of Top1mt increases topoisomerase I activity in mitochondria

The catalytic activity of topoisomerase I can be assessed *in vitro* by measuring its ability to relax a supercoiled DNA substrate. Topoisomerase I generates several topological forms (topoisomers) from the substrate depending on the number of superhelical-turns released. In agarose gel electrophoresis, compact supercoiled DNA migrates faster than relaxed DNA, allowing the separation and visualization of the DNA topoisomers.

To test the biochemical activity of wild type and YFP tagged variants of Top1mt heterologously expressed in mitochondria, I measured the DNA relaxation activity in salt extracts of isolated mitoplasts (Fig. 4.1.3). Mitoplast extracts from cells expressing the control construct (MTS-YFP) or the catalytically inactive Top1mt (MTS-YFP-Top1mt^{Y559F}) exhibited only a weak DNA relaxation activity provided by the endogenous Top1mt (Fig. 4.1.3.A and D). After 128 min incubation time, ~50% of the substrate was relaxed. Equivalent amounts of mitoplast extracts from cells overexpressing Top1mt and expressing MTS-YFP-Top1mt displayed a higher ability to relax supercoiled plasmid substrate. Here only 8 and 16 min incubation time was required to relax ~50% of the substrate (Fig. 4.1.3.B and C). This indicates that Top1mt as well as MTS-YFP-Top1mt were expressed as catalytically active forms since they enhanced the overall DNA relaxation activity extracted from the mitochondrial matrix. This increase in activity fitted the relative abundance of heterologous Top1mt proteins versus endogenous Top1mt protein shown in figure 4.1.2.E (compare lanes 1 and 2). Notably, although the expression levels of heterologue wild type and YFP tagged Top1mt was very similar (Fig.4.1.2.F compare lanes 1 and 2 with lanes 3 and 4), mitochondrial extracts from cells overexpressing Top1mt showed a higher relaxation activity compared to extracts from cells expressing MTS-YFP-Top1mt. Therefore, it is possible that the N-terminal fusion of Top1mt with YFP affects the catalytical properties of Top1mt.

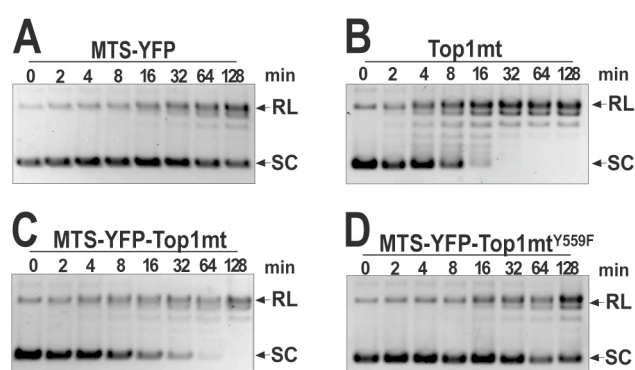


Figure 4.1.3. Mitochondrial targeting of transgenic Top1mt variants increases DNA-relaxation activity in mitochondria. 170 μ g of mitoplast extracts prepared from clones expressing MTS-YFP (A), Top1mt (B), MTS-YFP-Top1mt (C) and MTS-YFP-Top1mt^{Y559F} (D) were incubated with 0.4 μ g supercoiled pUC18 DNA at 37 °C for the time intervals indicated above. Position of relaxed (RL) and supercoiled (SC) plasmid forms is indicated on the right margin. Time points 0 min is DNA not exposed to mitochondrial extract.

Having established that the heterologously expressed proteins were targeted to the mitochondrial matrix and were fully catalytically active, I could proceed to analyse the consequences of these on mtDNA functions.

4.1.3 MTS-YFP-Top1mt associates with mitochondrial nucleoids without changing the overall topological state of mtDNA

Next, we monitored the cellular localisation of the heterologously expressed enzymes by confocal microscopy (Fig. 4.1.4.A). Comparison of MitoTracker images (right column) of untransfected cells (bottom row), and cells stably expressing MTS-YFP (top row), MTS-YFP-Top1mt (middle top row) or MTS-YFP-Top1mt^{Y559F} (middle bottom row) showed no difference in gross morphology of the mitochondrial compartment, which formed a largely connected reticulum, typically found in living mammalian cells (Rizzuto et al, 1998). This observation allowed me to exclude major effects on mitogenesis or the mitochondrial fusion/fission equilibrium. Comparison of YFP (right middle column) and MitoTracker (right column) within the same cell showed a complete overlap of fluorescent signals in the case of MTS-YFP expressing cells (top row), indicating that MTS-YFP is completely imported into mitochondria and then freely distributed in the entire mitochondrial matrix. MTS-YFP-Top1mt (middle top row) and MTS-YFP-Top1mt^{Y559F} (middle bottom row) were also exclusively localized in the mitochondrial compartment. However, they were not homogeneously distributed but rather accumulated at speckled sub-structures within the mitochondria (arrows, right middle column). It should be noted that frequency and intensity of these foci varied between individual cells within the same culture. Moreover, such foci were less apparent and less frequent for the active site mutant, where they were hardly detectable in some cells, suggesting that catalytic activity is not essential for, but to some extent stimulates, punctuate sub-mitochondrial localization of Top1mt.

The speckled distribution of MTS-YFP-Top1mt and MTS-YFP-Top1mt^{Y559F} in mitochondria is highly reminiscent of the staining of nucleoids (Ashley et al, 2005). These are foci within the mitochondrial matrix, where several copies of mtDNA are packaged together forming discrete mtDNA-protein complexes. To determine if MTS-YFP-Top1mt and MTS-YFP-Top1mt^{Y559F} foci represent nucleoid association we used immunocytochemistry with DNA-directed antibody (Fig. 4.1.4.B). Importantly, appearance and distribution of nucleoids in untransfected cells was identical to that found in cells stably expressing MTS-YFP, MTS-YFP-Top1mt or MTS-YFP-Top1mt^{Y559F}, suggesting that expression of these proteins has no negative effect on nucleoid composition. Comparison of nucleoids and YFP distribution in merged images show that all MTS-YFP-Top1mt and MTS-YFP-Top1mt^{Y559F} foci were positive for DNA, whereas the YFP signal showed no accumulation at several dots stained by

the DNA antibody.

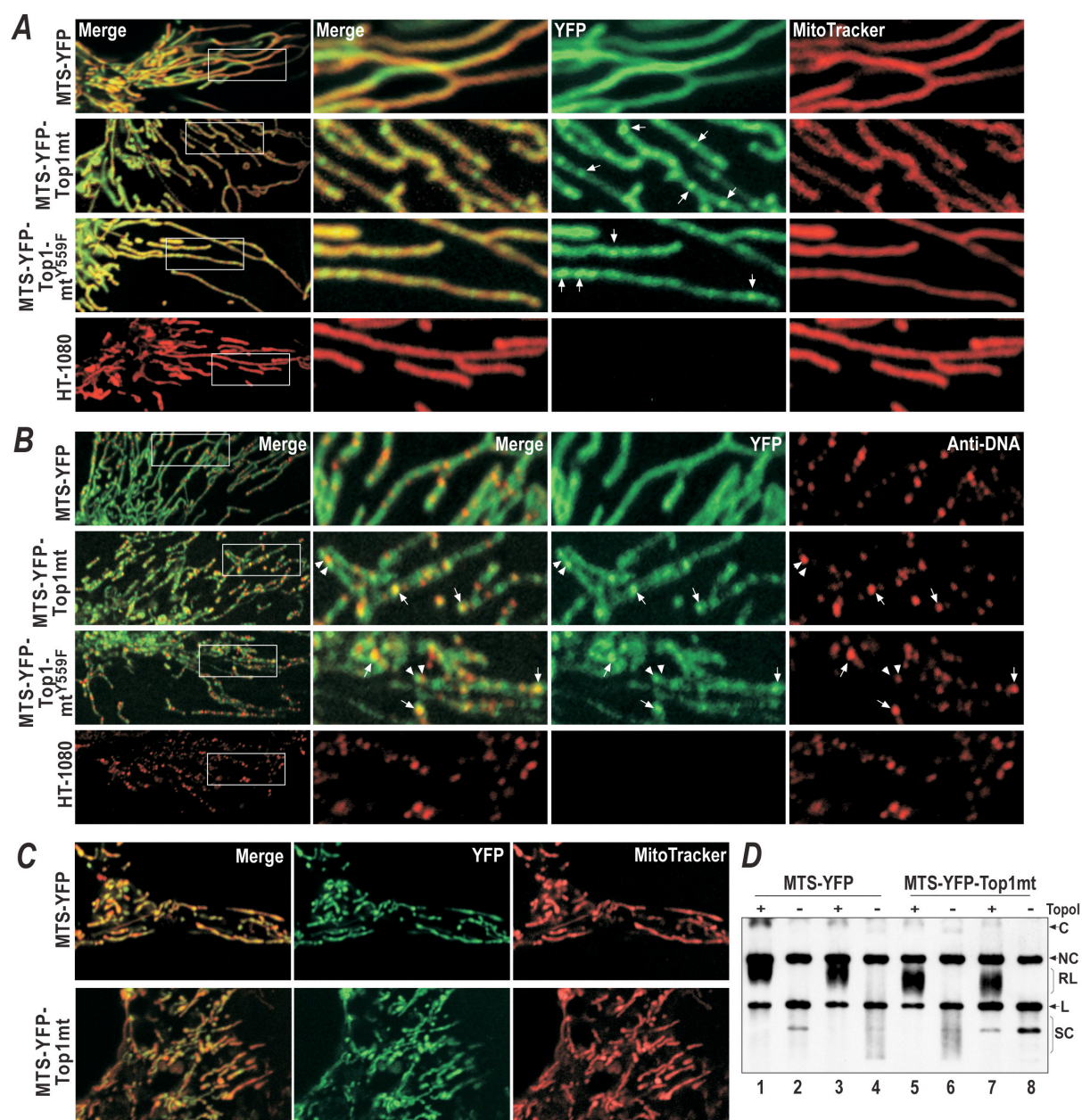


Figure 4.1.4. MTS-YFP-Top1mt is associated with mitochondrial nucleoids but does not affect overall topology of mtDNA. **A**) Confocal images of live clones stably expressing MTS-YFP (top), MTS-YFP-Top1mt (middle top), MTS-YFP-Top1mt^{Y559F} (middle bottom) and untransfected HT-1080 cells (bottom). Shown are images of YFP fluorescence (middle right), mitochondria-specific Mito Tracker Red fluorescence (right), and merged signals of both (left and middle left). The leftmost column shows a larger view of the cell where outlined boxes are enlarged 3-fold in detail images. MTS-YFP-Top1mt and MTS-YFP-Top1mt^{Y559F} foci are marked by arrows. **B**) The same cell clones as in A were fixed and counterstained with antibodies against DNA. Antibody-derived fluorescence is shown right. **C**) Confocal images of live 143B- ρ^0 cells transiently expressing MTS-YFP (top), MTS-YFP-Top1mt (bottom). Shown are images of YFP fluorescence (middle), Mito Tracker Red fluorescence (right), and merged images (left). MTS-YFP-Top1mt and MTS-YFP-Top1mt^{Y559F} foci positive or negative for mtDNA are marked by arrows or arrowheads, respectively. **D**) Overall topology of mtDNA. Total genomic DNA from cell clones expressing MTS-YFP (lanes 1-4) or MTS-YFP-Top1mt (lanes 5-8) was fractionated on a 0.5% agarose gel without EtBr, blotted and hybridized against a COXI probe. DNA from each clone was either left untreated (-) or pretreated with recombinant Top1 (+). Positions of catenanes (C), nicked (NC), relaxed (RL), linear (L) and supercoiled (SC) DNA topoisomers are indicated. Immunostains in A) and B) were performed by Stefan Sobek.

MTS-YFP-Top1mt lost its focal distribution and spread uniformly in the mitochondrial matrix, when transiently expressed in cells without mtDNA (ρ^0 cells) (Fig. 4.1.4.C). Together these results indicate that Top1mt associate with mtDNA.

Given the association of Top1mt with nucleoids shown in Figure 4.1.4.B and the known fact that mtDNA exists in various topological states (Pohjoismaki et al, 2006), I was curious whether the increase in mitochondrial DNA relaxation activity due to expression of MTS-YFP-Top1mt affected the overall topology of mtDNA. To address this question, I compared mtDNA topology between cell clones expressing MTS-YFP-Top1mt or MTS-YFP alone. For this purpose, purified genomic DNA (nuclear DNA and mtDNA) digested with restriction nucleases not cutting mtDNA was subjected to Southern blots and probed with mtDNA specific probes. (Figure 4.1.4.D). Several topological forms of mtDNA can be separated performing agarose gel electrophoresis in the absence of EtBr. In agreement with published data (Pohjoismaki et al, 2006), I observed a distribution of mtDNA into catenated (C), nicked (NC), linear (L), and supercoiled (SC) forms. The supercoiled form had the highest mobility and migrated as an inhomogeneous, ladder set of bands suggestive of various topoisomers. Those bands could be converted to a more homogeneous, slower migrating band by treatment with recombinant nuclear topoisomerase I confirming the relaxed state of the DNA (Figure 4.1.4.D, compare even with odd numbered lanes). However, the supercoiled portion of the mtDNA was not notably diminished in cell clones expressing MTS-YFP-Top1mt as compared to clones expressing MTS-YFP alone (compare lanes 2 and 4 with 6 and 8), and all other topological forms of mtDNA were also present in similar quantitative proportions in the two sets of cell clones. Therefore, I concluded that MTS-YFP-Top1mt activity did not significantly affect the overall topology of mtDNA at a global level.

4.1.4 Effect of increased Top1mt activity on mtDNA metabolism and mtDNA stability

Since the cell contains several copies of mtDNA (~1000 copies/cell) and their replication occurs in an asynchron manner, it is possible that only a minor fraction of these molecules are transcribed or replicated. Consequently, if enhanced Top1mt activity influences the topology of this subset of mtDNA molecules, it might have remained undetected in the analysis of the overall mtDNA topology. In fact, overexpression of several other proteins involved in mtDNA transcription and

replication have dramatic effects on mtDNA metabolism: For example, transient overexpression of TFAM in cultured cells increases mtDNA transcription (Maniura-Weber et al, 2004) but its prolonged overexpression leads to a paradoxical decrease of mtDNA transcription (Pohjoismaki et al, 2006). Moreover, transgenic mice overexpressing the mitochondrial DNA helicase Twinkle show a marked increment of mtDNA copies (Tyynismaa et al, 2004). Knowing that, I was curious to investigate the effect of Top1mt overexpression on mtDNA metabolism/ stability and the cellular consequences of that.

4.1.4.1 Deregulated Top1mt expression does not affect the mtDNA replication and stability

I investigated whether deregulated expression of Top1mt or YFP-tagged Top1mt affected maintenance and functionality of the mitochondrial genome. First, as a global measure of genome maintenance, I determined the average number of mtDNA copies per cell, using qPCR. I found that cells heterologously expressing Top1mt, MTS-YFP-Top1mt or MTS-YFP-Top1mt^{Y559F} had levels of mtDNA similar to cells expressing MTS-YFP alone (Figure 4.1.5). Therefore, enhanced mitochondrial activity of Top1mt had no significant effect on the replication rate of mtDNA. It is worth noting, that untransfected HT-1080 cells had ~20% more copies of mtDNA per cell. The ~20% decrease, however, appears to be a rather non-specific effect of cell transfection, since it also was observed in cell clones expressing YFP or YFP-fusion proteins in other cell compartments, e.g. the nucleus or the outer membrane (data not shown).

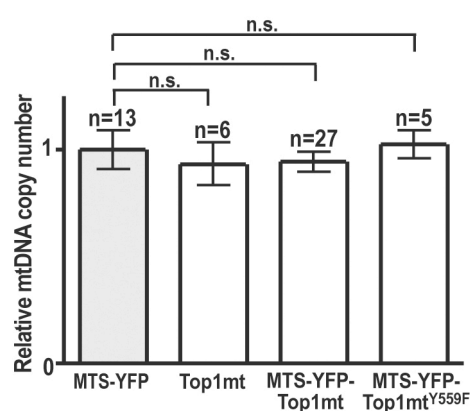


Figure 4.1.5. Mitochondrial targeting of Top1mt variants does not affect mtDNA copy number. Quantification of mtDNA copies per cell in clones expressing the constructs indicated below each column. MtDNA copies in each clone were determined using qPCR. All values were normalized to the mean value of the control clones expressing MTS-YFP (grey bar). The number of clones investigated is indicated above each bar (n) and error bars indicate the standard error of the mean (SEM). Values of each bar do not differ significantly from the control according to an unpaired T-test.

Thus, overexpression of Top1mt and expression of YFP-tagged Top1mt variants did not influence the mtDNA copy number. However, these data did not exclude that the enhanced Top1mt expression had an effect on the mtDNA stability. Defects of mtDNA replication can affect the mtDNA stability without influencing its copy number. For example, it is known that defective POLG and Twinkle induce mtDNA deletions (Trifunovic et al, 2005; Wanrooij et al, 2004), which are likely due to mtDNA replication stalling (Wanrooij et al, 2007).

To examine whether the increased Top1mt activity also affected the mtDNA stability, I quantified two already described mtDNA deletions: the 4977 bp Common Deletion (CD) (Wallace et al, 1995) and the 4865 bp deletion denoted 284. The amount of deleted mtDNA molecules were quantified using qPCR in clones expressing MTS-YFP and MTS-YFP-Top1mt as example for enhanced Top1mt activity. I found no differences between MTS-YFP-Top1mt expressing cells and control cell clones in the amount of both investigated deletions (Fig. 4.1.6), indicating that the increase of Top1mt activity in mitochondria apparently does not affect mtDNA replication.

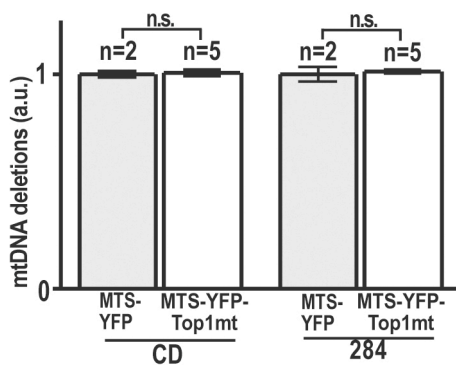


Figure 4.1.6. Mitochondrial targeting of MTS-YFP-Top1mt does not affect mtDNA integrity. Quantification of two different mtDNA deletions per cell in clones expressing MTS-YFP (grey bars) or MTS-YFP-Top1mt (white bars). Copies of deleted mtDNA were determined using qPCR. All values were normalized to the mean value of the control clones expressing MTS-YFP (grey bar). The number of clones investigated is indicated above each bar (n) and error bars indicate the SEM. Values of each bar do not differ significantly from the control according to an unpaired T-test.

4.1.4.2 MTS-YFP-Top1mt activity decreases steady-state levels of mtDNA transcripts

In the nuclear compartment, Top1 is believed to play its most important role in the transcription. Therefore, I was especially interested to examine the mtDNA transcription in cells having enhanced Top1mt activity in mitochondria. To investigate this, the steady-state level of 12S rRNA (a mtDNA transcript) was determined by Northern blotting (Figure 4.1.7.A). As loading control, the blot was reprobated for nuclear encoded 18S rRNA. In cell clones expressing MTS-YFP-Top1mt (lanes 7-9 and 13-15) the level of 12S rRNA were evidently lower as compared to cell

clones expressing MTS-YFP alone (lanes 1-3 and 10-12). In contrast, RNA levels were not reduced in cell clones expressing the wild type Top1mt (lanes 4-6) or the active site mutant MTS-YFP-Top1mt^{Y559F} (lanes 16-18). To obtain quantitative data on the effect of MTS-YFP-Top1mt, RNA levels of the mitochondrial transcripts COXI mRNA and 12S rRNA were determined by quantitative real time reverse transcriptase PCR (qRT-PCR) in comparison to mRNA levels of the mitochondrial protein succinate dehydrogenase subunit B (SDHB) encoded in the nuclear genome (Figure 4.1.7.B). 18S rRNA was amplified as internal standard. In cell clones expressing MTS-YFP-Top1mt the levels of the two transcripts from mtDNA were significantly lower (COXI, ~27%, and 12S rRNA, ~33%) as compared to cell clones expressing MTS-YFP alone (Figure 4.1.7.B, left and middle group of bars). In contrast, mRNA levels of the nucleus-encoded mitochondrial protein SDHB were slightly (~16%) but not significantly increased in the MTS-YFP-Top1mt expressing cell clones (Figure 4.1.7. right group of bars).

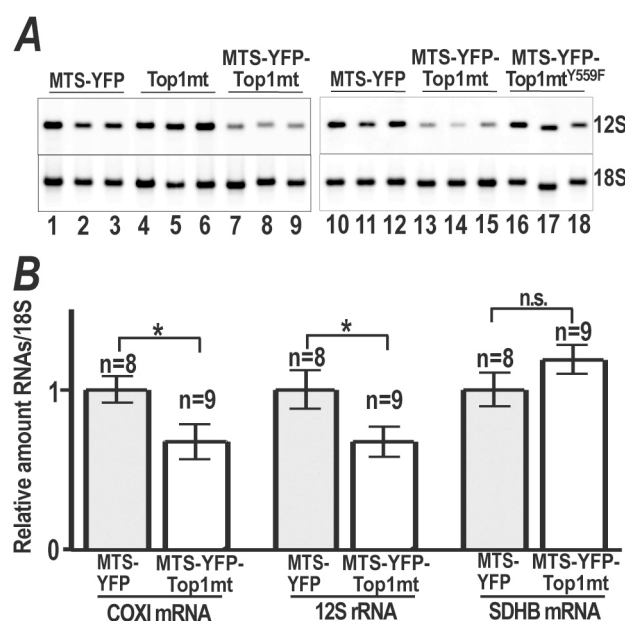


Figure 4.1.7. Expression of MTS-YFP-Top1mt lowers mtDNA transcripts levels. A) Northern blot analyses of 12S rRNA (top) from clones expressing MTS-YFP (lanes 1-3 and 10-12), Top1mt (lanes 4-6), MTS-YFP-Top1mt (lanes 7-9 and 13-15) or MTS-YFP-Top1mt^{Y559F} (lanes 16-18). 18S rRNA (bottom) was used as load control. B) COXI mRNA (left pair of columns), 12S rRNA (middle pair of columns) and SDHB mRNA (right pair of columns) levels determined by qRT-PCR in clones expressing MTS-YFP (grey bar) or MTS-YFP-Top1mt (white bar). All values are normalized first to the level of 18S rRNA and then to the mean value of MTS-YFP expressing clones. The number of clones investigated is indicated above each bar (n), and error bars indicate the SEM. COXI and 12S RNAs differed significantly (*: $p < 0.05$) from the control according to an unpaired T-test.

This finding clearly indicated that the expression of catalytic active MTS-YFP-Top1mt diminished mtDNA transcripts, whereas the catalytic inactive MTS-YFP-Top1mt^{Y559F} and the untagged Top1mt did not influence mtRNA amounts. These findings suggest an attenuating effect of the YFP-tagged Top1mt on mtDNA transcript levels that could result in a reduced abundance of mitochondrially

encoded proteins in cells expressing MTS-YFP-Top1mt. Most importantly, the difference between active or inactive YFP-tagged Top1mt demonstrates that the drop of mtDNA transcripts has to do with the biochemical function of Top1mt, and is not due to unspecific mtDNA binding. However, the fact that such an effect was not seen upon overexpression of untagged Top1mt suggests that it could also be due to the fusion with the fluorescent tag. It is possible that the catalytical properties of Top1mt were altered by the fusion of YFP at its N-terminal end (see Fig.4.1.3) or that somehow regulatory mechanisms of the protein were lost. In synopsis, the capacity of MTS-YFP-Top1mt to decrease mitochondrial transcripts not only depends on its catalytic activity (MTS-YFP-Top1mt versus MTS-YFP-Top1mt^{Y559F}), but also on the addition of MTS-YFP at its N-terminal end (MTS-YFP-Top1mt versus Top1mt). Notwithstanding, the MTS-YFP-Top1mt attenuating effect on mtDNA transcription is a powerful tool: Knockdown of TFAM, TFB1M and TFB2M abolishes completely the transcriptional process, leading to complete mtDNA depletion in the cell (Falkenberg et al, 2002; Larsson et al, 1998). However, to the best of my knowledge, there does not exist a way to inhibit exclusively transcription. In addition, the consequences of an impaired mtDNA transcription have so far not been investigated. Thus, even if the effect of MTS-YFP-Top1mt is not meaningful in physiological terms, it still offers a model to investigate the consequences of an attenuated mtDNA transcription *in vivo*.

4.1.5 Modest decrease of mtDNA transcripts drastically reduces the respiratory chain proteins

I have shown so far, that overexpressing YFP-fused Top1mt had an attenuating effect on mtDNA transcript levels, which could result in a reduced abundance of mitochondria-encoded proteins in cells subjected to MTS-YFP-Top1mt activity, thus leading to mitochondrial dysfunctions.

To address this issue, western blots of isolated mitoplasts were probed with antibodies directed against mitochondrial (COXI) and various nucleus-encoded respiratory chain subunits (NDUFA9, NDUF8, UQCRC2, COX4 and ATP5A1). Figure 4.1.8 shows a clear reduction of the mitochondrially encoded COXI (top panel) in cell clones expressing MTS-YFP-Top1mt (lanes 4-6 and 13-15) as compared to cell clones expressing MTS-YFP (lanes 1-3 and 10-13), Top1mt (lanes 7-9) or MTS-YFP-Top1mt^{Y559F} (lanes 16-18). Levels of nuclear encoded proteins were affected to variable extent: The complex I subunit NDUF8 (third panel) was dramatically

reduced, while all other subunits tested were either slightly (NDUFA9, second panel; UQCRC2, fourth panel and COX4, fifth panel) or not affected (ATP5A1, sixth panel). While COXI protein abundance mirrored its mRNA level, mRNA levels of nuclear encoded subunits were not diminished (see Fig.4.1.7). However, all respiratory complexes (except complex II) contain proteins encoded in the nucleus and in mitochondria, and abnormal mitochondrial protein synthesis has been reported to compromise assembly of the complexes (Park et al, 2007). Apparently, this defect in the complexes assembly is accompanied by a decrease in protein steady state levels of some nuclear encoded respiratory subunits (Park et al, 2007). Thus, it is plausible that the diminished level of most nuclear encoded subunits observed in figure 4.1.8 was a consequence of a defective complex assembly, and therefore a downstream effect of MTS-YFP-Top1mt action on mtDNA transcription. Of all tested nuclear encoded subunits only the α -subunit (ATP5A1) of complex V (ATPase-ATP synthase) was not reduced in cell clones expressing MTS-YFP-Top1mt. This finding is consistent with the notion that the ATP synthase subcomplex containing the α -subunit is known to remain stable and functional, even in the complete absence of mitochondrial protein synthesis (Buchet & Godinot, 1998).

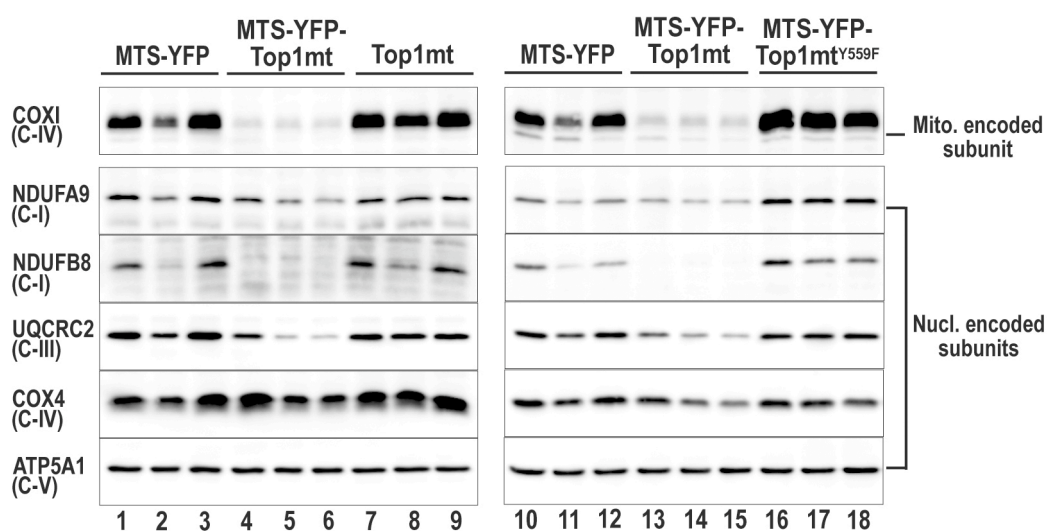


Figure 4.1.8. Expression of MTS-YFP-Top1mt lowers abundance of respiratory chain proteins. Western blot analysis of subunits of respiratory chain complexes from mitoplast lysates from selected single cell clones expressing MTS-YFP (lanes 1-3 and 10-12), Top1mt (lanes 7-9), MTS-YFP-Top1mt (lanes 4-6 and 13-15) or MTS-YFP-Top1mt^{Y559F} (lanes 16-18). MtDNA encoded subunit of complex IV (COXI) and nucleus encoded subunits of complex I (NDUFA9 and NDUFB8), complex III (UQCRC2), complex IV (COX4) and complex V (ATP5A1) were investigated.

Interestingly, densitometric analysis of immunoblots of several individual cell clones of each kind showed that steady state levels of COXI protein were even more diminished (by ~79% in comparison to ATP5A1) than corresponding levels of COXI mRNA (Figure 4.1.7.B). This suggests an over-proportional impact of reduced mtDNA transcript levels on mitochondrial protein synthesis. One possible explanation for this could be an additional defect in transcript maturation, i.e. a lack of excision of the tRNA sequences flanking mRNA and rRNA sequences in the polycistronic precursor (Ojala et al, 1981; Park et al, 2007). Therefore, I assessed the level of immature COXI mRNA by qRT-PCR using primer sets specifically amplifying tRNA flanked COXI (i.e. COXI precursor RNA). The ratio between immature and mature COXI mRNA determined was not increased in cells expressing MTS-YFP-Top1mt (Fig 4.1.9), excluding defects of RNA maturation. In contrast, the amount of unprocessed mtDNA transcripts in these cells was slightly (but not significantly) decreased. Thus, assuming that mtRNA processing is equally efficient in MTS-YFP-Top1mt and MTS-YFP expressing cells, it is possible that the lowered substrate (polycistronic RNAs) amount in MTS-YFP-Top1mt expressing cells undergo a more efficient maturation, explaining the decrease of unprocessed RNA. Another explanation for the over-proportional reduction of mitochondrial protein synthesis could be derived from the observation that expression of MTS-YFP-Top1mt affected levels of mitochondrial mRNA and rRNA (see Figure 4.1.7). Therefore, it is conceivable that mitochondrial protein production in the cells expressing MTS-YFP-Top1mt was compromised by a combined effect of decreased mRNA and less ribosomal activity. In addition, it is possible that unbalanced assembly of complexes from nuclear and mitochondrial protein synthesis compromises stability of the complexes.

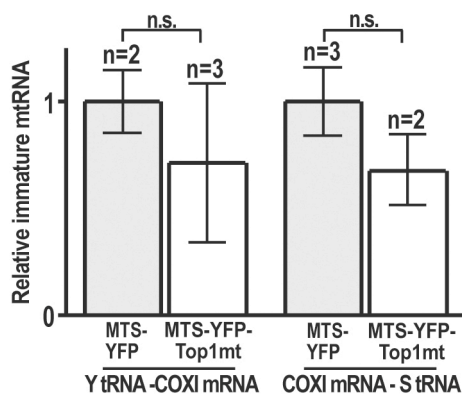


Figure 4.1.9. Expression of MTS-YFP-Top1mt does not affect the mitochondrial transcripts maturation. Quantification of immature COXI mRNA in clones expressing MTS-YFP (grey bars) and MTS-YFP-Top1mt (white bars). Unprocessed RNA was quantified by qRT-PCR using primers specifically amplifying regions upstream (Y tRNA-COXI mRNA, left pair of columns) and downstream COXI gene (COXI mRNA-S tRNA, right pair of columns). The ratio between immature and mature COXI mRNA in each clone was normalized to the mean value of the control clones expressing MTS-YFP. The number of clones investigated is indicated above each bar (n), and error bars indicate the SEM. Amounts of unprocessed mtRNA do not differ significantly from the control according to an unpaired T-test.

In summary, I could show, that the reduction of mtDNA transcripts affects dramatically not only the mitochondria-encoded proteins but also the nucleus-encoded subunits of the respiratory chain. Therefore, I next investigated what effect a reduced function of the respiratory chain had on the overall metabolic mitochondrial performance.

4.1.6 Defective respiratory chain assembly inhibits cell respiration and induces a metabolic switch to anaerobic glycolysis

Mitochondrial respiration is known to decline when mitochondrial complexes are inhibited by more than 50% (Rossignol et al, 1999). Therefore, it is plausible that, in MTS-YFP-Top1mt expressing cells, the ~79% decrease of respiratory chain proteins (see Figure 4.1.8) should lead to a functional reduction of the OXPHOS process.

To verify this, I determined the rate of oxygen consumption as a global measure of the overall function of the respiratory chain. As summarized in Figure 4.1.10.A, the rate of oxygen consumption in cell clones expressing MTS-YFP-Top1mt was significantly (~63%) lower than in cell clones expressing MTS-YFP alone. The absence of a slow growth phenotype or morphological defects in the cells is likely due to the ability of the HT-1080 cells to compensate for this by an increase in anaerobic glycolysis. To check this, I measured lactate, which is generated by the reduction of pyruvate during anaerobic metabolism (Figure 4.1.10.B). Lactate generation was ~79% increased in cells expressing MTS-YFP-Top1mt over a cultivation period of 48 h compared to control clones expressing MTS-YFP alone. Thus, decrease of respiratory chain proteins led to a functional reduction of the OXPHOS and the cells increased anaerobic glycolysis for ATP production.

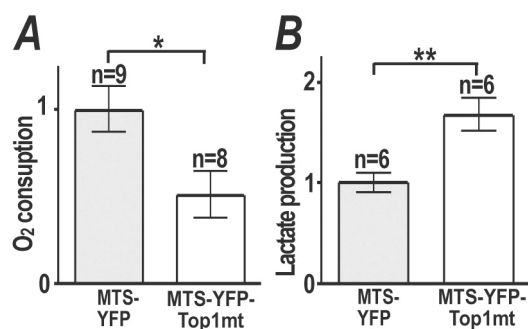


Figure 4.1.10. Expression of MTS-YFP-Top1mt leads to defects in respiratory chain functions. Oxygen consumption (A) and lactate production (B) of intact cells of various clones expressing MTS-YFP (grey bars) and MTS-YFP-Top1mt (white bars). All bars are normalized to the mean value of the control clones expressing MTS-YFP alone. The number of clones investigated is indicated above each bar (n), and error bars indicate the SEM. Asterisk-marked values differed significantly (*: $p < 0.05$; **: $p < 0.005$) from the control according to an unpaired T-test.

Inhibition of OXPHOS can lead to the accumulation of electrons in its initial steps. Especially in a defective OXPHOS process, these electrons can escape from the respiratory chain increasing ROS production (Bonawitz et al, 2006b). Thus, I was interested to investigate if respiratory chain impairment leads to a ROS increment in MTS-YFP-Top1mt expressing cells.

4.1.7 Defects of the respiratory chain lead to increased oxidative stress in mitochondria

To measure ROS levels in living cells, I used the MitoSOX dye, which is an indicator of mitochondrial superoxide anions. Staining of mitochondria with MitoSOX was on the average ~72% more intense in cells expressing MTS-YFP-Top1mt than in cells expressing MTS-YFP alone (Fig.4.1.11.A), which indicated a significant increase in mitochondrial production of superoxide anions. As positive control, I used antimycin A (AntA), which increases mitochondrial superoxide anions production by inhibition of electron transfer at complex III. Treatment with AntA did in both cases increased MitoSox fluorescence approximately 4-fold.

It has been reported that increased ROS levels induce the expression of ROS scavenging enzymes like the mitochondrial superoxide dismutase (SOD-2) and glutathione peroxidase 1 (St-Pierre et al, 2006). Thus, I examined the protein level of SOD-2 in MTS-YFP-Top1mt expressing cells by western analysis (Fig. 4.1.11.B). I found similar SOD-2 levels in cells expressing MTS-YFP-Top1mt (having increased ROS-levels) and control cells expressing MTS-YFP alone, which demonstrates that the cells did not react to an increased mitochondrial ROS production with a notable induction of SOD-2. Current belief holds that ROS in the mitochondrial matrix are responsible for mtDNA mutagenesis (Balaban et al, 2005; Richter et al, 1988). Thus, I investigated the impact of MTS-YFP-Top1mt on the mutation rate of mtDNA: Several cell clones expressing MTS-YFP-Top1mt or MTS-YFP were kept in continuous culture for three month before sequencing the entire COXI gene. I failed to detect a significant increase in mutations of the COXI gene in any of these cell clones, indicating a normal mutation rate in MTS-YFP-Top1mt expressing cells. This finding supports the idea that oxidative stress is not a major cause of mtDNA mutations in mammals (Lim et al, 2005; Stuart et al, 2005; Trifunovic et al, 2005). Alternatively, it could mean that increases in ROS levels or the time of exposure were insufficient for a significant impact on mtDNA stability as measured by COXI gene mutations. It could also be that cell clones bearing an increased load of mtDNA mutations could

not emerge from the highly proliferating cell population (Khrapko et al, 2003).

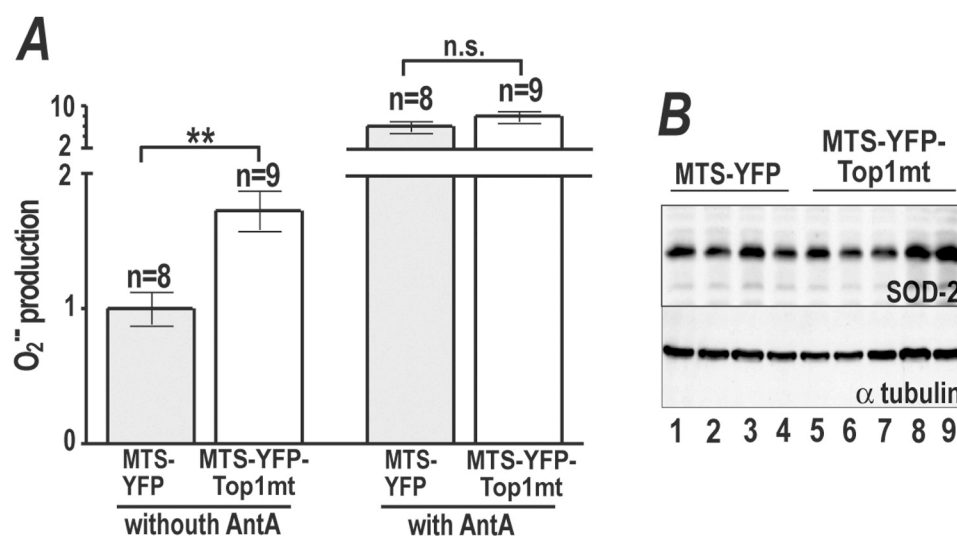


Figure 4.1.11. Expression of MTS-YFP-Top1mt increases oxidative stress in mitochondria but does not influence the expression of ROS scavenging enzymes. A) Superoxide production was determined with the mitochondrial superoxide indicator MitoSOXRed in cells expressing MTS-YFP (grey bars) and MTS-YFP-Top1mt (white bars). Cells were either untreated (left) or treated for 30 min with Antimycin A (AntA, right), a potent inhibitor of complex III. Since AntA treatment results in the formation of large quantities of ROS, it was used as positive control for superoxide production. All values were normalized to the respective mean value of YFP expressing clones. Each clone was measured at least twice and the number of clones investigated is indicated below each bar (n). Error bars indicate SEM. Asterisk-marked values differed significantly (**: $p < 0.005$) from the control according to an unpaired T-test. Note the different y-axis scales for the left vs. right bars. B) Western blot analyses of SOD-2 from whole cells lysates of MTS-YFP (lanes 1-4) and MTS-YFP-Top1mt (lanes 5-9) expressing clones.

4.2 Mitochondrial targeting of nuclear Top1

Among all the topoisomerases targeted to the mitochondrial matrix, Top1mt is the only one specifically developed for the mitochondrial compartment. The splitting of the topoisomerase I gene into Top1mt and Top1 is highly conserved in all vertebrates; however, the relevance of this splitting is still unknown. Top1mt and Top1 show a high degree of sequence homology and a nearly identical biochemical activity; nevertheless Top1 is excluded from the mitochondrial compartment, where Top1mt substitutes for it. Lower eukaryotes lack Top1mt and yeasts use Top1 activities in both the mitochondrial and the nuclear compartment. It is possible that nuclear Top1 in mitochondria would endanger mtDNA in vertebral species and that the separate encoding of Top1mt was necessary to preserve the mitochondrial genome. To investigate this, I targeted Top1 to the mitochondria and examined the consequence of that on mtDNA stability and mitochondrial functions.

4.2.1 The MTS of COX subunit VII is able to import Top1 into mitochondria

I targeted the topoisomerase I dedicated to the nuclear compartment to mitochondria. In the constructs used in this section, Top1 variants (Fig. 4.2.1) were fused at their N-terminal end to YFP and the MTS from COX subunit VIII (Rizzuto et al, 1995). Active full-length Top1 (MTS-YFP-Top1, fig 4.2.1. construct b), the inactive full length Top1 variant (MTS-YFP-Top1^{Y723F}, fig 4.2.1. construct c) and three N-terminally truncated versions of Top1 (Fig 4.2.1. constructs d, e and f) were targeted to mitochondria. In construct d, the first 190 residues were deleted (MTS-YFP-Top1¹⁹¹⁻⁷⁶⁵), removing all NLSs (Alsner et al, 1992; Mo et al, 2000a) without effecting catalytic activity *in vivo* or *in vitro* (Christensen et al, 2003). In construct e the active site tyrosine was mutated (MTS-YFP-Top1^{191-765, Y723F}) and in construct f the first 210 residues were lacking (MTS-YFP-Top1²¹¹⁻⁷⁶⁵). The latter construct lacked all amino acids encoded by the first eight exons of TOP1, and consequently contained only the regions conserved between Top1 and Top1mt (Zhang et al, 2004). Moreover it has an altered activity *in vitro* (Frohlich et al, 2007) and is resistant to the Top1 drug camptothecin *in vivo* (Christensen et al, 2003). The basic vector encoding for mitochondria-targeted YFP alone (MTS-YFP, fig 4.2.1. construct a) served as control.

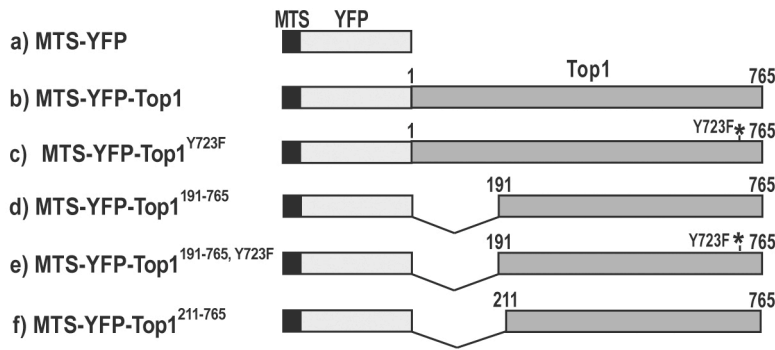


Figure 4.2.1. Targeting of Top1 variants to mitochondria. Schematic of the constructs studied in this section. Mitochondrial targeting of all constructs relied on the MTS of cytochrome C oxidase-subunit VIII (black).

When transfected into human HT-1080 cells, these constructs gave in all cases rise of viable cell lines supporting stable expression of the YFP-fused proteins. However, growth of cell clones expressing any of the YFP chimera was strictly dependent on the presence of uridine in the growth media. Moreover, the growth rates of these clones were markedly reduced compared to parental cells and to cell clones expressing MTS-YFP (see 4.2.7).

All selected clones were first screened under the microscope for YFP fluorescence and only clones showing mitochondrial localization of YFP were chosen and investigated further. To assess the integrity of the fusion proteins, to compare their relative expression levels, and to confirm targeting to the mitochondrial matrix, whole cells and isolated mitoplasts were subjected to western blotting and probed with YFP antibodies (Fig. 4.2.2).

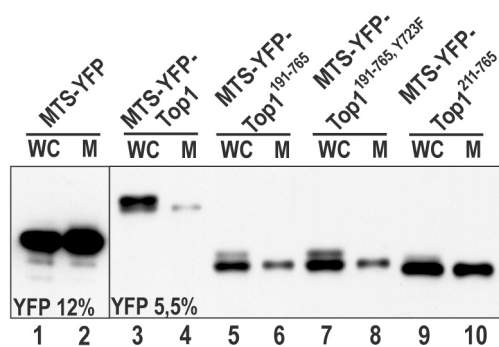


Figure 4.2.2. Generation of clones expressing Top1 variants in mitochondria. Immunoblot analysis of lysates from whole cells (WC) or isolated mitoplasts (M) from representative cell clones expressing the constructs indicated above. Samples were subjected to SDS PAGE (left panel 12% acrylamide, right panel 5.5% acrylamide) and Western blotting. Blots were probed with YFP antibodies.

Chimeric proteins were detected at expected size, and exhibited similar band intensities in extracts from whole cells and isolated mitoplasts. An additional band of higher apparent molecular size was seen in whole cells expressing the Top1 variants (Fig. 4.2.2, lanes 3, 5, 7, and 9). Most probably it represents the portion of the proteins not imported into the mitochondria where the MTS consequently is not cleaved off. In keeping with this notion, isolated mitoplasts only contained the faster migrating of the two bands (lanes 4, 6, 8, and 10). Thus, I could safely assume that yellow

fluorescence of the cells was due to the desired protein chimera, and that all fusion proteins were targeted to mitochondria and expressed there at similar levels.

The expression system described above allowed me to investigate the behaviour of Top1 in the mitochondrial compartment and perhaps clarify the reason for the evolution of Top1mt in vertebrates. However, it was critical first to determine if the expressed Top1 chimeras still maintained their biochemical properties also in the mitochondrial matrix.

4.2.2 Top1 maintains its biochemical activity in mitochondria

To test whether mitochondria-imported Top1 variants were active, I measured DNA relaxation activity in salt extracts of isolated mitoplasts (Fig. 4.2.3).

MTS-YFP-Top1¹⁹¹⁻⁷⁶⁵ and MTS-YFP-Top1^{191-765, Y765F} were chosen as examples of catalytically active and inactive variants of Top1. Mitoplast extracts from cells expressing MTS-YFP or the catalytically inactive mutant MTS-YFP-Top1^{191-765, Y765F} exhibited only a weak DNA-relaxation provided by the endogenous Top1mt (Fig. 4.2.3.A and C). In contrast, mitoplast extracts from cells expressing MTS-YFP-Top1¹⁹¹⁻⁷⁶⁵, an active version of Top1, had about 8-fold higher amounts of DNA-relaxation activity in the extracts (Fig. 4.2.3.B). These levels of, and differences in, extractable DNA-relaxation activities were similar as the ones observed in the experiments with heterologous expression of Top1 mt (see: Fig. 4.1.3).

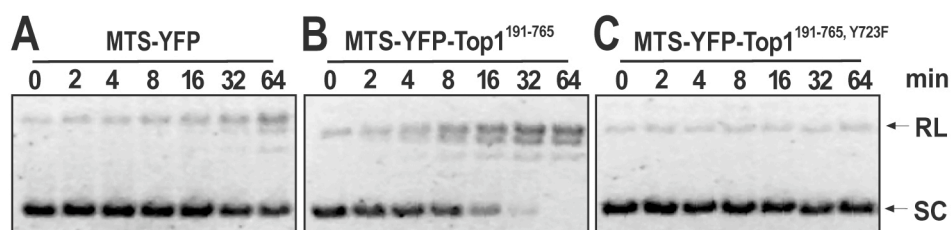


Figure 4.2.3. Top1 maintains its catalytic activity in mitochondria. Relaxation of supercoiled pUC18 plasmid DNA (400 ng) by mitoplast extracts (170 ng total protein) prepared from cell clones expressing MTS-YFP (A), MTS-YFP-Top1¹⁹¹⁻⁷⁶⁵ (B), or MTS-YFP-Top1^{191-765, Y723F} (C) at 37°C for the time indicated above. Position of Relaxed (RL) and supercoiled (SC) plasmid forms are indicated on the right margin. The time point at 0 min means that DNA not exposed to mitochondrial extract.

Thus, I succeeded in expressing YFP chimera of several Top1 variants in mitochondria. All chimera proteins localized in the mitochondrial matrix and maintained catalytic properties typical of Top1.

4.2.3 Mitochondrial targeting of Top1 leads to mtDNA depletion

To address the hypothesis of a detrimental effect of Top1 on the mitochondrial genome, I investigated the mtDNA stability in cells expressing mitochondria-targeted Top1 variants. As global measure of the mitochondrial genome maintenance, I determined the average copies of mtDNA by qPCR.

Surprisingly, I found that targeting of Top1 and its truncated variants to the mitochondrial matrix leads to a complete depletion of mtDNA (Table 4.2.1), no matter whether variants are catalytically active or not.

Construct	MtDNA copies/cell ± SEM	Number of investigated clones
MTS-YFP	1013.20 ± 331.93	13
MTS-YFP-Top1	0.07*** ± 0.04	2
MTS-YFP-Top1 ^{Y723F}	0.06*** ± 0.04	3
MTS-YFP-Top1 ¹⁹¹⁻⁷⁶⁵	0.05*** ± 0.03	3
MTS-YFP-Top1 ^{191-765, Y723F}	0.12*** ± 0.02	3
MTS-YFP-Top1 ²¹¹⁻⁷⁶⁵	0.03 *** ± 0.01	5

Table 4.1. MtDNA depletion in cells expressing mitochondria-targeted Top1 variants.

MtDNA copy numbers were determined by qPCR. Quantitative results are given as mean values ± standard error of the mean. Asterisk-marked values differed significantly ($p < 0.0001$) from the control MTS-YFP alone according to an unpaired T-test.

These results demonstrate that stable targeting of Top1 variants to mitochondria results in a phenotype similar to the so-called ρ^0 cells that have been depleted of mtDNA by long-term exposure to EtBr (King & Attardi, 1989). Top1-mediated depletion was most puzzling since it was also exerted by the inactive mutants MTS-YFP-Top1^{Y723F} and MTS-YFP-Top1^{191-765, Y723F} and, therefore, not linked to the catalytic activity of the enzyme.

4.2.4 Mitochondrial targeting of Top1 alters mitochondrial shape

Having demonstrated a deleterious effect on mtDNA, I investigated next the consequences on mitochondrial morphology using the mitochondria-specific probe MitoTracker (Fig. 4.2.4, right middle column).

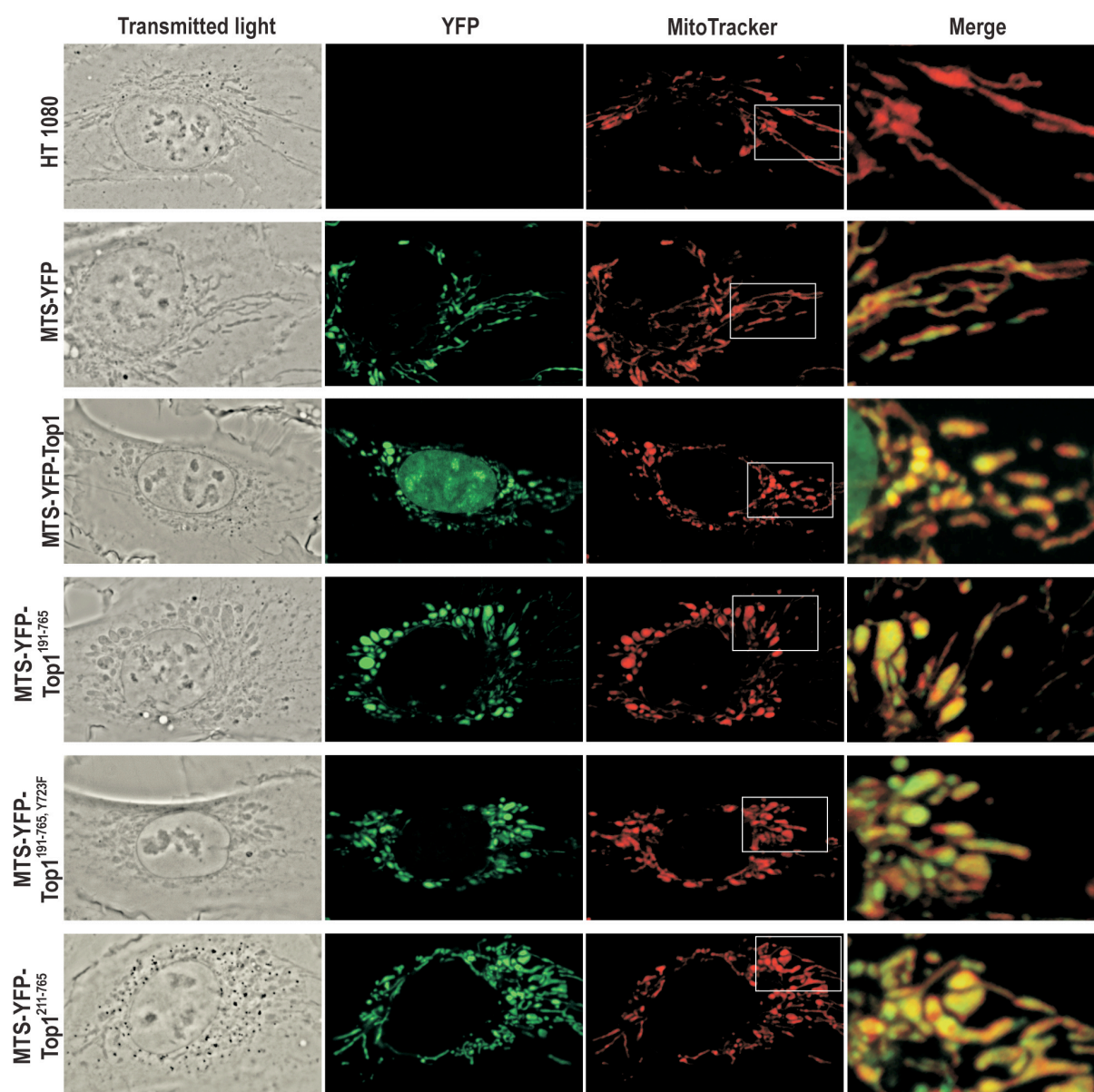


Figure 4.2.4. In vivo localization of mitochondria-targeted Top1 constructs. Each row shows representative confocal images of living HT-1080 cells stably expressing the construct indicated on the left margin. Shown are images of transmitted light (left), YFP fluorescence (middle left), mitochondria-specific Mito Tracker Red fluorescence (middle, right), and a merge of the latter two restricted to the area indicated in the Mito Tracker column at 3-fold magnification (right).

Cellular targeting of the chimeric proteins was judged by YFP fluorescence localization (Fig. 4.2.4, left middle column). These patterns largely coincide with the MitoTracker images (see merged images in right column) indicating that all fusion proteins were imported and distributed in the mitochondrial compartment. Consistent with the lack of mtDNA, the YFP signal does not show the focal distribution typical, for e.g., of MTS-YFP-Top1mt (compare Fig. 4.1.4): In the absence of nucleoids, YFP-Top1 chimeras distribute uniformly in the mitochondrial matrix.

MTS-YFP-Top1 showed a dual localization in mitochondria and the cell nucleus (row 3), since the N-terminal domain of the enzyme harbors multiple NLSs (Alsner et al, 1992; Mo et al, 2000a). This dual localization is consistent with the western blot results shown in figure 4.2.2. Truncation of this domain (MTS-YFP-Top1¹⁹¹⁻⁷⁶⁵, MTS-YFP-Top1^{191-765, Y723F}, MTS-YFP-Top1²¹⁰⁻⁷⁶⁵, rows 4-6) abolished nuclear targeting and created variants of the nuclear enzyme mostly localized in mitochondria. In contrast, in untransfected HT-1080 cells (row 1) and in a cell clone expressing MTS-YFP alone (row 2) the mitochondria form a largely connected reticulum, typically for living mammalian cells (Rizzuto et al, 1998). Evidently, significant changes in gross morphology of the mitochondrial organelle were observed in clones stably expressing mitochondria-targeted Top1 variants. Mitochondria were rounder and the entire compartment was less branched (rows 3-6). This mitochondrial morphology is consistent with previous reports on ρ^0 cells showing a similar alteration of the mitochondrial reticulum characterised by swollen regions linked by narrow connections. This morphology seems to be caused by the loss of mitochondrially encoded proteins followed by a disorganisation of the mitochondrial inner membrane (Gilkerson et al, 2000).

These data demonstrate that stable mitochondrial targeting of Top1 variants in human cells results in complete depletion of mtDNA and disorganization of the mitochondrial reticulum and this effect is independent of Top1 catalytical activity. Next, the cellular consequences of the Top1 mediated mtDNA depletion were analyzed. Since targeting of all Top1 variants induced the same detrimental phenotype, I limited my further investigations to cell clones expressing MTS-YFP-Top1¹⁹¹⁻⁷⁶⁵.

4.2.5 Mitochondrial targeting of Top1 depletes respiratory chain

First I examined the mtDNA gene products of MTS-YFP-Top1¹⁹¹⁻⁷⁶⁵ expressing cells. Consistent with the loss of the mitochondrial genome, mtDNA encoded RNAs (COXI, 12S) are absent (Fig 4.2.4.A). Interestingly, mRNA levels of the nuclear encoded SDHB (complex II subunit) were slightly decreased (~38%), as opposed to MTS-YFP-Top1mt expressing cells (see 4.1.4.2), were a ~30% reduction of mtDNA transcripts leads to a slight increase of the SDHB messenger. Possibly, the enhanced expression of nuclear encoded mitochondrial protein in MTS-YFP-Top1mt expressing cells is the compensatory response to an emergency situation. Since complex II and I are both electron acceptors of the OXPHOS, the cell could try to

compensate defects of complex I by increasing complex II activity. Possibly, in the case of a complete lack of respiratory chain activity, an increase in complex II activity is futile. Therefore, a decrease of SDHB mRNA could be the most opportune reaction to mtDNA depletion.

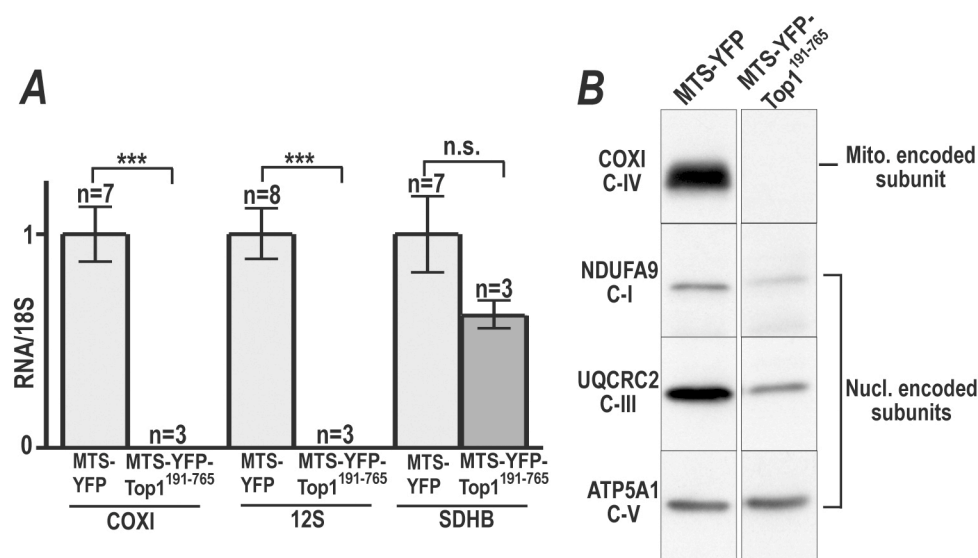


Figure 4.2.5 MtDNA depletion affects mtDNA as well as nuclear gene products. **A**) COXI mRNA (left), 12S rRNA (middle) and SDHB mRNA (right) levels are determined by qRT-PCR in clones expressing MTS-YFP (grey bars) or MTS-YFP-Top1¹⁹¹⁻⁷⁶⁵ (dark grey bar). All values are normalized first to the level of 18S rRNA and then to the mean value MTS-YFP expressing clones. The number of clones investigated is indicated above each bar (n), and error bars indicate the SEM. Asterisk-marked bars differed significantly (***: $p < 0.001$) from the control according to an unpaired T-test. **B**) Western blot analysis of subunits of respiratory chain complexes from mitoplast lysates of a representative clone expressing MTS-YFP (left) and MTS-YFP-Top1¹⁹¹⁻⁷⁶⁵ (right). MtDNA encoded subunit of complex IV (COXI) and nucleus encoded subunits of complex I (NDUFA9), complex III (UQCRC2) and complex V (ATP5A1) were investigated.

To investigate the condition of the respiratory chain of MTS-YFP-Top1¹⁹¹⁻⁷⁶⁵ expressing cells, western blots of isolated mitoplasts lysates were probed with antibodies against NDUFA9 (respiratory chain complex I), UQCRC2 (complex III), COXI (complex IV), or ATP5A (complex V) (Fig. 4.2.4.B). COXI, the mitochondrially encoded protein, was, as expected, not at all detectable. The nuclear encoded proteins NDUFA9 and UQCRC2 were also markedly reduced. This observation supports the hypothesis that proteins failing to be assembled in a corrected complex are degraded (Park et al, 2007). In contrast, the nuclear encoded subunit ATP5A of complex V remained unchanged in mtDNA depleted cells, according with previous observation of partial assembled complex V in ρ^0 cells (Buchet & Godinot, 1998).

4.2.6 Mitochondrial targeting of Top1 compromises cell respiration

I have shown that expression of MTS-YFP-Top1¹⁹¹⁻⁷⁶⁵ leads to depletion of mtDNA-encoded proteins and, furthermore, to the attenuation of several subunits of the respiratory chain that are nuclear encoded. Plausibly, this situation compromised operating of the OXPHOS. To investigate the functioning of the respiratory chain, I determined the rate of oxygen consumption in cells expressing MTS-YFP-Top1¹⁹¹⁻⁷⁶⁵ (Figure 4.2.6). As expected, the rate of oxygen consumption in cell expressing MTS-YFP-Top1¹⁹¹⁻⁷⁶⁵ was dramatically (80%) lower than in the control cell clones.

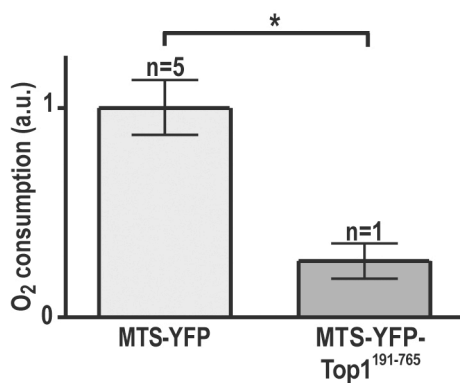


Figure 4.2.6. Defects in respiratory chain function in cell clones expressing MTS-YFP-Top1¹⁹¹⁻⁷⁶⁵. Oxygen consumption of intact cells of various clones expressing MTS-YFP (grey bar) and MTS-YFP-Top1¹⁹¹⁻⁷⁶⁵ (dark grey bar). All measurements were normalized to the mean value of the control clones. The number of clones investigated is indicated above each bar (n) and error bars indicate the SEM. Oxygen consumption of MTS-YFP-Top1¹⁹¹⁻⁷⁶⁵ expressing clones differed significantly (*: p<0.05) from the control according to an unpaired T-test.

The absence of a functional aerobic respiration was likely compensated by an increase in anaerobic glycolysis. Thus, I measured lactate in the growth media, which is generated by the reduction of pyruvate during anaerobic metabolism (Figure 4.2.7). Lactate generation was ~4-fold increased in cells expressing MTS-YFP-Top1¹⁹¹⁻⁷⁶⁵ over a cultivation period of 48 h compared to control clones expressing MTS-YFP alone. This finding is consistent with the reported observation that ρ^0 cells rely on glycolysis for their energy demand (King & Attardi, 1989).

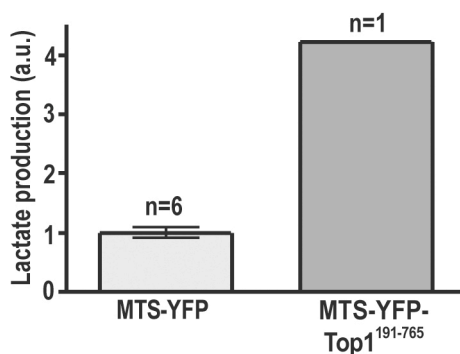


Figure 4.2.7. Increased anaerobic glycolysis in cells expressing MTS-YFP-Top1¹⁹¹⁻⁷⁶⁵. Lactate production of various clones expressing MTS-YFP (grey bar) and MTS-YFP-Top1¹⁹¹⁻⁷⁶⁵ (dark grey bar). Since the measurement of lactate production in MTS-YFP-Top1¹⁹¹⁻⁷⁶⁵ expressing cells was performed with only one clone, an error bar is not shown.

4.2.7 Mitochondrial targeting of Top1 causes uridine auxotrophy

As mentioned above, the generation of cell clones expressing mitochondria targeted YFP-Top1 chimera was possible only when uridine was added to the growth media. The nucleoside uridine serves in the cell as precursor for the synthesis of thymidine and cytidine, essential building elements of the DNA molecule. In the cell, the *de novo* synthesis of pyrimidine involves the mitochondrial enzyme dihydroorotate dehydrogenase. Since the function of this enzyme needs an operating respiratory chain, mtDNA depleted cells are not able to synthesize pyrimidine. Thus, ρ^0 cells are uridine auxotrophs (King & Attardi, 1989). Similar to ρ^0 cells, clones expressing MTS-YFP-Top1 variants only proliferated in the presence of uridine. This behaviour is demonstrated in figure 4.2.8.A.

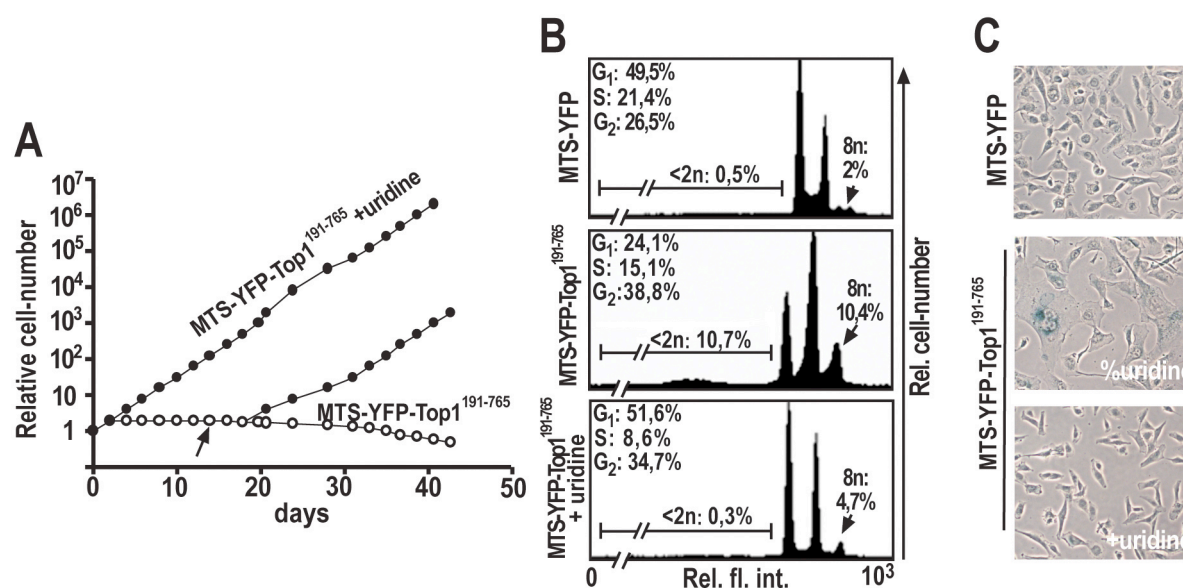


Figure 4.2.8. Growth of mtDNA depleted cells requires uridine supplementation. **A**) Growth rates of cells expressing MTS-YFP-Top1¹⁹¹⁻⁷⁶⁵ cultured in medium with (●) or without (○) uridine. Growth arrest can be reversed by supplementation with uridine. The arrow indicates the time-point, at which supplementation was started on a culture first grown in the absence of uridine for 14 days. Cells were diluted 1:2 upon confluence and relative cell numbers are calculated from numbers of splitting. Notably, it takes one population doubling before removal of uridine induces growth arrest and three before addition of uridine rescues growth arrest. **B**) Flow cytometric analysis of DNA content of cell clones expressing MTS-YFP (top) or MTS-YFP-Top1¹⁹¹⁻⁷⁶⁵ cultured for 30 days without (middle) or with uridine (bottom) before analysis. The numbers given in the histograms indicate percentage of apoptotic cells (<2n) and cell cycle distribution of living cells in G₁, S, or G₂ phase, or 8n cells. One representative experiment out of three is shown. **C**) Morphology and staining of senescence associated β-galactosidase activity of representative clones expressing MTS-YFP (top) or MTS-YFP-Top1¹⁹¹⁻⁷⁶⁵ cultured for 30 days without (middle) or with uridine (bottom). All the images were taken at the same magnification.

In the absence of uridine, cultures of a cell clone expressing MTS-YFP-Top1¹⁹¹⁻⁷⁶⁵ could be kept stationary for 30 days or more without significant loss in numbers (○). At any time during this period, cell proliferation could be recovered by addition of uridine to the medium (●). Cells could then be brought to stationary phase again by withdrawal of uridine. Growth arrest of these cells was probably due to an insufficient amount of pyrimidine resulting in an incomplete S phase and in the consequent block of the cell cycle. To investigate this, I analyzed the cell cycle state of cells expressing MTS-YFP-Top1¹⁹¹⁻⁷⁶⁵ using FACS analysis (Fig. 4.2.8.B).

I compared the cell cycle of growth-arrested cells, (cultivated without uridine) and proliferating cultures (cultivated with uridine) of the same clone expressing MTS-YFP-Top1¹⁹¹⁻⁷⁶⁵. I found a dramatic increase in hypodiploid nuclei, a reduced content of G₁ cells, and an elevated level of octaploid cells in arrested versus proliferating cultures. Consistent with the slight decrease in cell number observed during the stationary phase of growth arrest, the high rate of hypodiploid nuclei indicates an increased tendency of the cells to undergo apoptosis. Furthermore, the increased incidence of cells in G₂ and of octaploid cells indicates that most cells do not divide, but are arrested in G₂.

4.2.8 Mitochondrial targeting of Top1 induces cell senescence

During stationary phase, MTS-YFP-Top1¹⁹¹⁻⁷⁶⁵ expressing cells displayed a strikingly different phenotype characterized by inflated cell morphology and an enlarged cell size. Since this morphology was highly reminiscent of senescent phenotypes (Sumikawa et al, 2005), I tested if these cells were positive for senescence associated β -galactosidase staining (Dimri et al, 1995). Indeed, growth-arrested MTS-YFP-Top1¹⁹¹⁻⁷⁶⁵ expressing cells were positive for β -galactosidase activity (Fig. 4.2.8.C, row 2). Hence, removal of uridine induced a senescent like phenotype not found for cells clones expressing MTS-YFP alone (Fig. 4.2.8.C, row 1). Importantly, release of growth arrest upon addition of uridine also reversed the senescent like phenotype (Fig. 4.2.8.C, compare row 2 with 3).

4.2.9 mtDNA depletion induced by mitochondrial targeting of Top1 is a passive process

Having demonstrated that Top1, if targeted to mitochondria, induces mtDNA depletion, I wished to investigate how Top1 exerts this effect. Such knowledge is

essential to understand, why, in contrast, Top1mt is able to handle mtDNA safely. Several ways can be envisioned how Top1 could mediate mtDNA depletion: i) direct blockade of replication; ii) indirect blockade of replication (e.g. by depriving essential factors necessary for replication); iii) active destruction of mtDNA. Although I cannot exclude it, the latter option is unlikely, since the catalytic inactive Top1 variants also depleted mtDNA. To differentiate between these options, I needed first to investigate the timely progression of mtDNA loss. However, in the system described above I could only observe the start (before transfection, normal DNA) and the end-point (stable clones, mtDNA depleted) of the process. Therefore, I switched to a viral expression system allowing mitochondrial targeting of Top1 in a large fraction of a given cell population (see 3.2.3). We generated viruses efficiently delivering MTS-YFP-Top1 and as control MTS-YFP. Then we transduced HT-1080 cells with the described viruses to express MTS-YFP (○) or MTS-YFP -Top1 (●), and I determined mtDNA copy numbers at various population doublings (PD) after transduction (Fig. 4.2.9.A). In these kinetic experiments, cells were cultivated with uridine and the time point zero was defined as the moment where mitochondrial YFP fluorescence became clearly detectable by fluorescent microscopy (24 - 48 hours after transduction). Interestingly, at this timepoint mtDNA copy numbers were not diminished and remained stable for at least one more subsequent population doubling before starting to decline. Therefore, I can exclude that Top1 blocked mtDNA replication directly or that it actively degraded mtDNA. The phase after transduction, in which mtDNA copies remained unaffected, was followed by a rapid depletion of mtDNA during population doublings 2 to 6. The decline in mtDNA then leveled reaching a minimum near zero (<1 copy mt DNA per cell) after the ninth population doubling. This time course of mtDNA-depletion was best described by a model assuming a lag phase of 2 PD followed by an log-linear decay consistent with a two-fold dilution of mtDNA content in each cell division during PD 2 – 6 (Fig. 4.2.9.A, compare full and hatched lines).

This time course of mtDNA depletion is consistent with an indirect blockage of mtDNA replication via blockade of mtDNA transcription. These two processes are interdependent, because the primers required for initiation of mtDNA replication have to be generated first by mtDNA transcription (Wanrooij et al, 2008). Thus, a blockade of mitochondrial transcription should eventually abolish replication. To follow up on this notion, I determined the levels of COXI mtRNA (which is transcribed from mtDNA) during mtDNA depletion induced by MTS-YFP-Top1 (Fig. 4.2.9.B, ■). Evidently, a decline in COXI mRNA levels was immediately induced

Results

upon transduction with MTS-YFP-Top1 resulting in reductions of ~77, ~94, ~98, and >99% after 1, 2, 3, and 4 PD, respectively. Transduction of the inert control MTS-YFP had no effect (Fig. 4.2.9.B, □). Upon comparison of Fig. 4.2.9 A and B it becomes clear that expression of MTS-YFP-Top1 immediately reduces mtRNA level (during PD 1), whereas reduction in mtDNA copy numbers is a consequence that follows one or two PD later. In comparison, a reverse order of depletion of mtDNA (solid lines) and mtRNA (hatched lines) was seen upon treatment with the specific mtDNA replication inhibitor dideoxycytidine (ddC, Fig. 4.2.9.C) (Simpson et al, 1989), whereas treatment with EtBr that inhibits both transcription and replication (Seidel-Rogol & Shadel, 2002) led to simultaneous depletion of mtDNA and mtRNA (Fig. 4.2.9.D).

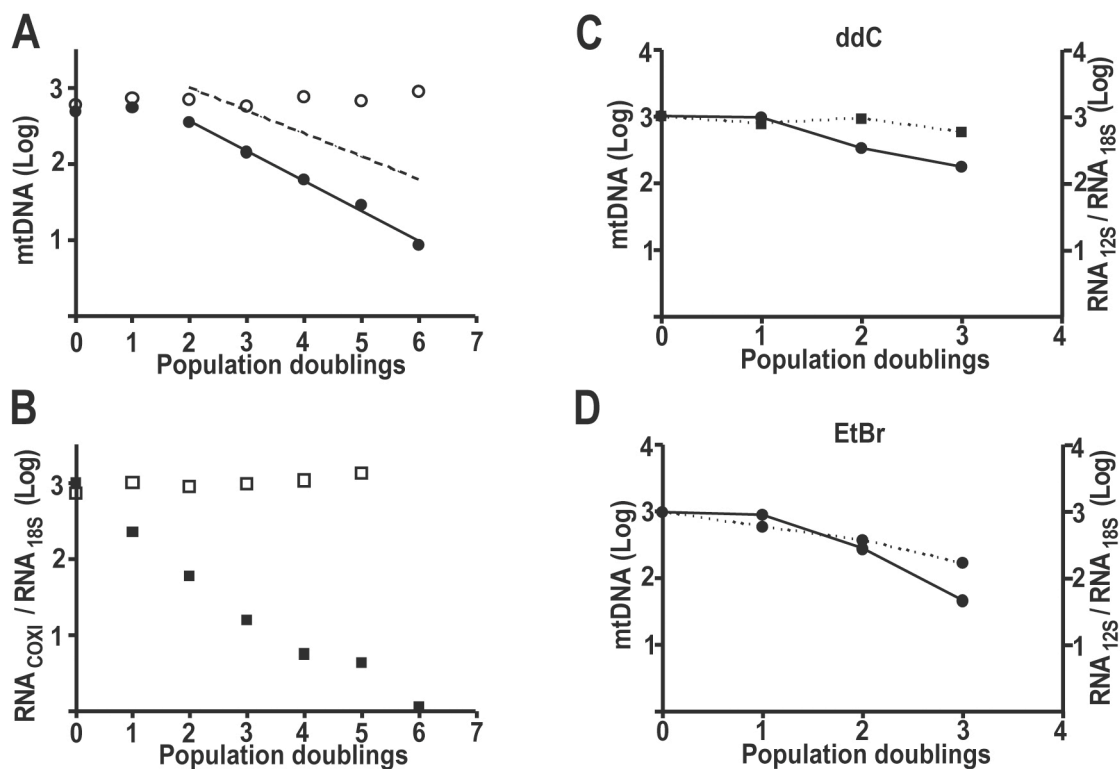


Figure 4.2.9 Mitochondrial targeting of Top1 inhibits mtDNA transcription and replication. A) Loss of mtDNA. MTS-YFP or MTS-YFP-Top1 were expressed in HT-1080 cells through a lentiviral vector system. Transduced cells were selected and cultured with uridine. MtDNA copy numbers of cells expressing MTS-YFP (○) or MTS-YFP-Top1 (●) were determined after each population doubling. Time zero was defined as the point at which fluorescent signals in the mitochondria was detectable (~24 hours after infection). The full line represents the regression of mtDNA copy numbers (logarithmic values) from population doubling 2 to 6. The hatched line represent the regression of theoretical values consistent with a model in which mtDNA is diluted two fold per cell division. The real and theoretical regression are nearly parallel (slope real = -0.3944 ± 0.0185 versus slope theoretical = 0.3) B) Loss of mtDNA transcripts precedes loss of mtDNA. Parallel to the mtDNA copy numbers, COXI mRNA was quantified in the cells expressing MTS-YFP (□) or MTS-YFP-Top1 (■) described above. MTS-YFP-Top1 expression has a prompt effect on COXI mRNA level, with a reduction of 77% and 94% after 1 and 2 population doublings respectively. C) and D) Depletion of mtDNA (full lines) and COXI mRNA (hatched lines) in HT-1080 cells treated with 20 μ M ddC (C) or 50 ng/ml EtBr (D).

These two control experiments show that I could discern between inhibition of mtDNA replication or -transcription, and that Top1 mediated mtDNA depletion clearly is a process preceded by selective blockade of transcription. In summary, these data confirm the above hypothesis that mitochondrial targeting of Top1 depletes mtDNA by inhibiting the synthesis of the replication primers. Given that these effects were likewise seen with active and inactive variants of Top 1 (see Tab. 4.1), and therefore, independent of enzymatic activity, I was curious to study them in more detail by analyzing the replication intermediates during Top1-mediated mtDNA depletion by two-dimensional neutral agarose gel electrophoresis (2DNAGE).

4.2.10 Mitochondrial targeting of Top1 blocks mtDNA replication initiation

2DNAGE allows resolving the replication intermediates (RIs) of mtDNA. MtDNA fragments are separated in a first dimension by size and in a second dimension by strand configuration, resolving RIs into a predictable sign pattern. Recently, 2DNAGE analyses have revealed two types of mtDNA RIs in higher eukaryotes that differ in their ribonucleotide content (Yasukawa et al, 2006). One type of RIs, denoted ERIOLS (extensive RNA incorporation on the lagging strand), incorporates RNA in the lagging strands and is therefore represented by RNA-DNA hybrids. Replication of the leading strand does not incorporate RNA and gives rise to another type of RIs, which follows a conventional strand-coupled DNA replication model (see 1.1.4.2). The knowledge provided by 2DNAGE suggests that, during replication of the leading strand, RNA is transiently incorporated on the lagging strand, and then replaced with DNA in a subsequent maturation step (Yasukawa et al, 2006).

Fig. 4.2.10.B shows 2DNAGE patterns of mtDNA from cells subjected to mitochondrial targeting of Top1. To obtain these patterns, extracted mtDNA was digested with HincII, generating fragments containing the region downstream O_H (the initiation and termination sites for replication). Digested mtDNA was then separated on a two-dimensional agarose gel and blotted. The fragments containing the control region were detected by hybridisation with a radioactively labelled cytochrome b probe. A schematic representation of the HincII fragment RIs is shown in figure 4.2.10.A. All fragments that are not in the process of being replicated were detected in the so called 1n spot. The subpopulation of mtDNA molecules, where the replication machinery passes through the analyzed mtDNA fragments, forms the y-

arc. The positions of ERIOLS (RNA-DNA intermediates) are depicted in grey. In particular, the bubble arcs (b) are indicative of replication initiation at O_H . In figure 4.2.10.B the RIs of cells expressing MTS-YFP (left) or MTS-YFP-Top1 (middle and right) are shown. We examined the situation of mtDNA replication in cells shortly subjected to Top1 activity and not yet having entered the phase of mtDNA depletion (PD0 in fig. 4.2.9.A) with that of cells having undergone three population doublings subsequent to Top1 expression in mitochondria and thus entered the log-linear phase of mtDNA depletion (PD3 in fig. 4.2.9.A). It is evident, that cells subjected to MTS-YFP-Top1 already after one cell doubling show much less RIs and lack the bubble arc (see arrow) as a sign of replication initiation. These features become more pronounced during three subsequent cell doublings, whereas atypical RIs indicative of stalled replication forks do not emerge. Thus, I could deduce that mitochondrial targeting of Top1 immediately inhibits the initiation of mtDNA replication but does not interfere with the continuation of replication forks already initiated.

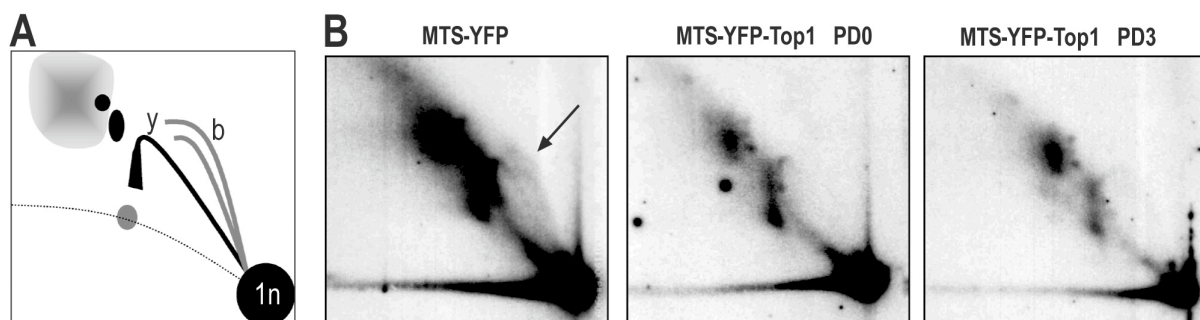


Figure 4.2.10. Analysis of replication intermediates. A) Schematic representation of RIs of the HincII fragment. The 1n spot represents all fragments that are not in the process of being replicated. RNA intermediates are depicted in grey, while conventional DNA intermediates are black. Most important, the bubble arcs (b) are indicative of replication initiation at O_H . B) 2DNAGE of mtDNA from cells expressing MTS-YFP (left) or MTS-YFP-Top1 shortly after expression initiation (middle) or after three population doublings (right). The mtDNA was digested with HincII and the fragment was detected with a radioactively labelled cytochrome b probe. Position of bubble arc is indicated by arrow. 2DNAGE were performed by S. Goffart.

4.3 The effects of Top1mt/Top1 hybrids

Vertebrates encode two genetically distinct topoisomerase I variants. The mitochondrial one (Top1mt) presumably arose by evolutionary duplication and modification of an early nuclear Top1 gene. I have shown that targeting of Top1 to mitochondria induces complete depletion of mtDNA whereas overexpression of Top1mt has no effect on the mtDNA stability. These findings clearly demonstrate that evolutionary splitting of topoisomerase I into Top1mt and Top1 was necessary to ensure the stability of the mitochondrial genome in human cells. Vertebral adaptation of Top1mt involves minor amino acid changes, because Top1mt and Top1 are highly conserved except for their targeting sequences. In this section, I aim to clarify which evolutionary changes in Top1mt enable safe handling of mtDNA. To investigate this, I inter-changed several regions of Top1 and Top1mt and tested the resulting Top1mt/Top1 hybrids for their effect on mtDNA stability. Since the highly divergent N-terminal domain of Top1 is not involved in the detrimental action on mtDNA, I will refer to Top1¹⁹¹⁻⁷⁶⁵ as full-length enzyme in the following.

4.3.1 Targeting of Top1mt/Top1 hybrids to mitochondria

Based on the crystal structure and biochemical investigations, Top1 can be divided into four domains (Redinbo et al, 1998): the N-terminal domain (a.a. 1–214), the core domain (a.a. 215–635), the linker (a.a. 636–698), and the C-terminal domain (a.a. 699–765) that contains the active site Tyr⁷²³. The largely unfolded N-terminal domain has been implicated in the nuclear localization of Top1 (Mo et al, 2000a) but it is not strictly required for the catalytic function *in vitro* (Alsner et al, 1992; Stewart et al, 1996). The C-terminal domain together with catalytic residues of the core domain constitutes the catalytic domain of Top1 (Cheng et al, 1998; Jensen & Svejstrup, 1996; Krogh & Shuman, 2000; Levin et al, 1993; Megonigal et al, 1997). Top1mt can similarly be classified into four domains, depending on the sequence alignments with Top1: The N-terminal domain (a.a. 1–51), the core domain (a.a. 52–470), the linker (a.a. 471–533) and the C-terminal domain (a.a. 534–601) containing the active site Tyr⁵⁵⁹ (Fig. 4.3.1.A). For studying which of the evolutionary changes in Top1mt have defused the repressive potential of Top1 and enabled safe handling of mtDNA, several regions of Top1mt and Top1 were inter-changed, generating Top1/Top1mt hybrids. Sites for swapping were chosen on the basis of Top1mt and Top1 protein alignment.

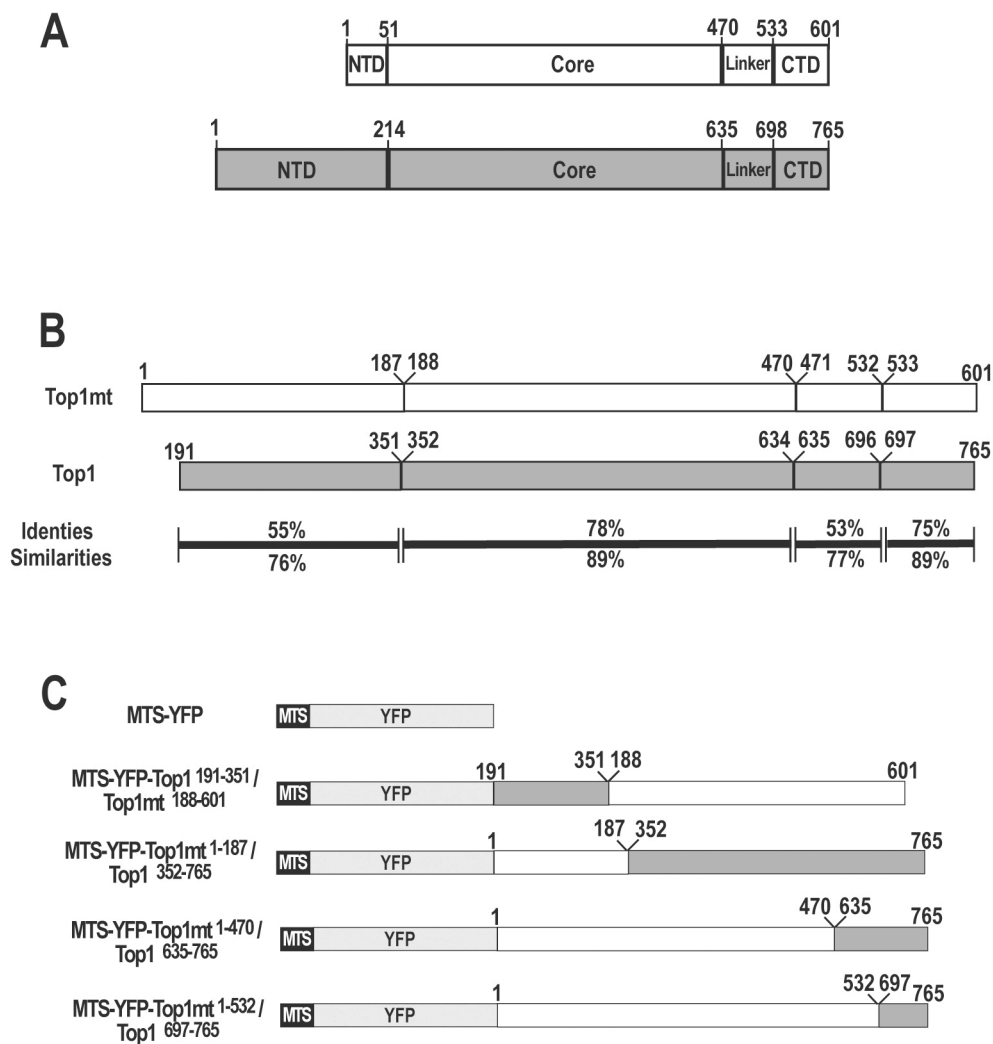


Figure 4.3.1. Top1mt/Top1 hybrids design. A) Structure comparison between Top1mt (white) and Top1 (grey). N-terminal domain (NTD), core, linker and C-terminal domain (CTD) are defined according to Top1 crystal structure. B) Sites chosen for the swapping strategy in the highly conserved catalytic domain of Top1mt and Top1. Percentages of identical and similar amino acids are indicated below each marked region. C) Schematic of the generated Top1mt/Top1 hybrids.

As described in (Zhang et al, 2001), the similarity between the two proteins is striking: Except for the N-terminal domain (NTD), Top1mt and Top1 are highly conserved, showing an overall identity of ~70% and similarity of ~85%. Since MTS-YFP-Top1¹⁹¹⁻⁷⁶⁵ and MTS-YFP-Top1²¹¹⁻⁷⁶⁵ also induced mtDNA depletion, the highly divergent NTD could be excluded as being responsible for the detrimental effect of Top1, and we assumed that the evolutionary adaptation of Top1mt must have involved mainly changes in the highly conserved catalytic domain. Within this domain, two regions exhibit a lower degree of homology: The first amino acids of the

core domain (Top1¹⁹¹⁻³⁵¹ and Top1mt³⁴⁻¹⁸⁷) and the linker domain (Top1⁶³⁶⁻⁶⁹⁷ and Top1mt⁴⁷¹⁻⁵³³) show only 55% or 53% identity and 76% or 77% similarity respectively (Fig. 4.3.1.B). Under the assumption that the regions most divergent between Top1 and Top1mt would most likely determine the functional alteration of mtDNA, I swapped Top1¹⁹¹⁻³⁵¹ and Top1mt¹⁻¹⁸⁷ generating the two hybrids proteins Top1¹⁹¹⁻³⁵¹/Top1mt¹⁸⁸⁻⁶⁰¹ and Top1mt¹⁻¹⁸⁷/Top1³⁵²⁻⁷⁶⁵. Furthermore, I exchanged the linker and C-terminal domain and the C-terminal domain alone of Top1mt with the corresponding domains of Top1, generating Top1mt¹⁻⁴⁷⁰/Top1⁶³⁵⁻⁷⁶⁵ and Top1mt¹⁻⁵³²/Top1⁶⁹⁷⁻⁷⁶⁵ respectively (Fig. 4.3.1.B). To allow targeting to the mitochondrial matrix, these hybrids were then fused at the N-terminus with MTS-YFP, generating MTS-YFP-Top1¹⁹¹⁻³⁵¹/Top1mt¹⁸⁸⁻⁶⁰¹, MTS-YFP-Top1mt¹⁻¹⁸⁷/Top1³⁵²⁻⁷⁶⁵, MTS-YFP-Top1mt¹⁻⁴⁷⁰/Top1⁶³⁵⁻⁷⁶⁵ and MTS-YFP-Top1mt¹⁻¹⁸⁷/Top1³⁵²⁻⁷⁶⁵. The basic vector MTS-YFP served as control (Fig 4.3.1.C).

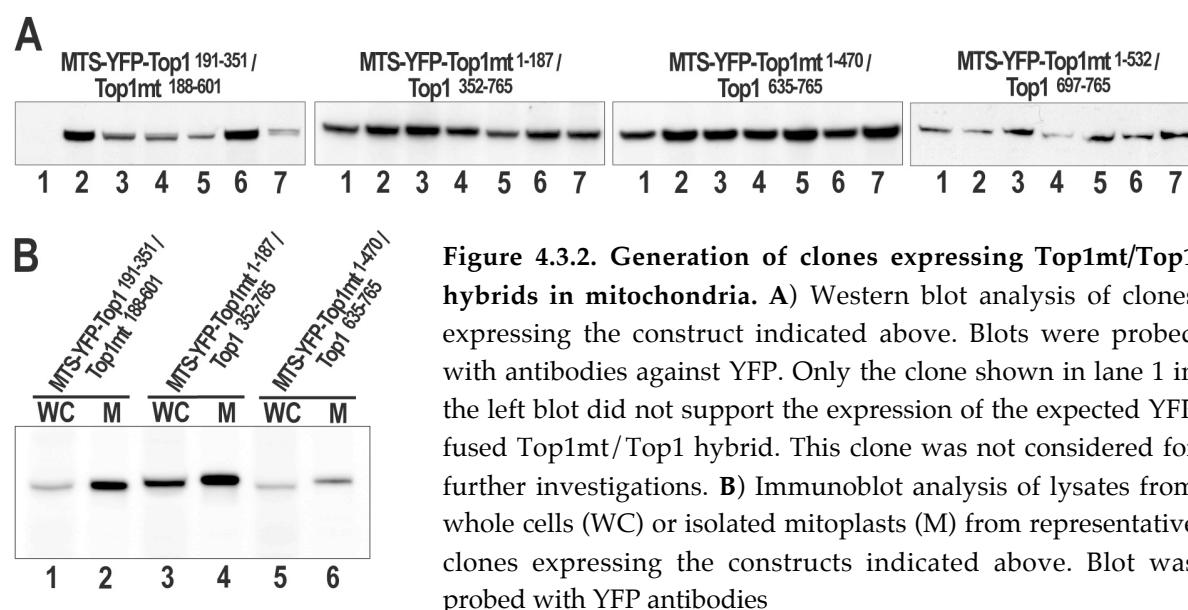


Figure 4.3.2. Generation of clones expressing Top1mt/Top1 hybrids in mitochondria. **A**) Western blot analysis of clones expressing the construct indicated above. Blots were probed with antibodies against YFP. Only the clone shown in lane 1 in the left blot did not support the expression of the expected YFP fused Top1mt/Top1 hybrid. This clone was not considered for further investigations. **B**) Immunoblot analysis of lysates from whole cells (WC) or isolated mitoplasts (M) from representative clones expressing the constructs indicated above. Blot was probed with YFP antibodies

The mitochondria-targeted YFP-Top1mt/Top1 hybrids were expressed in human HT-1080 cells. Stably expressing clones were isolated, expanded and screened under the microscope for YFP fluorescence. Cell lysates of clones showing the expected mitochondrial YFP localization were used for western blotting and probed with YFP antibody (Fig. 4.3.2.A). All constructs gave rise to several clones stably expressing an intact YFP-Top1mt/Top1 hybrid protein. To confirm that the intact fusion protein was entirely localized in the mitochondrial matrix, lysates of isolated mitoplasts were subjected to western blotting, and probed with YFP antibody (Fig. 4.3.2.B lanes 2, 4

and 6). All Top1mt/Top1 hybrids were detected at expected size, and exhibited similar band intensities in extracts from whole cells and isolated mitoplasts, indicating a predominantly mitochondrial localization of the engineered proteins.

Thus, a successful expression of YFP fused Top1mt/Top1 hybrids in mitochondria was achieved. The generated hybrid proteins were then tested with respect to their impact on mtDNA. However, a prerequisite for these investigations was that the generated hybrid proteins were correctly folded and catalytically active, which was tested first.

4.3.2 Top1mt/Top1 hybrids maintain their catalytic properties

To test if the Top1mt/Top1 hybrids were active, I determined DNA-relaxation activity in extracts of isolated mitoplasts. A representative result is shown in figure 4.3.3: Endogenous Top1mt activity co-extracted from the mitoplasts was hardly detectable. Consequently, extracts from mitoplasts of cells expressing MTS-YFP alone exhibited a weak DNA-relaxation activity (Fig 4.3.3.A). In contrast, mitoplast extracts of cells expressing MTS-YFP-Top1¹⁹¹⁻³⁵¹/Top1mt¹⁸⁸⁻⁶⁰¹, MTS-YFP-Top1mt¹⁻¹⁸⁷/Top1³⁵²⁻⁷⁶⁵ and MTS-YFP-Top1mt¹⁻⁴⁷⁰/Top1⁶³⁵⁻⁷⁶⁵ exhibited an increase in DNA-relaxation activity (Fig 4.3.3.B, C and D), due to the presence of the Top1mt/Top1 hybrids. Thus, the chimeric enzymes maintained the basic catalytic properties of Top1 or Top1mt and therefore were correctly folded.

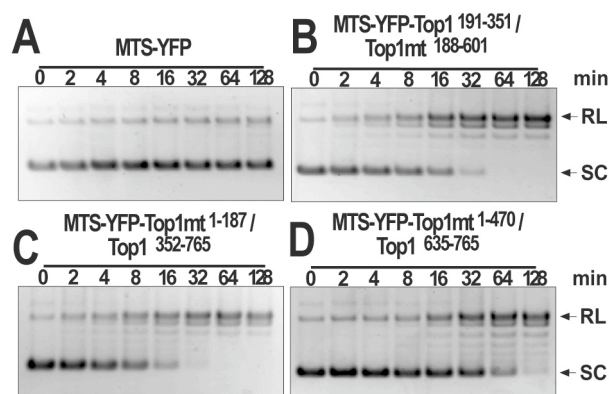


Figure 4.3.3. Top1mt/Top1 hybrids are catalytically active in mitochondria. Relaxation activity of Top1mt/Top1 hybrids from mitoplast extracts prepared from cell clones expressing MTS-YFP (A), MTS-YFP-Top1¹⁹¹⁻³⁵¹ / Top1mt¹⁸⁸⁻⁶⁰¹ (B), MTS-YFP-Top1mt¹⁻¹⁸⁷ / Top1³⁵²⁻⁷⁶⁵ (C) and MTS-YFP-Top1mt¹⁻⁴⁷⁰ / Top1⁶³⁵⁻⁷⁶⁵ (D) at 37°C for the time indicated above. Position of relaxed (RL) and supercoiled (SC) plasmid forms is indicated on the right margin.

4.3.3 mtDNA transcription-repressive properties reside in the core domain of Top1

Having shown that Top1/Top1mt hybrids are targeted to the mitochondrial matrix and are biochemical active there, I examined, how Top1/Top1mt hybrids affected mtDNA abundance. For this purpose, I determined the average number of mtDNA copies in cell clones expressing the various YFP-tagged Top1/Top1mt hybrids. MtDNA amounts of clones expressing MTS-YFP, MTS-YFP-Top1mt and MTS-YFP-Top1 already shown in section 4.1 and 4.2 are included below to enable an easier comparison with the hybrids proteins (Fig 4.3.4.A). I found that cells expressing MTS-YFP-Top1mt¹⁻⁴⁷⁰/Top1⁶³⁵⁻⁷⁶⁵ and MTS-YFP-Top1mt¹⁻⁵³²/Top1⁶⁹⁷⁻⁷⁶⁵ had mtDNA levels similar to cells expressing MTS-YFP alone or MTS-YFP-Top1mt, suggesting that linker and C-terminal domain of Top1 do not confer Top1mt the repressive effect. Interestingly, expression of the truncated version of Top1 (MTS-YFP-Top1¹⁹¹⁻³⁵¹/Top1mt¹⁸⁸⁻⁶⁰¹) induced complete mtDNA depletion, demonstrating that the repressive properties of Top1 are fully retained in a fragment encompassing residues 191-351. The hybrid MTS-YFP-Top1mt¹⁻¹⁸⁷/Top1³⁵²⁻⁷⁶⁵ did not deplete mtDNA, however, it induced a slight but significant decreased of mtDNA copies. In the previous section (see 4.2), I have shown that MTS-YFP-Top1mt activity in mitochondria decreases the level of mtDNA transcripts by about 30%. However, despite the link between mtDNA replication and transcription (Wanrooij et al, 2008), these cells had a normal amount of DNA. These findings indicate that a decrease in transcription by 30% does still allow for adequate replication of mtDNA suggesting that mtDNA replication proceeds normally until a certain lower threshold of transcription is reached where levels of mtDNA transcripts become too low to support proper replication initiation. Northern blot analysis of the mtDNA transcript 12S RNA seems to confirm this hypothesis (Fig. 4.3.4.B) in so far as 12S rRNA tended to be lower in MTS-YFP-Top1mt¹⁻¹⁸⁷/Top1³⁵²⁻⁷⁶⁵ expressing cells than in MTS-YFP-Top1mt expressing cells (Fig. 4.3.4.B, compare lanes 7-9 with 13-15). However, it should to be noted that MTS-YFP-Top1mt¹⁻¹⁸⁷/Top1³⁵²⁻⁷⁶⁵ expressing clones showed a certain variance in the amount of 12S transcript, which makes interpretation of these data difficult.

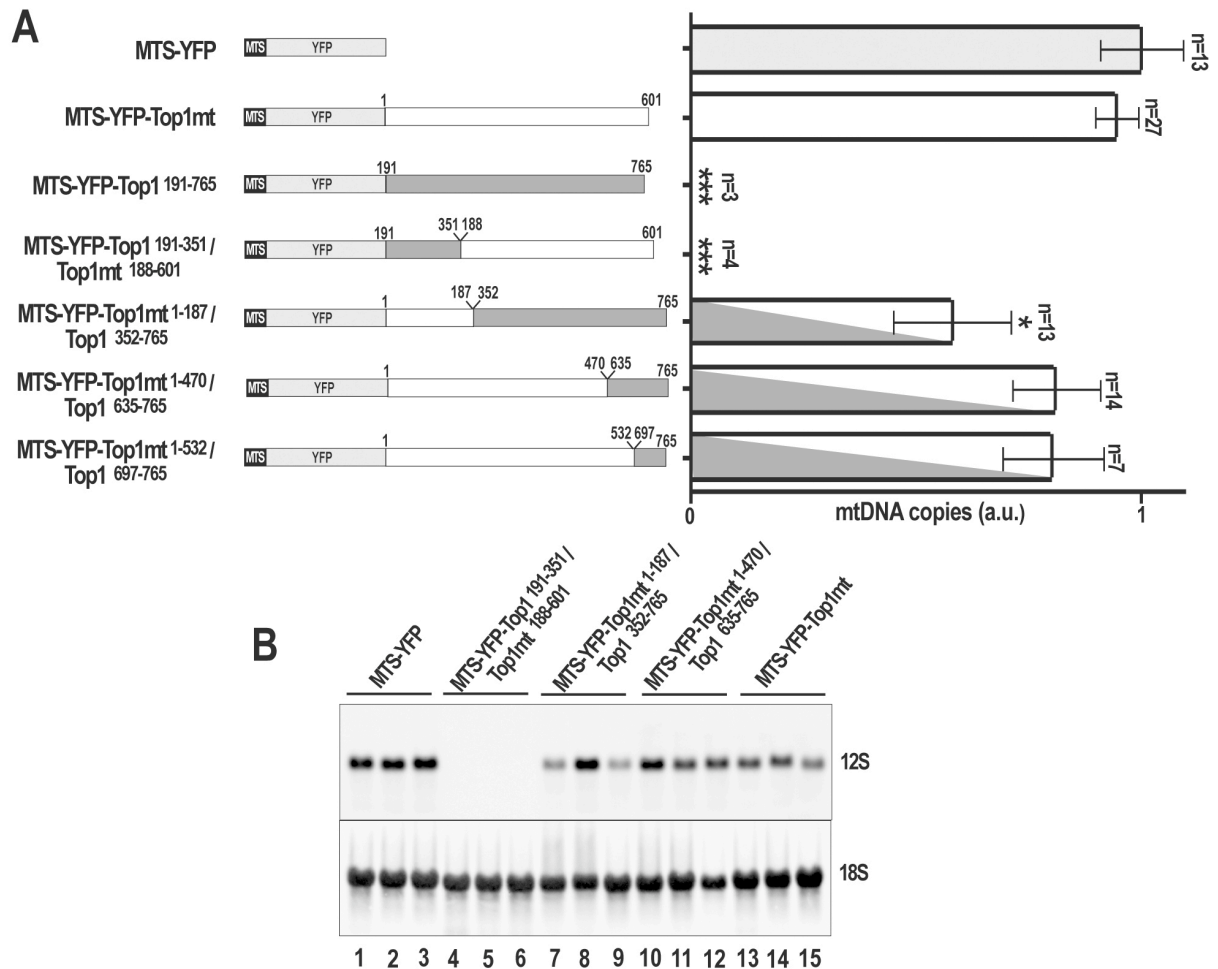


Figure 4.3.4. Effects of mitochondrial targeting of Top1mt/Top1 hybrids on mtDNA copies and transcripts. **A**) Quantification of mtDNA copies per cell in clones expressing the constructs indicated beside each column. MTS-YFP-Top1mt and MTS-YFP-Top1 are also included in the graph. All values are normalized to the mean value of the control clones expressing MTS-YFP. The number of clones investigated is indicated above each bar (n), and error bars indicate the SEM. Significant differences between each bar and the control cells are marked with asterisks (***: $p < 0.001$; *: $p < 0.05$) according to an unpaired T-test. **B**) Northern blot analysis of 12S rRNA (top) from cell clones expressing MTS-YFP (lanes 1-3), MTS-YFP-Top1¹⁹¹⁻³⁵¹/Top1mt¹⁸⁸⁻⁶⁰¹ (lanes 4-6), MTS-YFP-Top1mt¹⁻¹⁸⁷/Top1³⁵²⁻⁷⁶⁵ (lanes 7-9), MTS-YFP-Top1mt¹⁻⁴⁷⁰/Top1⁶³⁵⁻⁷⁶⁵ (lanes 10-12) and MTS-YFP-Top1mt (lanes 13-15). 18S rRNA (bottom) was used as load control.

4.3.4 Top1¹⁹¹⁻³⁵¹ manifests its repressive effect only in the context of a complete topoisomerase I enzyme.

The results of the swapping experiments summarized in figure 4.3.4.A show that mtDNA-destructive properties of Top1 are fully retained in all enzyme chimera

harbouring residues 191-352 of the core domain of Top1, while all other regions of Top1 could replace the corresponding regions in Top1mt without affecting mtDNA replication. However, it is unclear whether the core portion Top1¹⁹¹⁻³⁵¹ exerted these repressive effects on mtDNA replication by itself or only in the context of a complete enzyme. To address this, I targeted the core fragment Top1¹⁹¹⁻³⁵¹ alone to the mitochondria (using the construct MTS-YFP-Top1¹⁹¹⁻³⁵¹, see Fig 4.3.5.A) and tested whether the expression of this construct resulted in a depletion of mtDNA.

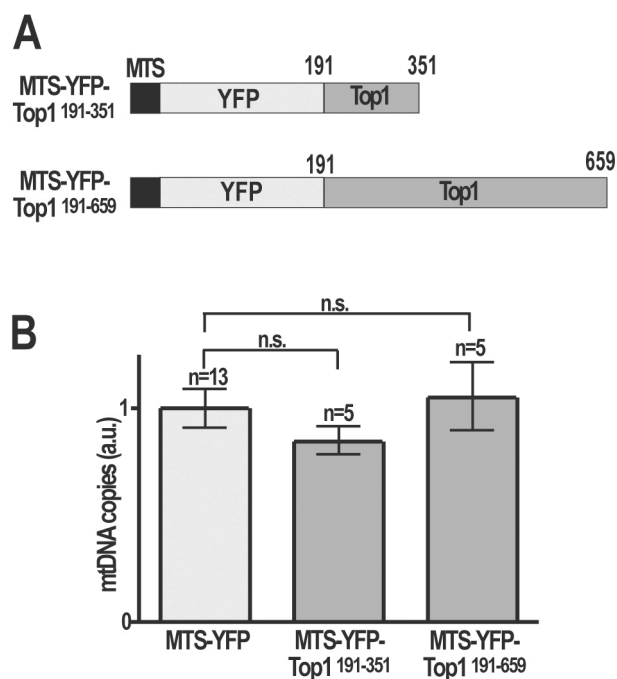


Figure 4.3.5 MtdNA quantification of clones expressing Top1 truncated variants. **A)** Schematic of the Top1 truncated variants considered. **B)** Quantification of mtDNA copies per cell in clones expressing MTS-YFP-Top1¹⁹¹⁻³⁵¹ or MTS-YFP-Top1¹⁹¹⁻⁶⁵⁹. MtDNA copies were normalized to the mean value of the MTS-YFP expressing clones. Above each bar the number of clones investigated (n) is indicated. MtDNA amounts of MTS-YFP-Top1¹⁹¹⁻³⁵¹ and MTS-YFP-Top1¹⁹¹⁻⁶⁵⁹ expressing cells did not differ significantly from the control according to an unpaired T-test.

I found that cells expressing MTS-YFP-Top1¹⁹¹⁻³⁵¹ had a normal amount of mtDNA (Fig 4.3.5.B), suggesting that Top1¹⁹¹⁻³⁵¹ manifests its repressive effect only in the context of a complete topoisomerase I. This result was not surprising and accorded to published observations that Top1 CTD (a.a. 713–765), although containing the active site tyrosine, lacks in itself topoisomerase I activity (Stewart et al, 1997). Furthermore, fragment complementation studies have shown that core and C-terminal domains together represent the minimal requirement for DNA relaxation *in vitro* (Stewart et al, 1997). Moreover, fragments encompassing core or C-terminal domains can interact *in vitro* to reconstitute the enzymatic activity of Top1, suggesting that the interaction of these domains provides the DNA clamping function essential for the activity of Top1. Given that Top1¹⁹¹⁻³⁵¹ in itself did not have a repressive effect on mtDNA replication, whereas this effect was unmasked in all enzyme chimera combining this domain with a C-terminal domain stemming either from Top1 or Top1mt, it can be concluded that the interaction with the CTD plays a crucial role in

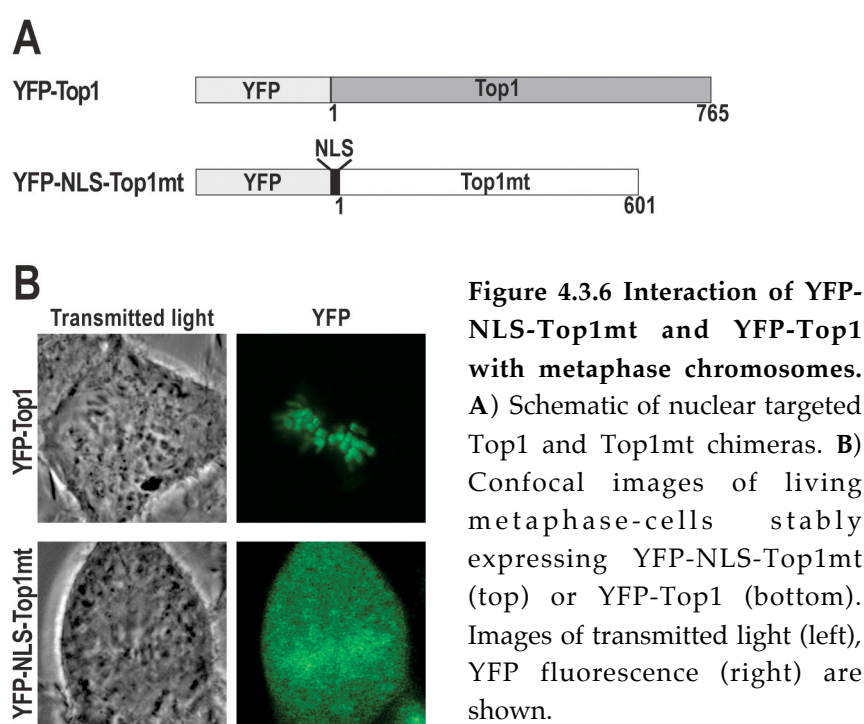
the repressive properties of Top1¹⁹¹⁻³⁵¹. To address this point, I investigated a fragment of Top1 encompassing residues 191-659. Top1¹⁹¹⁻⁶⁵⁹ is lacking the CTD and therefore inactive, but it can be reconstituted *in vitro* to full activity by addition of a recombinant CTD (Stewart et al, 1997). For targeting to the mitochondrial matrix, Top1¹⁹¹⁻⁶⁵⁹ was fused at the N-terminal with MTS-YFP, generating MTS-YFP-Top1¹⁹¹⁻⁶⁵⁹ (Fig. 4.3.5.A). I found that HT-1080 cells expressing this construct had a normal amount of mtDNA, confirming my assumption that the core domain of Top1 has to act in concert with a CTD to exert its repressive effect on mtDNA transcription/-replication and induce the ρ^0 phenotype. It should be noted however, that requirement of interactions with a CTD does not include that this domain needs to have an active site, since Top1^{191-765, Y723F} also induced depletion of mtDNA although it lacks the active site tyrosin and is catalytically inactive.

4.3.5 Top1 and Top1mt differ in their interaction with nuclear genomic DNA

I have demonstrated that vertebral adaptation of Top1 to functioning in the mitochondrial context involves amino acid changes in the core domain (a.a. 191-351). It remains unclear how and why these amino acid changes defuse or attenuate the unfavourable interactions of nuclear Top1 with mtDNA. Clearly, catalytic activity does not play a role in this, since the dominant negative effect of Top1 on mtDNA is fully retained in an active site mutant. On the other hand, these effects appear to require all domains constituting the core enzyme, which suggests that conformational alterations of the entire enzyme molecule could play a role in adapting it to the handling of mtDNA. My data furthermore suggest, that such conformational changes could be related to the way the enzymes clamps around DNA, since the relevant alterations in the core domain of Top1 seem to modify its interactions with the C-terminal domain, which are crucial in forming and operating the DNA-clamp. Given finally the impact of the DNA-clamp on the way the enzyme handles DNA in general, it is plausible to speculate that the crucial difference between Top1 and Top1mt could be related to their DNA interactions in the context of the chromatin or nucleoid, respectively.

To gain some insight into this, I did a crossover experiment targeting Top1mt to the cell nucleus and comparing its ability to interact with nuclear genomic DNA to that of Top1 (Fig. 4.3.6.). To do this, Top1mt was fused to YFP to allow visualization and a NLS was added to target it to the nucleus. Cells stably expressing the emerging

construct YFP-NLS-Top1mt were compared with cells expressing YFP-Top1 (Christensen et al, 2002a) (Fig. 4.3.6.A). Thus, I was able to compare in the cell nucleus the ectopic behaviour of mtTop1 with the orthotopic behaviour of Top1. As shown in Fig. 4.3.6.B, in metaphase cells YFP-NLS-Top1mt did scarcely interact with, and accumulate on, the chromosomes, while YFP-Top1 was entirely accumulated on the chromosomes as previously reported (Christensen et al, 2002a). These data support the above reasoning in so far as they show that the two enzymes have a fundamentally different propensity of targeting DNA in a biological context, although they have a similar affinity to “naked” DNA in a test tube (Zhang et al, 2001).



4.3.6 Evolutional change of Top1mt occurs in a highly conserved region

The results presented up to here in section 4.3. identify the first region in the core domain as the one bearing the genetic differences crucial for the different effects of Top1 and Top1mt on mtDNA. In the next step, I subjected this domain to a detailed analysis of genetic divergence between Top1 and Top1mt and checked by construction of further hybrid proteins which of these differences in coding DNA-sequence had an impact on mtDNA handling by the enzymes.

Considering the crystal structure of Top1 (see 1.2.3.1), the relevant region coincides

with the entire subdomain II (residues 233-319) and part of subdomain I (residues 215-232 and 320-433) of the core domain. Subdomains I and II form the cap region of Top1, whereas subdomain III (residue 434-635), together with linker, and C-terminal domain, forms the lower lobe of Top1. In the closed clamp configuration of the enzyme, the two lobes of Top1 are joined through a hinge region on one side of the DNA molecule (corresponding with the region between Subdomain III and II, residues 430-440) and contact each other in the lips region on the opposite side (residues 367-369 of subdomain I and residues 497-499 of subdomain III).

An amino acid alignment of the first regions of the core domain of Top1 and Top1mt is shown in figure 4.3.7.A. The secondary structure, as predicted from the crystal structure of Top1 (Redinbo et al, 1998), is aligned underneath. It is readily apparent that the aligned region can be divided into two distinct portions, differing in their degree of homology: The first half encompassing residues 206-286 is more conserved. Here 56 of 80 amino acids (70%) are identical in Top1 and Top1mt. In contrast, the second half encompassing residues 287-351 shows a higher genetic divergence with only 33 of 65 amino acids (51%) identical. The less conserved half is located adjacent to the “lips” of Top1 (a.a. 367-369) that open and close the space between cap and base of the protein. Differences in amino acid composition in this region could therefore have an impact on the way Top1 clamps around DNA, a function which I suspect to play a role in the overall functional differences between the two enzyme forms. To test the assumption that differences in the amino acid composition of this second half of the region are responsible for the functional differences between Top1 and Top1mt, I created chimera between the two enzymes swapped after residue 286 of Top1 and 122 of Top1mt, respectively (indicated in red in Fig. 4.3.7.A), thus generating the two hybrids protein Top1¹⁹¹⁻²⁸⁶/Top1mt¹²³⁻⁶⁰¹ and Top1mt¹⁻¹²²/Top1²⁸⁷⁻⁷⁶⁵ (schematic drawing in Fig. 4.3.7.B). Moreover, I analysed the putative impact of amino acid substitutions in this sub-region on the structure of Top1mt as compared to Top1: Although the crystal structure of Top1mt is not yet known, *in silico* analysis (Scratch Protein Predictor <http://www.ics.uci.edu/~baldig/scratch/index.html>) suggests a secondary structure very similar to that of Top1. The only major structural difference is predicted in region Top1³⁰⁰⁻³⁴⁰, where in Top 1 two long α helices (α 5 and α 6) form the “nose-cone”. In Top1mt these two helices seem to be replaced by a single long α helix. To test the functional relevance of this specific replacement, I replaced the double “nose-cone” α helices of Top1 with the single one of Top1mt and *vice versa* (Fig. 4.3.7.B, chimeric constructs Top1mt¹⁻¹²²/Top1²⁸⁷⁻³⁵¹/Top1mt¹⁸⁸⁻⁶⁰¹ and Top1¹⁹¹⁻²⁸⁶/Top1mt¹²³⁻¹⁸⁷/Top1³⁵²⁻⁷⁶⁵).

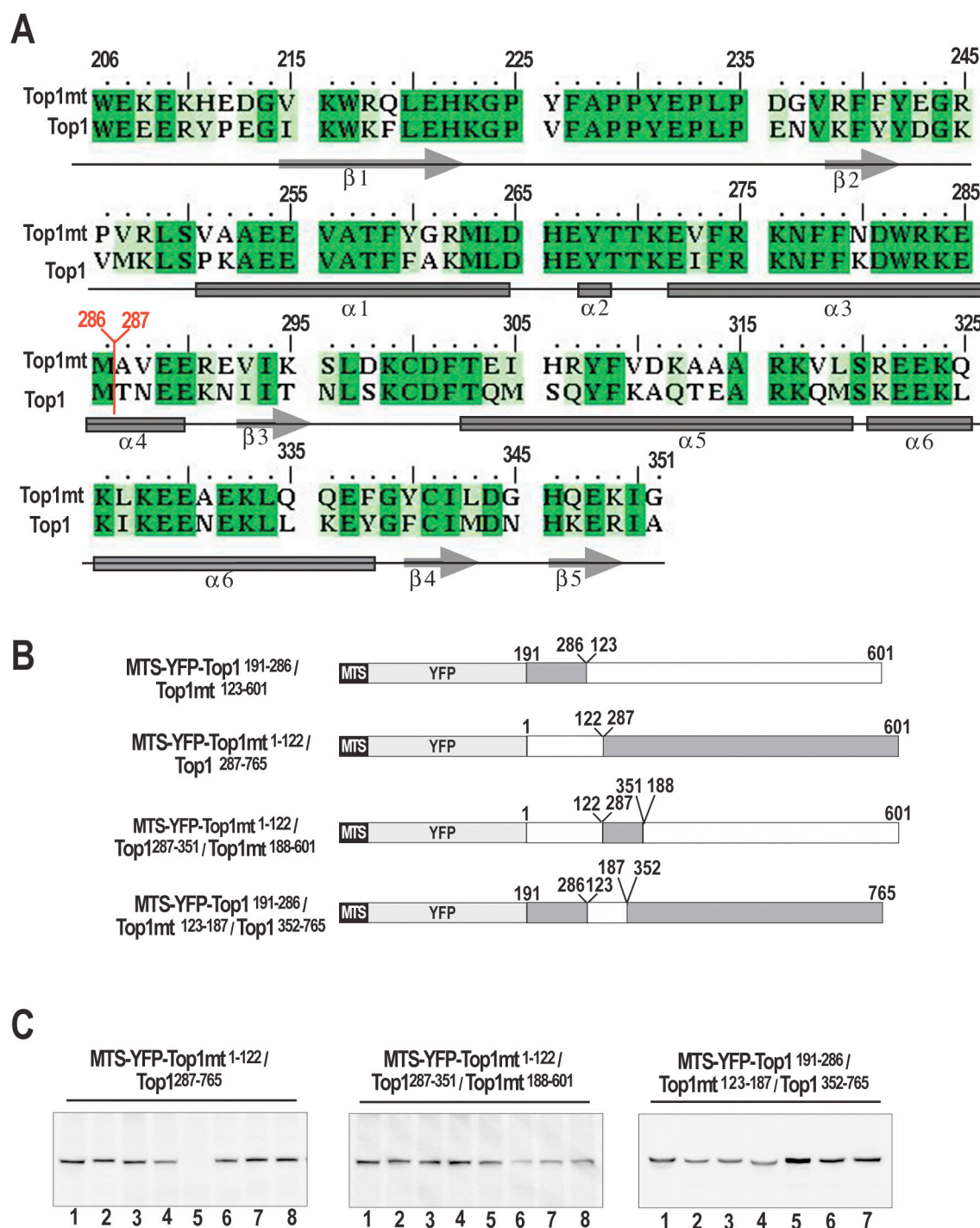


Figure 4.3.7. Generation of further Top1mt/Top1 hybrids and expression of this in mitochondria. A) Protein sequence alignment between Top1²⁰⁶⁻³⁵¹ and Top1mt⁴²⁻¹⁸⁷. Top1²⁰⁶ was chosen as start for the alignment since it represents the first residue of Top1 13-exon signature. The identical and similar amino acids are in dark and light green respectively. The numeration indicated above the alignment refers to Top1 amino acid sequence. Under the alignment the secondary structure of Top1 is shown. The position chosen as Top1 and Top1mt swapping site is marked in red. B) Schematic representation of the generated Top1mt/Top1 hybrids C) Western blot analysis of whole cell lysates of clones expressing the construct indicated above. Blots were stained with YFP antibodies.

Results

These chimeric constructs were fused to MTS-YFP and transfected into HT-1080 cells, and cell clones with stable mitochondrial expression of the fluorescent proteins were selected and expanded. Selection for expression of the two constructs where the N-terminal half of Top1mt was combined with the C-terminal half of Top1 (MTS-YFP-Top1mt¹⁻¹²²/Top1²⁸⁷⁻⁷⁶⁵), where the double helix “nose cone” of Top1 was incorporated into the context of Top1mt (MTS-YFP-Top1mt¹⁻¹²²/Top1²⁸⁷⁻³⁵¹/Top1mt¹⁸⁸⁻⁶⁰¹) or where the single helix “nose cone” of Top1mt was incorporated into the context of Top1 (MTS-YFP-Top1¹⁹¹⁻²⁸⁶/Top1mt¹²³⁻¹⁸⁷/Top1³⁵²⁻⁷⁶⁵) gave rise to many cell clones. YFP-directed immunoblotting analysis showed that these cells supported the expression of an intact fusion protein (Fig. 4.3.7.C). In contrast, expression of the construct where the N-terminal half of Top1 was combined with the C-terminal half of Top1mt (MTS-YFP-Top1¹⁹¹⁻²⁸⁶/Top1mt¹²³⁻⁶⁰¹) failed completely.

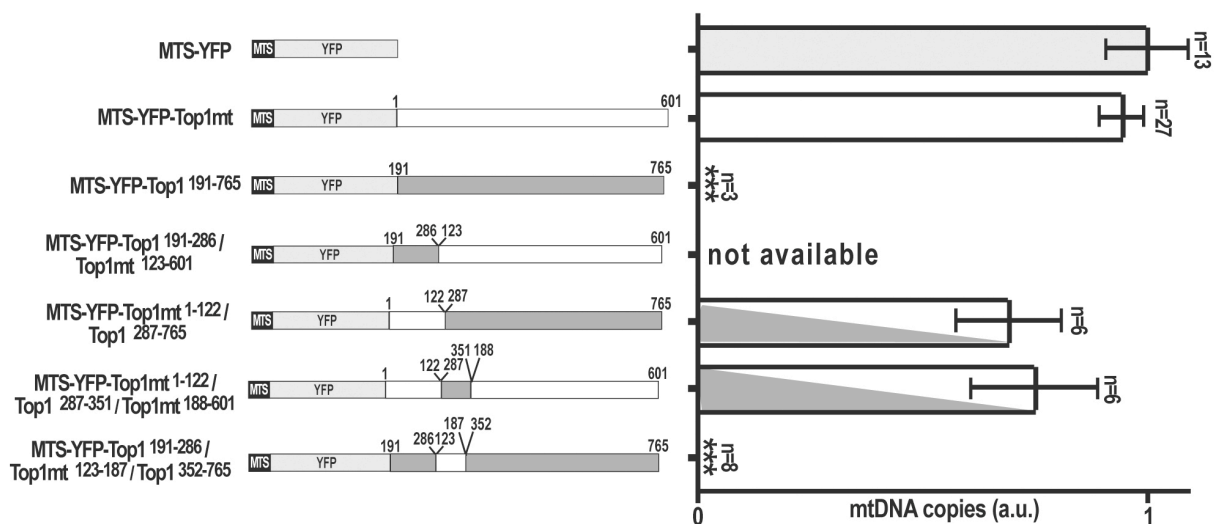


Figure 4.3.8. Quantification of mtDNA copies in cells expressing Top1mt/Top1 hybrids in mitochondria. Quantification of mtDNA copies per cell in clones expressing the constructs indicated beside each column. All values are normalized to the mean value of the control clones expressing MTS-YFP. The number of clones investigated is indicated above each bar (n), and error bars indicate the SEM. Significant differences between each bar and the control cells are marked with asterisks (***) $p < 0.001$ according to an unpaired T-test.

To corroborate these observations, I determined the average number of mtDNA copies in the cell clones available. These data are plotted in Fig. 4.3.8, together with the data obtained for cells expressing just MTS-YFP, MTS-YFP-Top1mt or MTS-YFP-Top1 (already presented in section 4.1 and 4.2). In the cells expressing the N-terminal

half of Top1mt combined with the C-terminal half of Top1 (MTS-YFP-Top1mt¹⁻¹²²/Top1²⁸⁷⁻⁷⁶⁵) or the double helix “nose cone” of Top1 in the context of Top1mt (MTS-YFP-Top1mt¹⁻¹²²/Top1²⁸⁷⁻³⁵¹/Top1mt¹⁸⁸⁻⁶⁰¹), mtDNA levels were only slightly diminished as compared to cells expressing just MTS-YFP. In contrast, in the single clone presenting the single helix “nose cone” of Top1mt in the context of Top1 (MTS-YFP-Top1¹⁹¹⁻²⁸⁶/Top1mt¹²³⁻¹⁸⁷/Top1³⁵²⁻⁷⁶⁵), mtDNA was completely depleted. In summary, these findings show that, contrary to my expectations, it is the extreme N-terminal and highly conserved region of the core domain of Top 1 (a.a. residues 191-286) that confers the repressive effect on mtDNA. All constructs delivering this portion in the context of a minimally functional Top1 enzyme to the mitochondrial matrix induced complete loss of mtDNA. In contrast, all constructs not having this portion did not induce significant depletion of mtDNA, irrespective of how the rest of the enzyme was composed. Most notably, the significant structural differences predicted in the “nose cone” of Top1 and Top1mt play no role in the adaptation of the enzyme to a state not repressing mtDNA replication/-transcription.

5. Discussion

Topoisomerase activity is believed to be an essential cofactor of mtDNA metabolism (Wang et al, 2002). In keeping with this, all three topoisomerase subfamilies present in the vertebrate cell nucleus, type IA, IB and IIA, are also represented in the mitochondria by Top3 α , Top1mt and Top2 β , respectively. Vertebrate evolution has split topoisomerase I into two genetically independent variants Top1 and Top1mt, which are responsible for the nuclear and for the mitochondrial compartment, respectively. The meaning of this splitting is very puzzling, since these two enzymes show an extremely high sequence homology and a nearly identical biochemical activity (Zhang et al, 2001). Moreover, the development of Top1mt was not required in non-vertebrates that utilize Top1 in both nucleus and mitochondria (Tua et al, 1997; Wang et al, 1995). Most notably, the gene of Top1mt was found to be inessential for mouse development, even though its loss may have negative effects on the adult mouse that are still unknown (Zhang et al, 2007). Since the separate encoding does not seem to provide for an essential function, I formed the hypothesis that it might serve to improve regulation and diminish harmful properties that Top1 possibly has when interacting with mtDNA. Implicit in this assumption is that unregulated overexpression of Top1mt and ectopic expression of nuclear Top1 in the mitochondria should have adverse effects on mitochondrial function and mtDNA maintenance. Here, I tested this experimentally. I demonstrate that elevation of Top1mt activity could influence mtDNA transcription, while targeting of Top1 to the mitochondria has similar effects albeit at a much more dramatic level. To my knowledge, there is no comparable study available that addresses this issue.

5.1 Mitochondrial targeting of Top1 is incompatible with a correct mtDNA metabolism in human cells

I found that cells stably expressing mitochondria-targeted variants of nuclear Top1 completely lost their mtDNA and showed a phenotype also seen in ρ^0 cells, which are depleted of mtDNA by continuous exposure to EtBr (Gilkerson et al, 2000; King & Attardi, 1989). This dramatic effect of Top1 in mitochondria must be due to specific

structural properties of nuclear Top1 and not to its overexpression, because overexpression of Top1mt at similar levels did not lead to a loss of mtDNA. Therefore, the evolution of Top1mt was obviously necessary to allow for stable propagation of the mitochondrial genome in vertebrates.

5.1.1 Effects on cell-physiology of Top1 mitochondrial targeting

Cells expressing mitochondria-targeted Top1 missed a functioning OXPHOS and their energy production relied entirely on anaerobic glycolysis (see 4.2.6). In addition in the absence of a functional respiratory chain, thymidine and cytidine were not synthesised thereby inducing growth arrest. Growth arrested cells developed hallmarks of cell senescence such as a notable increase in cell size and a cytochemically detectable β -galactosidase staining (see 4.2.8). Senescence was first identified about 50 years ago as a phenomenon in which cultured primary cells stop growing after about 50 cell divisions (Hayflick, 1965). Telomere shortening and the induction of tumour suppressor p16 contribute to limit the lifetime of the cells, which undergo an irreversible growth arrest predominantly in G_1/S phase of the cell cycle (Pazolli & Stewart, 2008). Cell senescence is not only a physiological process of aged cells but also represents a defence mechanism. In fact, senescence can also be induced by different stress stimuli such as oncogene expression, DNA damage and oxidative stress (Campisi, 2005). However, the growth arrest in cells expressing mitochondria-targeted Top1 shown here occurred preferentially in the G_2 phase as consequence of a defective mtDNA synthesis. Moreover, the senescent phenotype found in these cells could be reverted by addition of uridine (see 4.2.7). This reversibility and the increased levels of cells in G_2 – phase contrasts typical features of cell senescence and, at the moment, it is not clear how to interpret the phenotype of senescence in cells depleted of mtDNA due to ectopic expression of Top1. In addition, it should be considered that the β -galactosidase staining is a rather unspecific marker for senescence, since other factors such as different cell culture conditions can also increase β -galactosidase activity in the cell (Severino et al, 2000). It is possible that the Top1-mediated mtDNA depletion evoked a cellular response similar to stress induced cell senescence. However, to confirm this assumption, further investigation of the downstream effectors of senescence like p16 are needed.

5.1.2 Which evolutionary changes have generated or defused the mtDNA repressive potential of Top1 or Top1mt, respectively?

I have invested a lot of experimental effort into finding out which evolutionary differences between Top1mt and Top1 allow safe handling of mtDNA by the one but not the other form of the enzyme. Previous investigations have shown that differences between Top1 and Top1mt result in a slight alteration of optimal catalytic conditions for the two enzymes *in vitro* (Zhang et al, 2001). However, mitochondrial targeting of Top1 active site mutants (Top1^{Y723F} and Top1^{191-765, Y723F}) also depleted mtDNA, demonstrating that the detrimental properties of Top1 did not depend on its catalytic activity. Therefore the adaptation in the pH-optimum of DNA catalysis is clearly not reason why nuclear Top1 acts repressive on mtDNA. Another potential outcome of the amino acid changes of Top1mt could involve the DNA binding properties of the enzyme. Top1 is a bi-lobed clamp-like protein that completely encompasses the DNA duplex (Champoux, 2001; Leppard & Champoux, 2005). In the nucleus, it is able to interact with DNA packaged in a highly complex chromatin structure (Felsenfeld & Groudine, 2003). Given the different structure and organisation of nuclear and mitochondrial DNA, Top1 could be too “aggressive” to act in the mitochondrial compartment and it is plausible to assume that Top1mt represents an attenuated variant of Top1. In support of this hypothesis, I found that Top1mt targeted to the nucleus was less prone to interact with nuclear genomic DNA than the corresponding fragment of Top1 (see 4.3.5). Clearly these data do not provide a direct evidence for differences in the affinity for DNA of Top1 and Top1mt, since it cannot be excluded that Top1mt is inactive in the nucleus. Nevertheless, this observation supports the hypothesis that Top1 and Top1mt have a different ability and/or fashion to bind DNA in the cell.

Since N-terminally truncated variants of Top1 (Top1¹⁹¹⁻⁷⁶⁵ and Top1²¹¹⁻⁷⁶⁵) also depleted mtDNA (see 4.2.3), the detrimental properties of the enzyme must reside in the amino acid sequence of the catalytic domain (Top1²¹⁵⁻⁷⁶⁵ corresponding to Top1mt⁵²⁻⁶⁰¹). Since this region is highly conserved in Top1 and Top1mt (70% identities and 85% similarities) (Zhang et al, 2001), only minor divergences between the two enzymes can be responsible for their completely different impact on mtDNA. Within the highly conserved catalytic domain, the linker domain (Top1⁶³⁵⁻⁶⁹⁸ corresponding to Top1mt⁴⁷⁰⁻⁵³³) and the N-terminal region of the core (Top1mt¹⁻¹⁸⁷ corresponding to Top1¹⁹¹⁻³⁵¹) show the lowest degree of homology between Top1mt and Top1 (see 4.3.1). The linker of Top1 is a flexible, positively charged coiled-coil

structure that connects core and C-terminal domain in a conformation that wraps completely around DNA. Since loss of the linker strongly reduces the affinity of Top1 for DNA (Stewart et al, 1997), this domain was the initial candidate conferring mtDNA destructive properties to Top1. However, the linker domain of Top1mt and Top1 could be ex-changed without conferring repressive or tolerant effects on mtDNA accordingly (see 4.3.3), suggesting that evolutionary changes of this region are not involved in these effects. In contrast, when Top1mt¹⁻¹⁸⁷ was exchanged with Top1¹⁹¹⁻³⁵¹, Top1mt became detrimental for mtDNA and, *vice versa*, substitution of Top1¹⁹¹⁻³⁵¹ with Top1mt¹⁻¹⁸⁷ could rescue Top1 detrimental phenotype (see 4.3.3). Thus, the mtDNA destructive properties of Top1 reside in the first region of the core domain (Top1¹⁹¹⁻³⁵¹). Considering the structure of Top1 clamping DNA, Top1¹⁹¹⁻³⁵¹ forms part of the cap region and is characterized by two long nose-cone helices (see 1.2.3.1). Since positively charged, these helices could play a prominent role in the affinity of Top1 for DNA similar to the linker domain. Moreover, *in silico* analysis of Top1mt secondary structure predicts that the nose-cone helices are replaced by a single long helix in Top1mt (see 4.3.6). However, inter-changing these helices did not abrogate the detrimental effect of Top1 and, *vice versa*, Top1mt still allowed stable mtDNA propagation. Thus, the evolutionary changes allowing Top1mt to work in the mitochondrial context must reside in the extreme N-terminal region of its core domain (Top1mt¹⁻¹²² corresponding to Top1¹⁹¹⁻²⁸⁷). Importantly, targeting of C-terminally truncated variants of Top1, carrying only the detrimental region Top1¹⁹¹⁻²⁸⁷, did not deplete mtDNA (see 4.3.4). Thus, Top1¹⁹¹⁻²⁸⁷ triggers mtDNA-repressive properties only in the context of a complete topoisomerase I. Taken together these data show that the correct folding of Top1 in the clamp-like conformation is necessary to bring about the repression of mtDNA.

5.1.3 How does Top1 deplete mtDNA?

Analysis of the mtDNA and RNA depletion kinetics following expression of mitochondria targeted Top1 (see 4.2.10) showed that the primary effect is a repression mtDNA transcription leading to a loss of primers for replication and a serial a serial dilution of mtDNA copies in the cell population until complete depletion (see 4.2.9). Analysis of the replication intermediates showed that Top1 did not interfere with already initiated replication events but rather reduced *de novo* mtDNA transcripts. This could result from the active inhibition of mtDNA transcription or from interference with mtRNA stability. My data do not permit to

discriminate between these two alternatives. However, the evidence that mtRNA reduction led to a block of replication strongly suggests the inhibition of *de novo* mtDNA transcription. The transcription intermediates revealed a strong decrease of RNA-rich RIs in the early phase of Top1 expression as well as in the course of mtDNA depletion. This reduction is consistent with the general decline of all RIs. However, there were still some RNA rich RIs detectable, which is in some contrast to the almost complete depletion of mtDNA transcripts measured with RT-qPCR (see fig. 4.2.9.B). Two major hypotheses have been proposed as rationale of RNA-DNA hybrids generation during mtDNA replication: One hypothesis assumes that RNA is synthesized *de novo* by POLRMT primase activity. Another theory excludes the predominant role of *de novo* transcription in the generation of RNA rich RIs, proposing instead that already produced transcripts hybridize with the lagging strand (Yasukawa et al, 2006). My findings show an almost complete depletion of mtDNA transcripts but a persistence of RNA-rich RIs. This supports the latter model suggesting that, even when mtDNA transcription was strongly inhibited, already initiated replication could complete without interruption using already produced transcripts. The dominant negative effect induced by mitochondrial targeting of Top1 variants is not without precedence. For example, heterologous expression of mutated twinkle or POLG in HEK293 cells also strongly lowers mtDNA copy number by blocking mtDNA synthesis (Jazayeri et al, 2003; Spelbrink et al, 2000; Wanrooij et al, 2007). In the same model, manipulation of the TFAM expression level also results in mtDNA reduction (Pohjoismaki et al, 2006). Moreover, RNA interference of TFB2M in *D. melanogaster* Schneider cells reduces mtDNA transcription, consequently decreasing mtDNA copy number threefold (Matsushima et al, 2004). From this it has been concluded that a correct propagation of mtDNA requires the cooperation of both transcription and replication. The transcriptional process produces the RNA primers that are then used by POLG to initiate replication. In the mitochondria, POLRMT has dual functions and acts as RNA polymerase and primase producing long polycistronic transcripts as well as short RNA primers (Wanrooij et al, 2008). Moreover, during vertebrate mtDNA replication, RNA is transiently incorporated throughout the lagging strand, generating RNA-DNA hybrids noted as RNA-rich RIs (Yasukawa et al, 2006) (see 4.2.10).

Identification of the genetic changes in Top1mt versus Top1 responsible for the repressive effect on mtDNA offers the opportunity to speculate about mechanism(s) by which Top1 mediates mtDNA depletion. Having demonstrated that the mitochondrial targeting of Top1 leads to a blockage of mtDNA replication due to the strong reduction of mtDNA transcription, it is possible that Top1 might interfere with essential cofactor/s of mtDNA transcription. As suggested above, the effect of Top1 on mtDNA could be due to the strong binding affinity of the enzyme. The first persuasive hint comes from the correct folding of Top1 in the clamp-like conformation, but not its catalytical activity, was necessary to endanger mtDNA. A second hint is provided by Top1 structural data: A few amino acids (Top1²⁰¹⁻²¹⁴) of the detrimental region of Top1 are in contact with the putative hinge region of the enzyme (fig. 5.1). Thus, the N-terminal region may play a role in Top1 opening and closing around DNA (Redinbo et al, 2000) and could consequently modulate DNA binding of Top1. The different ability of Top1 and Top1mt to interact with nuclear DNA, as demonstrated here by the nuclear targeting of Top1mt, supports this theory indirectly (see 4.3.5).

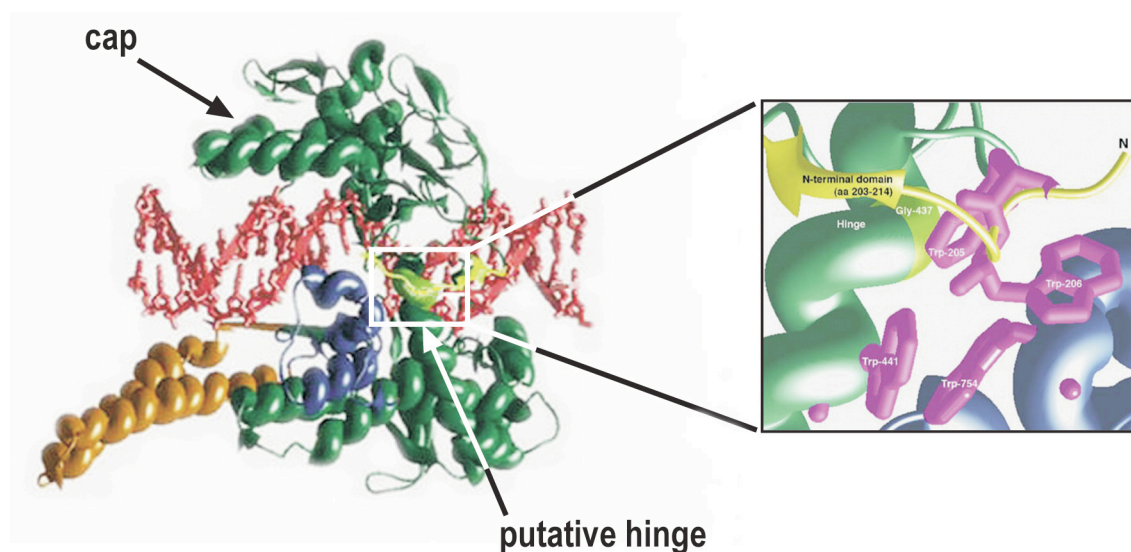


Fig. 5.1: Top1 N-terminal region interacts with the hinge. Left is shown a schematic representation of Top1 crystal structure in association with DNA (red). The N-terminal, core, linker and C-terminal domains are depicted in yellow, green, orange and blue, respectively. The region where NTD interact with the putative hinge of the enzyme (outlined box) is shown in detail in the stereo view on the right side. Hydrophobic residues (magenta) of NTD (yellow), core (green) and CTD (blue) form a cluster in close proximity of Top1 putative hinge (Gly-437, light green), probably influencing the clamp of Top1 around its substrate. Figure adapted from (Leppard & Champoux, 2005).

Thus, a too firm binding of Top1 to mtDNA could be the reason why mtDNA transcription gets blocked. In this context, a recent *in vitro* study showed a dramatic reduction of POLRMT primase activity if mtDNA was coated with mtSSB (Wanrooij et al, 2008). However, it is unlikely that Top1 also inhibits mtDNA transcription by coating mtDNA. RIs of cells subjected to Top1 action did not show signs of replication stalling (see 4.2.10) indicating that Top1 did not represent a physical barrier for the replication fork. Top1 does not possess strict substrate specificity at nucleotide sequence level (Been et al, 1984) but it prefers supercoiled over relaxed DNA (Camilloni et al, 1988; Muller et al, 1985). Thus, it is plausible that Top1 recognizes specific tertiary-DNA structure of mtDNA such as the D-loop. In fact, it has been recently shown that Top1mt associates with mtDNA directly downstream of this regulatory region of mtDNA (Zhang & Pommier, 2008). A strong accumulation of Top1 at the D-loop may exclude essential transcription factors from the promoters inhibiting mtDNA transcription.

The interaction of Top1 with other proteins represents another possible explanation for its inhibitory effect on mtDNA transcription. In this regard, the folding of the enzyme could play a key role, defining the boundary surface for the contact between Top1 and other protein partners. It is proposed that, through interaction with transcription factors, Top1 can act as repressor of basal transcription in a manner that is independent of its relaxation activity (Merino et al, 1993). Interestingly, the cap region of Top1, shown here to be involved in the repression of mtDNA transcription, can interact with the RNA recognition motive (RRM) of several splicing factors in the nucleus (Trzcinska-Daneluti et al, 2007).

In addition to the prominent role in the management of the topological state of DNA, Top1 has an additional function as kinase in the nucleus (Rossi et al, 1996). Top1 binds and phosphorylates transcription factors, which regulate the splicing process and, hence, the gene expression. Interestingly, the kinase activity of Top1 is independent of its catalytic activity (Rossi et al, 1998). Similar to splicing factors, members of the rRNA methyltransferases family like TFB1M and TFB2M possess the capacity to bind RNA and/or ssDNA (Falkenberg et al, 2002). Top1 could therefore target TFB1M and TFB2M and inhibit their function. In fact, TFB2M knockdown in Schneider cells leads to a phenotype similar to that caused by Top1 in mitochondria because it also shows a reduced mtDNA transcription and decreased mtDNA copy number (Matsushima et al, 2004).

5.2 Heterologous expression of Top1mt

Top1mt is the only topoisomerase specifically developed for the mitochondrial compartment (Zhang et al, 2001). This genetic feature suggests that activity of Top1mt may be critical in vertebrates. Similar to the functions of Top1 in the nuclear compartment, Top1mt could be a key player in the metabolism of the mitochondrial genome. The fact that the gene of Top1mt was found to be inessential for mouse development (Zhang et al, 2007) argues against this. On the other hand, I have shown that at least the nuclear form of the enzyme represses mtDNA transcription and –thereby replication, which is detrimental to mitochondrial function. It could be envisaged that such a potential is still present in Top1mt, albeit masked or attenuated. To address this, I have here induced a deregulated over-expression of Top1mt to investigate the effects exerted by enhanced levels of Top1mt activity in the mitochondrial matrix on mtDNA metabolism.

5.2.1 Top1mt possesses an inherent potential to inhibit transcription of mitochondrial genes

I found that overexpression of wild type Top1mt or expression of mitochondria-targeted YFP fused Top1mt (MTS-YFP-Top1mt) or catalytical inactive variant (MTS-YFP-Top1mt^{Y559F}) did not affect the average number of mtDNA copies (see 4.1.4.1). The consequence of an enhanced Top1mt activity on the transcription was puzzling: MTS-YFP-Top1mt induced a significant decrease in mtDNA transcripts, an effect not inflicted by the active site mutant MTS-YFP-Top1mt^{Y559F} or MTS-YFP alone. Since overexpression of untagged Top1mt had no effects on mtDNA transcripts, I concluded that it was YFP that conferred negative properties to Top1mt. These properties must be inherent to Top1mt, since the tag alone, had no effect. In fact, only active Top1mt possessed the potential to lower mtDNA transcripts. Such enhancement of inborn enzyme properties by the addition of tags has previously been reported for TFAM, where mtDNA transcription was more severely affected by expression of epitope tagged TFAM than by overexpression of natural TFAM (Pohjoismaki et al, 2006). It is not clear how the tag releases the negative capability buried within Top1mt. One possibility is that, the tag influences the catalytic properties of Top1mt. Top1mt relaxation activity measured in mitoplast extracts seems to be higher than the activity of MTS-YFP-Top1mt (see 4.1.2). However, I did

not detect changes in the overall relaxation state of mtDNA in clones expressing MTS-YFP-Top1mt, suggesting that it is not Top1mt's ability to relax mtDNA that is influenced by MTS-YFP. It is possible that MTS-YFP-Top1mt affects mtDNA topology in a manner not detectable in the relaxation activity assay performed here. Another possibility is that, as for Top1 (Leppard & Champoux, 2005), the activity of Top1mt is regulated by interactions with other mitochondrial proteins. The MTS-YFP tag could disturb such interactions. Alternatively, the tag could hamper putative post-translational modifications of Top1mt. These possibilities are not necessarily mutually exclusive, and it is possible that one could induce the other. For example, the fusion to YFP could interrupt interactions between Top1mt and an unknown protein that normally modulates the activity of Top1mt and restricts its potential to inhibit mtDNA transcription.

5.1.2 *In vivo* effects of attenuated mtDNA transcription

Clearly, MTS-YFP-Top1mt is not a natural occurring protein and it is unknown whether the transcriptional defects, which derive from its expression, have a physiological relevance. Nevertheless, MTS-YFP-Top1mt offered a powerful tool to investigate the effects of an attenuated mtDNA transcription *in vivo*. The consequences of a moderately reduced mtDNA transcription in the cell have so far not been studied. This is probably due to lack of a tool that inhibits exclusively transcription, since chemical inhibitors like EtBr and ddC reduce both transcription and replication, and manipulation of essential transcription factors such as TFAM and TFB2M lead to much more dramatic effects on the mtDNA metabolism that also decrease of mtDNA copies in the cell (Larsson et al, 1998; Matsushima et al, 2004). Thus, I investigated the consequence of a moderate attenuation of mtDNA transcription.

Interestingly, I found that a very modest reduction in mtDNA transcript levels (~30%) had an over-proportional impact on the level of the mitochondrially encoded proteins of the respiratory chain (e.g. a ~80%-decrease in the mitochondrially encoded COXI subunit). This was probably due to the fact that levels of mitochondrial mRNA and rRNA were likewise affected and mitochondrial protein production was compromised by a combined effect of decreased mRNA and lesser ribosomal activity. Alternatively, the enhanced activity of MTS-YFP-Top1mt could simultaneously affect transcriptional and translational processes. TFB1M and TFB2M are cofactors involved in both mtDNA transcription and mitochondrial ribosome

biogenesis (Cotney & Shadel, 2006; Falkenberg et al, 2002). TFB2M is less efficient in the transduction process than TFB1M but is much more active as transcription factor and *vice versa* (Cotney & Shadel, 2006). Therefore, a hypothetical interference of Top1mt with TFB1M functionality could affect translation more than mtDNA transcription.

A second interesting finding was that reduction in mitochondrially produced components also led to a significant decrease in several nuclear encoded subunits of the respiratory chain complexes. These findings are in agreement with a study reporting that abnormal mitochondrial protein synthesis compromises assembly of these complexes (Park et al, 2007).

Thirdly, I found that imbalances in the composition of the respiratory chain thus provoked, severely affected the OXPHOS decreasing the rate of oxygen consumption by ~63% and inducing compensatory enhancement of anaerobic metabolism to a significant extent. It is known that a defective OXPHOS process can also result in electrons escaping from the respiratory chain and generating ROS (Bonawitz et al, 2006b), however it has been subject of some debate whether these two effects (decrease in OXPHOS and increase in ROS-production) can be simultaneously induced by a single noxis. I show here clearly, that imbalances in the respiratory chain induced by overexpression of MTS-YFP-Top1mt do indeed also exhibit features of impaired fidelity of electron transport as measured by an increased (~72%) production of superoxide anions. However, these increases in ROS seemed to be not significant in terms of cell survival, since they did not induce compensatory expression of scavenging enzymes like the mitochondrial superoxide dismutase (SOD-2) (Akashi et al, 1995; Esposito et al, 1999; St-Pierre et al, 2006), which however, could also be due to the fact that my cell model is unable to respond to oxidative stress in this way (Esposito et al, 1999). Moreover, I failed to detect a significant increase in mutations of the COXI gene in these cell clones constitutively subjected to increased ROS, indicating a normal mutation rate in MTS-YFP-Top1mt expressing cells. This finding supports the idea that oxidative stress is not a major cause of mtDNA mutations in mammals (Lim et al, 2005; Stuart et al, 2005; Trifunovic et al, 2005). However, it should be noted that-ROS induced mtDNA mutagenesis might have remained undetected in my experimental approach. It could be that increases in ROS levels or the time of exposure were insufficient for a significant impact on mtDNA stability as measured by COXI gene mutations. It could also be that cell clones bearing an increased load of mtDNA mutations did not emerge from the highly proliferating cell population (Khrapko et al, 2003).

5.1.3 Top1mt associates with mitochondrial nucleoids

This is the first study examining the sub-mitochondrial distribution of Top1mt. My major finding is that YFP tagged Top1mt accumulated in the living cell at discrete foci within the mitochondria (see 4.1.3). Moreover these foci could be divided into two subsets: One subset coincided with mitochondrial nucleoids, whereas another subset was found adjacent to but not coincident with mtDNA-antibodies. That biofluorescent Top1mt co-localises with mitochondrial nucleoids is consistent with published biochemical studies (Bogenhagen et al, 2008; Zhang & Pommier, 2008). Notwithstanding, the present study adds significant additional details in so far as I show that the composition of individual nucleoids differs with respect to Top1mt. Such information was not gained by biochemical analyses that are an average of all mitochondrial nucleoids. In contrast, I show here a considerable variance, which is most probably due to the transcriptional and replicative status of individual nucleoids at the time of observation. I propose that nucleoids where I did not detect an accumulation of MTS-YFP-Top1mt are in a physiological status not requiring Top1mt activity. While, in nucleoids delineated by MTS-YFP-Top1mt mtDNAs are actively being metabolized. Moreover, the inactive mutant MTS-YFP-Top1mt^{Y559F} had a lesser propensity to accumulate with nucleoids. This active site mutant protein is capable of binding DNA but unable to catalyze DNA cleavage. Thus, it is feasible that MTS-YFP-Top1mt^{Y559F} will bind to mtDNA “requiring” Top1mt activity but will reside there only shortly due its lack of nicking closing activity.

5.3 Concluding remarks

In this work, I contribute to clarifying the meaning of the evolutionary splitting of Top1/Top1mt. Targeting of Top1 to human mitochondria is evidently incompatible with stable mtDNA propagation, affects dramatically the transcriptional process leading ultimately to complete mtDNA depletion. The mtDNA depletion effect of Top1 in mitochondria is similar to that caused by expression of mutated variants of POLG and Twinkle (Jazayeri et al, 2003; Wanrooij et al, 2007). An analogous strong decrease of mtDNA copy-numbers has been observed upon downregulation of several cofactors of mtDNA metabolism such as TFAM (Maniura-Weber et al, 2004; Pohjoismaki et al, 2006), TFB2M (Matsushima et al, 2004), Twinkle (Tyyntismaa et al, 2004) or mtSSB (Farr et al, 2004).

The incompatibility between Top1 and mtDNA was bypassed in vertebrates by the development of Top1mt and I propose that modifications in the folding of Top1mt play a key role in this process. It is not quite clear, however, whether Top1mt is an attenuated form adapted to the requirements of mtDNA, or whether Top1 is a more aggressive form, which in the course of adaptation to the increasing complexity of the vertebrate nuclear genome acquired properties that made it incompatible with mtDNA. As the two enzymes have evolved from a common ancestor that was used in both organelles, the latter possibility seems intuitively more plausible. However, this single ancestor seems not to resemble Top1mt, as would be expected from such reasoning. For example yeasts use a single form of Top1 in the nucleus and the mitochondria (Tua et al, 1997). Protein sequence alignment of *S. cerevisiae*, *S. pombe* and *human* Top1 and *human* Top1mt revealed that both yeast Top1's are more similar to the human nuclear variant Top1 than to Top1mt (Table 5.1). This seems to indicate that the major evolutionary changes took place in Top1mt and that the ultimate outcome of topoisomerase I splitting during evolution was the adaptation of the mitochondrial form and not a further improvement of the nuclear form.

(% identities / % similarities)

<i>human</i> Top1	100/100			
<i>human</i> Top1mt	53/66	100/100		
<i>S. cerevisiae</i> Top1	39/53	35/51	100/100	
<i>S. pombe</i> Top1	37/53	35/47	48/66	100/100
	<i>human</i> Top1	<i>human</i> Top1mt	<i>S. cerevisiae</i> Top1	<i>S. pombe</i> Top1

Table 5.1: Homology of amino acid sequences of *S. cerevisiae*, *S. pombe* and *human* Top1 and *human*Top1mt.

Thus the most likely explanation is that in the course of vertebral evolution Top1 became incompatible with the mitochondrial compartment requiring the development of a specialized topoisomerase I variant, namely Top1mt. This raises the question of why Top1 became dominantly repressive to mtDNA in vertebrates and why the single form of the enzyme operating e.g. in yeasts does not induce mtDNA depletion. One possible explanation is provided by the differences in mtDNA transcription and/or replication between yeasts and vertebrates. For example, in *S. cerevisiae*, Abf2 (yeast TFAM homologue) is not essential for transcription (Diffley & Stillman, 1991). Thus, supposing that the detrimental effect

of Top1 in human mitochondria is due to the competition between Top1 and TFAM on the promoter, the negligibility of Abf2 in the transcriptional process could permit the action of Top1 in yeast mitochondria. Otherwise, differences in the structure between yeasts and vertebrate Top1 could also explain their different effect on mtDNA. However, the structure of *S. cerevisiae* Top1 cap region is similar to that of human Top1 is similar to (Lue et al, 1995).

Top1mt activity may be critical in vertebrate mitochondria, as it appears to require a specific gene, TOP1mt. However, the specific function of Top1mt in mitochondria is not clear. Recently, it has been ascribed a role of this enzyme in the pausing of the replication machinery downstream from the D-loop (Zhang & Pommier, 2008) (see 1.2.4). In spite of this, TOP1mt is not essential for development in the mice (Zhang et al, 2007). In addition to that, I found that overexpression of Top1mt has no effects on mtDNA metabolism. This result was surprising because overexpression of several other cofactors of mtDNA metabolism such as TFAM, TFB2M and Twinkle results in marked effects on mtDNA (Cotney et al, 2007; Maniura-Weber et al, 2004; Pohjoismaki et al, 2006; Tynismaa et al, 2004). Knowledge about Top1 knockout and its overexpression raise the possibility that Top1mt does not have essential functions. In contrast to the situation in the nuclear compartment, where Top1 plays vital roles in DNA metabolism, Top1mt seems to have a marginal effect in mitochondria. It is possible that the other topoisomerases present in the mitochondria (Top3 α and Top2 β) are able to sustain alone a basal mtDNA metabolism. On the other hand, Top1mt is expressed at high levels in organs with large mitochondrial mass (Zhang et al, 2001) and is upregulated in cells where mitochondrial biogenesis is induced via E2F1 knockdown (Goto et al, 2006). This suggests that Top1mt is to some extent involved in mitochondrial biogenesis. Interestingly, PGC-1 α , a key transcriptional co-activator of mitochondrial biogenesis, is not essential for development in mice (Leone et al, 2005). However, knockout of PGC-1 α in mice causes a reduced basal expression of many mitochondrial genes in tissues with high mitochondrial activity requirement leading to functional deficiencies of the respiratory chain (Arany et al, 2005; Leone et al, 2005). With age PGC-1 α ^{-/-} mice develop a wide range of disorders such as cardiac dysfunctions, reduced exercise capacity, altered thermogenic response. A similar phenotype was inflicted by PGC-1 β knockout, another transcriptional co-activator of mitochondrial biogenesis (Sonoda et al, 2007). The evolution of long living vertebrate developed new life conditions and stress stimuli. The development of Top1mt in this context could suggest that it has a role in the adaptation to an extended lifetime

and/or to the new environmental conditions. Studies are ongoing to determine the eventual pathological phenotype of TOP1^{-/-} mice (Zhang & Pommier, 2008); evaluation of the performance of these mice under stress stimuli could clarify whether Top1mt plays an essential role in the mitochondrial biogenesis.

6. References

- Ahmad F, Stewart E (2005) The N-terminal region of the *Schizosaccharomyces pombe* RecQ helicase, Rqh1p, physically interacts with Topoisomerase III and is required for Rqh1p function. *Mol Genet Genomics* **273**: 102-114
- Akashi M, Hachiya M, Paquette RL, Osawa Y, Shimizu S, Suzuki G (1995) Irradiation increases manganese superoxide dismutase mRNA levels in human fibroblasts. Possible mechanisms for its accumulation. *J Biol Chem* **270**: 15864-15869
- Allen RG, Tresini M (2000) Oxidative stress and gene regulation. *Free Radic Biol Med* **28**: 463-499
- Alsner J, Svejstrup JQ, Kjeldsen E, Sorensen BS, Westergaard O (1992) Identification of an N-terminal domain of eukaryotic DNA topoisomerase I dispensable for catalytic activity but essential for in vivo function. *J Biol Chem* **267**: 12408-12411
- Arany Z, He H, Lin J, Hoyer K, Handschin C, Toka O, Ahmad F, Matsui T, Chin S, Wu PH, Rybkin II, Shelton JM, Manieri M, Cinti S, Schoen FJ, Bassel-Duby R, Rosenzweig A, Ingwall JS, Spiegelman BM (2005) Transcriptional coactivator PGC-1 alpha controls the energy state and contractile function of cardiac muscle. *Cell Metab* **1**: 259-271
- Ashley N, Harris D, Poulton J (2005) Detection of mitochondrial DNA depletion in living human cells using PicoGreen staining. *Exp Cell Res* **303**: 432-446
- Baker SD, Wadkins RM, Stewart CF, Beck WT, Danks MK (1995) Cell cycle analysis of amount and distribution of nuclear DNA topoisomerase I as determined by fluorescence digital imaging microscopy. *Cytometry* **19**: 134-145
- Bakshi RP, Shapiro TA (2004) RNA interference of *Trypanosoma brucei* topoisomerase IB: both subunits are essential. *Mol Biochem Parasitol* **136**: 249-255
- Balaban RS, Nemoto S, Finkel T (2005) Mitochondria, oxidants, and aging. *Cell* **120**: 483-495

- Been MD, Burgess RR, Champoux JJ (1984) Nucleotide sequence preference at rat liver and wheat germ type 1 DNA topoisomerase breakage sites in duplex SV40 DNA. *Nucleic Acids Res* **12**: 3097-3114
- Bodley AL, Chakraborty AK, Xie S, Burri C, Shapiro TA (2003) An unusual type IB topoisomerase from African trypanosomes. *Proc Natl Acad Sci U S A* **100**: 7539-7544
- Bogenhagen DF, Rousseau D, Burke S (2008) The layered structure of human mitochondrial DNA nucleoids. *J Biol Chem* **283**: 3665-3675
- Bogenhagen DF, Wang Y, Shen EL, Kobayashi R (2003) Protein components of mitochondrial DNA nucleoids in higher eukaryotes. *Mol Cell Proteomics* **2**: 1205-1216
- Bolender N, Sickmann A, Wagner R, Meisinger C, Pfanner N (2008) Multiple pathways for sorting mitochondrial precursor proteins. *EMBO Rep* **9**: 42-49
- Bonawitz ND, Clayton DA, Shadel GS (2006a) Initiation and beyond: multiple functions of the human mitochondrial transcription machinery. *Mol Cell* **24**: 813-825
- Bonawitz ND, Rodeheffer MS, Shadel GS (2006b) Defective mitochondrial gene expression results in reactive oxygen species-mediated inhibition of respiration and reduction of yeast life span. *Mol Cell Biol* **26**: 4818-4829
- Brill SJ, Sternglanz R (1988) Transcription-dependent DNA supercoiling in yeast DNA topoisomerase mutants. *Cell* **54**: 403-411
- Buchet K, Godinot C (1998) Functional F1-ATPase essential in maintaining growth and membrane potential of human mitochondrial DNA-depleted rho degrees cells. *J Biol Chem* **273**: 22983-22989
- Camilloni G, Di Martino E, Caserta M, di Mauro E (1988) Eukaryotic DNA topoisomerase I reaction is topology dependent. *Nucleic Acids Res* **16**: 7071-7085
- Campisi J (2005) Suppressing cancer: the importance of being senescent. *Science* **309**: 886-887

- Carey JF, Schultz SJ, Sisson L, Fazzio TG, Champoux JJ (2003) DNA relaxation by human topoisomerase I occurs in the closed clamp conformation of the protein. *Proc Natl Acad Sci U S A* **100**: 5640-5645
- Carpenter AJ, Porter AC (2004) Construction, characterization, and complementation of a conditional-lethal DNA topoisomerase IIalpha mutant human cell line. *Mol Biol Cell* **15**: 5700-5711
- Castora FJ, Kelly WG (1986) ATP inhibits nuclear and mitochondrial type I topoisomerases from human leukemia cells. *Proc Natl Acad Sci U S A* **83**: 1680-1684
- Champoux JJ (2001) DNA Topoisomerases: Structure, Function, and Mechanism. *Annu Rev Biochem* **70**: 369-413.
- Chen H, Chomyn A, Chan DC (2005) Disruption of fusion results in mitochondrial heterogeneity and dysfunction. *J Biol Chem* **280**: 26185-26192
- Cheng C, Kussie P, Pavletich N, Shuman S (1998) Conservation of structure and mechanism between eukaryotic topoisomerase I and site-specific recombinases. *Cell* **92**: 841-850
- Cheok CF, Bachrati CZ, Chan KL, Ralf C, Wu L, Hickson ID (2005) Roles of the Bloom's syndrome helicase in the maintenance of genome stability. *Biochem Soc Trans* **33**: 1456-1459
- Christensen MO, Barthelmes HU, Boege F, Mielke C (2002a) The N-terminal domain anchors human topoisomerase I at fibrillar centers of nucleoli and nucleolar organizer regions of mitotic chromosomes. *J Biol Chem* **277**: 35932-35938
- Christensen MO, Barthelmes HU, Boege F, Mielke C (2003) Residues 190-210 of human topoisomerase I are required for enzyme activity in vivo but not in vitro. *Nucleic Acids Res* **31**: 7255-7263
- Christensen MO, Krokowski RM, Barthelmes HU, Hock R, Boege F, Mielke C (2004) Distinct effects of topoisomerase I and RNA polymerase I inhibitors suggest a dual

mechanism of nucleolar/nucleoplasmic partitioning of topoisomerase I. *J Biol Chem* **279**: 21873-21882

Christensen MO, Larsen MK, Barthelmes HU, Hock R, Andersen CL, Kjeldsen E, Knudsen BR, Westergaard O, Boege F, Mielke C (2002b) Dynamics of human DNA topoisomerases IIalpha and IIbeta in living cells. *J Cell Biol* **157**: 31-44

Clayton DA (1982) Replication of animal mitochondrial DNA. *Cell* **28**: 693-705

Clayton DA (1991) Replication and transcription of vertebrate mitochondrial DNA. *Annu Rev Cell Biol* **7**: 453-478

Cliften PF, Park JY, Davis BP, Jang SH, Jaehning JA (1997) Identification of three regions essential for interaction between a sigma-like factor and core RNA polymerase. *Genes Dev* **11**: 2897-2909

Costanzo MC, Fox TD (1990) Control of mitochondrial gene expression in *Saccharomyces cerevisiae*. *Annu Rev Genet* **24**: 91-113

Cotney J, Shadel GS (2006) Evidence for an early gene duplication event in the evolution of the mitochondrial transcription factor B family and maintenance of rRNA methyltransferase activity in human mtTFB1 and mtTFB2. *J Mol Evol* **63**: 707-717

Cotney J, Wang Z, Shadel GS (2007) Relative abundance of the human mitochondrial transcription system and distinct roles for h-mtTFB1 and h-mtTFB2 in mitochondrial biogenesis and gene expression. *Nucleic Acids Res* **35**: 4042-4054

Das BB, Sen N, Ganguly A, Majumder HK (2004) Reconstitution and functional characterization of the unusual bi-subunit type I DNA topoisomerase from *Leishmania donovani*. *FEBS Lett* **565**: 81-88

Diffley JF, Stillman B (1991) A close relative of the nuclear, chromosomal high-mobility group protein HMG1 in yeast mitochondria. *Proc Natl Acad Sci U S A* **88**: 7864-7868

- Dimri GP, Lee X, Basile G, Acosta M, Scott G, Roskelley C, Medrano EE, Linskens M, Rubelj I, Pereira-Smith O, et al. (1995) A biomarker that identifies senescent human cells in culture and in aging skin in vivo. *Proc Natl Acad Sci U S A* **92**: 9363-9367
- Druzhyzna NM, Wilson GL, LeDoux SP (2008) Mitochondrial DNA repair in aging and disease. *Mech Ageing Dev* **129**: 383-390
- Esposito LA, Melov S, Panov A, Cottrell BA, Wallace DC (1999) Mitochondrial disease in mouse results in increased oxidative stress. *Proc Natl Acad Sci U S A* **96**: 4820-4825
- Fairfield FR, Bauer WR, Simpson MV (1985) Studies on mitochondrial type I topoisomerase and on its function. *Biochim Biophys Acta* **824**: 45-57
- Falkenberg M, Gaspari M, Rantanen A, Trifunovic A, Larsson NG, Gustafsson CM (2002) Mitochondrial transcription factors B1 and B2 activate transcription of human mtDNA. *Nat Genet* **31**: 289-294
- Fan L, Kim S, Farr CL, Schaefer KT, Randolph KM, Tainer JA, Kaguni LS (2006) A novel processive mechanism for DNA synthesis revealed by structure, modeling and mutagenesis of the accessory subunit of human mitochondrial DNA polymerase. *J Mol Biol* **358**: 1229-1243
- Farr CL, Matsushima Y, Lagina AT, 3rd, Luo N, Kaguni LS (2004) Physiological and biochemical defects in functional interactions of mitochondrial DNA polymerase and DNA-binding mutants of single-stranded DNA-binding protein. *J Biol Chem* **279**: 17047-17053
- Felsenfeld G, Groudine M (2003) Controlling the double helix. *Nature* **421**: 448-453
- Fernandez-Silva P, Martinez-Azorin F, Micol V, Attardi G (1997) The human mitochondrial transcription termination factor (mTERF) is a multizipper protein but binds to DNA as a monomer, with evidence pointing to intramolecular leucine zipper interactions. *Embo J* **16**: 1066-1079

Fisher RP, Topper JN, Clayton DA (1987) Promoter selection in human mitochondria involves binding of a transcription factor to orientation-independent upstream regulatory elements. *Cell* **50**: 247-258

Frohlich RF, Veigaard C, Andersen FF, McClendon AK, Gentry AC, Andersen AH, Osheroff N, Stevnsner T, Knudsen BR (2007) Tryptophane-205 of human topoisomerase I is essential for camptothecin inhibition of negative but not positive supercoil removal. *Nucleic Acids Res* **35**: 6170-6180

Gilkerson RW, Margineantu DH, Capaldi RA, Selker JM (2000) Mitochondrial DNA depletion causes morphological changes in the mitochondrial reticulum of cultured human cells. *FEBS Lett* **474**: 1-4

Goto Y, Hayashi R, Kang D, Yoshida K (2006) Acute loss of transcription factor E2F1 induces mitochondrial biogenesis in HeLa cells. *J Cell Physiol* **209**: 923-934

Grue P, Grasser A, Sehested M, Jensen PB, Uhse A, Straub T, Ness W, Boege F (1998) Essential mitotic functions of DNA topoisomerase IIalpha are not adopted by topoisomerase IIbeta in human H69 cells. *J Biol Chem* **273**: 33660-33666

Hanahan D (1983) Studies on transformation of Escherichia coli with plasmids. *J Mol Biol* **166**: 557-580

Hannan KM, Hannan RD, Rothblum LI (1998) Transcription by RNA polymerase I. *Front Biosci* **3**: d376-398

Harman D (1972) The biologic clock: the mitochondria? *J Am Geriatr Soc* **20**: 145-147

Hayflick L (1965) The Limited in Vitro Lifetime of Human Diploid Cell Strains. *Exp Cell Res* **37**: 614-636

Heck MM, Hittelman WN, Earnshaw WC (1988) Differential expression of DNA topoisomerases I and II during the eukaryotic cell cycle. *Proc Natl Acad Sci U S A* **85**: 1086-1090

- Holt IJ, He J, Mao CC, Boyd-Kirkup JD, Martinsson P, Sembongi H, Reyes A, Spelbrink JN (2007) Mammalian mitochondrial nucleoids: organizing an independently minded genome. *Mitochondrion* **7**: 311-321
- Holt IJ, Lorimer HE, Jacobs HT (2000) Coupled leading- and lagging-strand synthesis of mammalian mitochondrial DNA. *Cell* **100**: 515-524
- Horton RM, Hunt HD, Ho SN, Pullen JK, Pease LR (1989) Engineering hybrid genes without the use of restriction enzymes: gene splicing by overlap extension. *Gene* **77**: 61-68
- Huang TT, Carlson EJ, Gillespie AM, Shi Y, Epstein CJ (2000) Ubiquitous overexpression of CuZn superoxide dismutase does not extend life span in mice. *J Gerontol A Biol Sci Med Sci* **55**: B5-9
- Hyvarinen AK, Pohjoismaki JL, Reyes A, Wanrooij S, Yasukawa T, Karhunen PJ, Spelbrink JN, Holt IJ, Jacobs HT (2007) The mitochondrial transcription termination factor mTERF modulates replication pausing in human mitochondrial DNA. *Nucleic Acids Res* **35**: 6458-6474
- Iborra FJ, Kimura H, Cook PR (2004) The functional organization of mitochondrial genomes in human cells. *BMC Biol* **2**: 9
- Jazayeri M, Andreyev A, Will Y, Ward M, Anderson CM, Clevenger W (2003) Inducible expression of a dominant negative DNA polymerase-gamma depletes mitochondrial DNA and produces a rho0 phenotype. *J Biol Chem* **278**: 9823-9830
- Jensen AD, Svejstrup JQ (1996) Purification and characterization of human topoisomerase I mutants. *Eur J Biochem* **236**: 389-394
- Ju BG, Lunyak VV, Perissi V, Garcia-Bassets I, Rose DW, Glass CK, Rosenfeld MG (2006) A topoisomerase IIbeta-mediated dsDNA break required for regulated transcription. *Science* **312**: 1798-1802
- Juan CC, Hwang JL, Liu AA, Whang-Peng J, Knutsen T, Huebner K, Croce CM, Zhang H, Wang JC, Liu LF (1988) Human DNA topoisomerase I is encoded by a

References

single-copy gene that maps to chromosome region 20q12-13.2. *Proc Natl Acad Sci U S A* **85**: 8910-8913

Kaguni LS (2004) DNA polymerase gamma, the mitochondrial replicase. *Annu Rev Biochem* **73**: 293-320

Kajander OA, Karhunen PJ, Holt IJ, Jacobs HT (2001) Prominent mitochondrial DNA recombination intermediates in human heart muscle. *EMBO Rep* **2**: 1007-1012

Kanki T, Ohgaki K, Gaspari M, Gustafsson CM, Fukuoh A, Sasaki N, Hamasaki N, Kang D (2004) Architectural role of mitochondrial transcription factor A in maintenance of human mitochondrial DNA. *Mol Cell Biol* **24**: 9823-9834

Kaufman BA, Durisic N, Mativetsky JM, Costantino S, Hancock MA, Grutter P, Shoubridge EA (2007) The mitochondrial transcription factor TFAM coordinates the assembly of multiple DNA molecules into nucleoid-like structures. *Mol Biol Cell* **18**: 3225-3236

Khrapko K, Nekhaeva E, Kraytsberg Y, Kunz W (2003) Clonal expansions of mitochondrial genomes: implications for in vivo mutational spectra. *Mutat Res* **522**: 13-19

Kimura K, Saijo M, Ui M, Enomoto T (1994) Growth state- and cell cycle-dependent fluctuation in the expression of two forms of DNA topoisomerase II and possible specific modification of the higher molecular weight form in the M phase. *J Biol Chem* **269**: 1173-1176

King MP, Attardi G (1989) Human cells lacking mtDNA: repopulation with exogenous mitochondria by complementation. *Science* **246**: 500-503

Korhonen JA, Gaspari M, Falkenberg M (2003) TWINKLE Has 5' -> 3' DNA helicase activity and is specifically stimulated by mitochondrial single-stranded DNA-binding protein. *J Biol Chem* **278**: 48627-48632

Korhonen JA, Pham XH, Pellegrini M, Falkenberg M (2004) Reconstitution of a minimal mtDNA replisome in vitro. *Embo J* **23**: 2423-2429

- Krishnan KJ, Reeve AK, Samuels DC, Chinnery PF, Blackwood JK, Taylor RW, Wanrooij S, Spelbrink JN, Lightowlers RN, Turnbull DM (2008) What causes mitochondrial DNA deletions in human cells? *Nat Genet* **40**: 275-279
- Krogh BO, Shuman S (2000) Catalytic mechanism of DNA topoisomerase IB. *Mol Cell* **5**: 1035-1041
- Kulikowicz T, Shapiro TA (2006) Distinct genes encode type II Topoisomerases for the nucleus and mitochondrion in the protozoan parasite *Trypanosoma brucei*. *J Biol Chem* **281**: 3048-3056
- Lakshmipathy U, Campbell C (1999) The human DNA ligase III gene encodes nuclear and mitochondrial proteins. *Mol Cell Biol* **19**: 3869-3876
- Larsson NG, Clayton DA (1995) Molecular genetic aspects of human mitochondrial disorders. *Annu Rev Genet* **29**: 151-178
- Larsson NG, Wang J, Wilhelmsson H, Oldfors A, Rustin P, Lewandoski M, Barsh GS, Clayton DA (1998) Mitochondrial transcription factor A is necessary for mtDNA maintenance and embryogenesis in mice. *Nat Genet* **18**: 231-236
- Lebel M, Spillare EA, Harris CC, Leder P (1999) The Werner syndrome gene product co-purifies with the DNA replication complex and interacts with PCNA and topoisomerase I. *J Biol Chem* **274**: 37795-37799
- Lee MP, Brown SD, Chen A, Hsieh TS (1993) DNA topoisomerase I is essential in *Drosophila melanogaster*. *Proc Natl Acad Sci U S A* **90**: 6656-6660
- Leone TC, Lehman JJ, Finck BN, Schaeffer PJ, Wende AR, Boudina S, Courtois M, Wozniak DF, Sambandam N, Bernal-Mizrachi C, Chen Z, Holloszy JO, Medeiros DM, Schmidt RE, Saffitz JE, Abel ED, Semenkovich CF, Kelly DP (2005) PGC-1alpha deficiency causes multi-system energy metabolic derangements: muscle dysfunction, abnormal weight control and hepatic steatosis. *PLoS Biol* **3**: e101

Leppard JB, Champoux JJ (2005) Human DNA topoisomerase I: relaxation, roles, and damage control. *Chromosoma* **114**: 75-85

Leshar DT, Pommier Y, Stewart L, Redinbo MR (2002) 8-Oxoguanine rearranges the active site of human topoisomerase I. *Proc Natl Acad Sci U S A* **99**: 12102-12107

Levin NA, Bjornsti MA, Fink GR (1993) A novel mutation in DNA topoisomerase I of yeast causes DNA damage and RAD9-dependent cell cycle arrest. *Genetics* **133**: 799-814

Lim KS, Jeyaseelan K, Whiteman M, Jenner A, Halliwell B (2005) Oxidative damage in mitochondrial DNA is not extensive. *Ann N Y Acad Sci* **1042**: 210-220

Linka RM, Porter AC, Volkov A, Mielke C, Boege F, Christensen MO (2007) C-terminal regions of topoisomerase IIalpha and IIbeta determine isoform-specific functioning of the enzymes in vivo. *Nucleic Acids Res* **35**: 3810-3822

Liu M, Spremulli L (2000) Interaction of mammalian mitochondrial ribosomes with the inner membrane. *J Biol Chem* **275**: 29400-29406

Low RL, Orton S, Friedman DB (2003) A truncated form of DNA topoisomerase IIbeta associates with the mtDNA genome in mammalian mitochondria. *Eur J Biochem* **270**: 4173-4186

Lucas P, Lasserre JP, Plissonneau J, Castroviejo M (2004) Absence of accessory subunit in the DNA polymerase gamma purified from yeast mitochondria. *Mitochondrion* **4**: 13-20

Lue N, Sharma A, Mondragon A, Wang JC (1995) A 26 kDa yeast DNA topoisomerase I fragment: crystallographic structure and mechanistic implications. *Structure* **3**: 1315-1322

Lyu YL, Wang JC (2003) Aberrant lamination in the cerebral cortex of mouse embryos lacking DNA topoisomerase IIbeta. *Proc Natl Acad Sci U S A* **100**: 7123-7128

- Maniura-Weber K, Goffart S, Garstka HL, Montoya J, Wiesner RJ (2004) Transient overexpression of mitochondrial transcription factor A (TFAM) is sufficient to stimulate mitochondrial DNA transcription, but not sufficient to increase mtDNA copy number in cultured cells. *Nucleic Acids Res* **32**: 6015-6027
- Mankouri HW, Hickson ID (2006) Top3 processes recombination intermediates and modulates checkpoint activity after DNA damage. *Mol Biol Cell* **17**: 4473-4483
- Mason PA, Matheson EC, Hall AG, Lightowlers RN (2003) Mismatch repair activity in mammalian mitochondria. *Nucleic Acids Res* **31**: 1052-1058
- Matsushima Y, Garesse R, Kaguni LS (2004) Drosophila mitochondrial transcription factor B2 regulates mitochondrial DNA copy number and transcription in schneider cells. *J Biol Chem* **279**: 26900-26905
- McCulloch V, Shadel GS (2003) Human mitochondrial transcription factor B1 interacts with the C-terminal activation region of h-mtTFA and stimulates transcription independently of its RNA methyltransferase activity. *Mol Cell Biol* **23**: 5816-5824
- Megonigal MD, Fertala J, Bjornsti MA (1997) Alterations in the catalytic activity of yeast DNA topoisomerase I result in cell cycle arrest and cell death. *J Biol Chem* **272**: 12801-12808
- Merino A, Madden KR, Lane WS, Champoux JJ, Reinberg D (1993) DNA topoisomerase I is involved in both repression and activation of transcription. *Nature* **365**: 227-232
- Meyer KN, Kjeldsen E, Straub T, Knudsen BR, Hickson ID, Kikuchi A, Kreipe H, Boege F (1997) Cell cycle-coupled relocation of types I and II topoisomerases and modulation of catalytic enzyme activities. *J Cell Biol* **136**: 775-788
- Mielke C, Tummler M, Schubeler D, von Hoegen I, Hauser H (2000) Stabilized, long-term expression of heterodimeric proteins from tricistronic mRNA. *Gene* **254**: 1-8

Miwa S, Riyahi K, Partridge L, Brand MD (2004) Lack of correlation between mitochondrial reactive oxygen species production and life span in *Drosophila*. *Ann N Y Acad Sci* **1019**: 388-391

Mo YY, Wang C, Beck WT (2000a) A novel nuclear localization signal in human DNA topoisomerase I. *J Biol Chem* **275**: 41107-41113.

Mo YY, Wang P, Beck WT (2000b) Functional expression of human DNA topoisomerase I and its subcellular localization in HeLa cells. *Exp Cell Res* **256**: 480-490

Montoya J, Christianson T, Levens D, Rabinowitz M, Attardi G (1982) Identification of initiation sites for heavy-strand and light-strand transcription in human mitochondrial DNA. *Proc Natl Acad Sci U S A* **79**: 7195-7199

Morham SG, Kluckman KD, Voulomanos N, Smithies O (1996) Targeted disruption of the mouse topoisomerase I gene by camptothecin selection. *Mol Cell Biol* **16**: 6804-6809

Muller MT, Pfund WP, Mehta VB, Trask DK (1985) Eukaryotic type I topoisomerase is enriched in the nucleolus and catalytically active on ribosomal DNA. *Embo J* **4**: 1237-1243

Ojala D, Montoya J, Attardi G (1981) tRNA punctuation model of RNA processing in human mitochondria. *Nature* **290**: 470-474

Okamoto K, Shaw JM (2005) Mitochondrial morphology and dynamics in yeast and multicellular eukaryotes. *Annu Rev Genet* **39**: 503-536

Park CB, Asin-Cayuela J, Camara Y, Shi Y, Pellegrini M, Gaspari M, Wibom R, Hultenby K, Erdjument-Bromage H, Tempst P, Falkenberg M, Gustafsson CM, Larsson NG (2007) MTERF3 is a negative regulator of mammalian mtDNA transcription. *Cell* **130**: 273-285

Pazolli E, Stewart SA (2008) Senescence: the good the bad and the dysfunctional. *Curr Opin Genet Dev* **18**: 42-47

- Perez-Campo R, Lopez-Torres M, Cadenas S, Rojas C, Barja G (1998) The rate of free radical production as a determinant of the rate of aging: evidence from the comparative approach. *J Comp Physiol [B]* **168**: 149-158
- Plank JL, Chu SH, Pohlhaus JR, Wilson-Sali T, Hsieh TS (2005) *Drosophila melanogaster* topoisomerase III α preferentially relaxes a positively or negatively supercoiled bubble substrate and is essential during development. *J Biol Chem* **280**: 3564-3573
- Pohjoismaki JL, Wanrooij S, Hyvarinen AK, Goffart S, Holt IJ, Spelbrink JN, Jacobs HT (2006) Alterations to the expression level of mitochondrial transcription factor A, TFAM, modify the mode of mitochondrial DNA replication in cultured human cells. *Nucleic Acids Res* **34**: 5815-5828
- Rasheed S, Nelson-Rees WA, Toth EM, Arnstein P, Gardner MB (1974) Characterization of a newly derived human sarcoma cell line (HT-1080). *Cancer* **33**: 1027-1033
- Redinbo MR, Champoux JJ, Hol WG (2000) Novel insights into catalytic mechanism from a crystal structure of human topoisomerase I in complex with DNA. *Biochemistry* **39**: 6832-6840
- Redinbo MR, Stewart L, Kuhn P, Champoux JJ, Hol WG (1998) Crystal structures of human topoisomerase I in covalent and noncovalent complexes with DNA. *Science* **279**: 1504-1513
- Richter C, Park JW, Ames BN (1988) Normal oxidative damage to mitochondrial and nuclear DNA is extensive. *Proc Natl Acad Sci U S A* **85**: 6465-6467
- Riedl SJ, Salvesen GS (2007) The apoptosome: signalling platform of cell death. *Nat Rev Mol Cell Biol* **8**: 405-413
- Rizzuto R, Brini M, Pizzo P, Murgia M, Pozzan T (1995) Chimeric green fluorescent protein as a tool for visualizing subcellular organelles in living cells. *Curr Biol* **5**: 635-642

Rizzuto R, Pinton P, Carrington W, Fay FS, Fogarty KE, Lifshitz LM, Tuft RA, Pozzan T (1998) Close contacts with the endoplasmic reticulum as determinants of mitochondrial Ca²⁺ responses. *Science* **280**: 1763-1766

Rodeheffer MS, Boone BE, Bryan AC, Shadel GS (2001) Nam1p, a protein involved in RNA processing and translation, is coupled to transcription through an interaction with yeast mitochondrial RNA polymerase. *J Biol Chem* **276**: 8616-8622

Rodeheffer MS, Shadel GS (2003) Multiple interactions involving the amino-terminal domain of yeast mtRNA polymerase determine the efficiency of mitochondrial protein synthesis. *J Biol Chem* **278**: 18695-18701

Rossi F, Labourier E, Forne T, Divita G, Derancourt J, Riou JF, Antoine E, Cathala G, Brunel C, Tazi J (1996) Specific phosphorylation of SR proteins by mammalian DNA topoisomerase I. *Nature* **381**: 80-82

Rossi F, Labourier E, Gallouzi IE, Derancourt J, Allemand E, Divita G, Tazi J (1998) The C-terminal domain but not the tyrosine 723 of human DNA topoisomerase I active site contributes to kinase activity. *Nucleic Acids Res* **26**: 2963-2970

Rossignol R, Malgat M, Mazat JP, Letellier T (1999) Threshold effect and tissue specificity. Implication for mitochondrial cytopathies. *J Biol Chem* **274**: 33426-33432

Sanchirico ME, Fox TD, Mason TL (1998) Accumulation of mitochondrially synthesized *Saccharomyces cerevisiae* Cox2p and Cox3p depends on targeting information in untranslated portions of their mRNAs. *Embo J* **17**: 5796-5804

Schapira AH (2006) Mitochondrial disease. *Lancet* **368**: 70-82

Schriner SE, Linford NJ, Martin GM, Treuting P, Ogburn CE, Emond M, Coskun PE, Ladiges W, Wolf N, Van Remmen H, Wallace DC, Rabinovitch PS (2005) Extension of murine life span by overexpression of catalase targeted to mitochondria. *Science* **308**: 1909-1911

- Seidel-Rogol BL, McCulloch V, Shadel GS (2003) Human mitochondrial transcription factor B1 methylates ribosomal RNA at a conserved stem-loop. *Nat Genet* **33**: 23-24
- Seidel-Rogol BL, Shadel GS (2002) Modulation of mitochondrial transcription in response to mtDNA depletion and repletion in HeLa cells. *Nucleic Acids Res* **30**: 1929-1934
- Severino J, Allen RG, Balin S, Balin A, Cristofalo VJ (2000) Is beta-galactosidase staining a marker of senescence in vitro and in vivo? *Exp Cell Res* **257**: 162-171
- Shaiu WL, Hsieh TS (1998) Targeting to transcriptionally active loci by the hydrophilic N-terminal domain of *Drosophila* DNA topoisomerase I. *Mol Cell Biol* **18**: 4358-4367
- Shimamoto A, Nishikawa K, Kitao S, Furuichi Y (2000) Human RecQ5beta, a large isomer of RecQ5 DNA helicase, localizes in the nucleoplasm and interacts with topoisomerases 3alpha and 3beta. *Nucleic Acids Res* **28**: 1647-1655
- Simpson MV, Chin CD, Keilbaugh SA, Lin TS, Prusoff WH (1989) Studies on the inhibition of mitochondrial DNA replication by 3'-azido-3'-deoxythymidine and other dideoxynucleoside analogs which inhibit HIV-1 replication. *Biochem Pharmacol* **38**: 1033-1036
- Slesarev AI, Stetter KO, Lake JA, Gellert M, Krah R, Kozyavkin SA (1993) DNA topoisomerase V is a relative of eukaryotic topoisomerase I from a hyperthermophilic prokaryote. *Nature* **364**: 735-737
- Sonoda J, Mehl IR, Chong LW, Nofsinger RR, Evans RM (2007) PGC-1beta controls mitochondrial metabolism to modulate circadian activity, adaptive thermogenesis, and hepatic steatosis. *Proc Natl Acad Sci U S A* **104**: 5223-5228
- Spelbrink JN, Toivonen JM, Hakkaart GA, Kurkela JM, Cooper HM, Lehtinen SK, Lecrenier N, Back JW, Speijer D, Foury F, Jacobs HT (2000) In vivo functional analysis of the human mitochondrial DNA polymerase POLG expressed in cultured human cells. *J Biol Chem* **275**: 24818-24828

- St-Pierre J, Buckingham JA, Roebuck SJ, Brand MD (2002) Topology of superoxide production from different sites in the mitochondrial electron transport chain. *J Biol Chem* **277**: 44784-44790
- St-Pierre J, Drori S, Uldry M, Silvaggi JM, Rhee J, Jager S, Handschin C, Zheng K, Lin J, Yang W, Simon DK, Bachoo R, Spiegelman BM (2006) Suppression of reactive oxygen species and neurodegeneration by the PGC-1 transcriptional coactivators. *Cell* **127**: 397-408
- Stewart L, Ireton GC, Champoux JJ (1996) The domain organization of human topoisomerase I. *J Biol Chem* **271**: 7602-7608
- Stewart L, Ireton GC, Champoux JJ (1997) Reconstitution of human topoisomerase I by fragment complementation. *J Mol Biol* **269**: 355-372
- Stewart L, Redinbo MR, Qiu X, Hol WG, Champoux JJ (1998) A model for the mechanism of human topoisomerase I. *Science* **279**: 1534-1541
- Stuart JA, Bourque BM, de Souza-Pinto NC, Bohr VA (2005) No evidence of mitochondrial respiratory dysfunction in OGG1-null mice deficient in removal of 8-oxodeoxyguanine from mitochondrial DNA. *Free Radic Biol Med* **38**: 737-745
- Stuart JA, Brown MF (2006) Mitochondrial DNA maintenance and bioenergetics. *Biochim Biophys Acta* **1757**: 79-89
- Sumikawa E, Matsumoto Y, Sakemura R, Fujii M, Ayusawa D (2005) Prolonged unbalanced growth induces cellular senescence markers linked with mechano transduction in normal and tumor cells. *Biochem Biophys Res Commun* **335**: 558-565
- Takao M, Aburatani H, Kobayashi K, Yasui A (1998) Mitochondrial targeting of human DNA glycosylases for repair of oxidative DNA damage. *Nucleic Acids Res* **26**: 2917-2922
- Thompson JD, Higgins DG, Gibson TJ (1994) CLUSTAL W: improving the sensitivity of progressive multiple sequence alignment through sequence weighting, position-specific gap penalties and weight matrix choice. *Nucleic Acids Res* **22**: 4673-4680

- Thrash C, Bankier AT, Barrell BG, Sternglanz R (1985) Cloning, characterization, and sequence of the yeast DNA topoisomerase I gene. *Proc Natl Acad Sci U S A* **82**: 4374-4378
- Thyagarajan B, Padua RA, Campbell C (1996) Mammalian mitochondria possess homologous DNA recombination activity. *J Biol Chem* **271**: 27536-27543
- Trifunovic A, Hansson A, Wredenberg A, Rovio AT, Dufour E, Khvorostov I, Spelbrink JN, Wibom R, Jacobs HT, Larsson NG (2005) Somatic mtDNA mutations cause aging phenotypes without affecting reactive oxygen species production. *Proc Natl Acad Sci U S A* **102**: 17993-17998
- Trifunovic A, Larsson NG (2008) Mitochondrial dysfunction as a cause of ageing. *J Intern Med* **263**: 167-178
- Trifunovic A, Wredenberg A, Falkenberg M, Spelbrink JN, Rovio AT, Bruder CE, Bohlooly YM, Gidlof S, Oldfors A, Wibom R, Tornell J, Jacobs HT, Larsson NG (2004) Premature ageing in mice expressing defective mitochondrial DNA polymerase. *Nature* **429**: 417-423
- Trzcinska-Daneluti AM, Gorecki A, Czubaty A, Kowalska-Loth B, Girstun A, Murawska M, Lesyng B, Staron K (2007) RRM proteins interacting with the cap region of topoisomerase I. *J Mol Biol* **369**: 1098-1112
- Tsutsui H, Kinugawa S, Matsushima S (2008) Mitochondrial oxidative stress and dysfunction in myocardial remodelling. *Cardiovasc Res*
- Tua A, Wang J, Kulpa V, Wernette CM (1997) Mitochondrial DNA topoisomerase I of *Saccharomyces cerevisiae*. *Biochimie* **79**: 341-350
- Tyynismaa H, Mjosund KP, Wanrooij S, Lappalainen I, Ylikallio E, Jalanko A, Spelbrink JN, Paetau A, Suomalainen A (2005) Mutant mitochondrial helicase Twinkle causes multiple mtDNA deletions and a late-onset mitochondrial disease in mice. *Proc Natl Acad Sci U S A* **102**: 17687-17692

Tyynismaa H, Sembongi H, Bokori-Brown M, Granycome C, Ashley N, Poulton J, Jalanko A, Spelbrink JN, Holt IJ, Suomalainen A (2004) Twinkle helicase is essential for mtDNA maintenance and regulates mtDNA copy number. *Hum Mol Genet* **13**: 3219-3227

Van Remmen H, Ikeno Y, Hamilton M, Pahlavani M, Wolf N, Thorpe SR, Alderson NL, Baynes JW, Epstein CJ, Huang TT, Nelson J, Strong R, Richardson A (2003) Life-long reduction in MnSOD activity results in increased DNA damage and higher incidence of cancer but does not accelerate aging. *Physiol Genomics* **16**: 29-37

Van Remmen H, Qi W, Sabia M, Freeman G, Estlack L, Yang H, Mao Guo Z, Huang TT, Strong R, Lee S, Epstein CJ, Richardson A (2004) Multiple deficiencies in antioxidant enzymes in mice result in a compound increase in sensitivity to oxidative stress. *Free Radic Biol Med* **36**: 1625-1634

Vermulst M, Bielas JH, Kujoth GC, Ladiges WC, Rabinovitch PS, Prolla TA, Loeb LA (2007) Mitochondrial point mutations do not limit the natural lifespan of mice. *Nat Genet* **39**: 540-543

Vermulst M, Wanagat J, Kujoth GC, Bielas JH, Rabinovitch PS, Prolla TA, Loeb LA (2008) DNA deletions and clonal mutations drive premature aging in mitochondrial mutator mice. *Nat Genet* **40**: 392-394

Wallace DC, Shoffner JM, Trounce I, Brown MD, Ballinger SW, Corral-Debrinski M, Horton T, Jun AS, Lott MT (1995) Mitochondrial DNA mutations in human degenerative diseases and aging. *Biochim Biophys Acta* **1271**: 141-151

Wallis JW, Chrebet G, Brodsky G, Rolfe M, Rothstein R (1989) A hyper-recombination mutation in *S. cerevisiae* identifies a novel eukaryotic topoisomerase. *Cell* **58**: 409-419

Wang J, Kearney K, Derby M, Wernette CM (1995) On the relationship of the ATP-independent, mitochondrial associated DNA topoisomerase of *Saccharomyces cerevisiae* to the nuclear topoisomerase I. *Biochem Biophys Res Commun* **214**: 723-729

- Wang JC (2002) Cellular roles of DNA topoisomerases: a molecular perspective. *Nat Rev Mol Cell Biol* **3**: 430-440
- Wang Y, Lyu YL, Wang JC (2002) Dual localization of human DNA topoisomerase IIIalpha to mitochondria and nucleus. *Proc Natl Acad Sci U S A* **99**: 12114-12119
- Wang Z, Cotney J, Shadel GS (2007) Human mitochondrial ribosomal protein MRPL12 interacts directly with mitochondrial RNA polymerase to modulate mitochondrial gene expression. *J Biol Chem* **282**: 12610-12618
- Wanrooij S, Fuste JM, Farge G, Shi Y, Gustafsson CM, Falkenberg M (2008) Human mitochondrial RNA polymerase primes lagging-strand DNA synthesis in vitro. *Proc Natl Acad Sci U S A* **105**: 11122-11127
- Wanrooij S, Goffart S, Pohjoismaki JL, Yasukawa T, Spelbrink JN (2007) Expression of catalytic mutants of the mtDNA helicase Twinkle and polymerase POLG causes distinct replication stalling phenotypes. *Nucleic Acids Res* **35**: 3238-3251
- Wanrooij S, Luoma P, van Goethem G, van Broeckhoven C, Suomalainen A, Spelbrink JN (2004) Twinkle and POLG defects enhance age-dependent accumulation of mutations in the control region of mtDNA. *Nucleic Acids Res* **32**: 3053-3064
- Woessner RD, Mattern MR, Mirabelli CK, Johnson RK, Drake FH (1991) Proliferation- and cell cycle-dependent differences in expression of the 170 kilodalton and 180 kilodalton forms of topoisomerase II in NIH-3T3 cells. *Cell Growth Differ* **2**: 209-214
- Xu B, Clayton DA (1992) Assignment of a yeast protein necessary for mitochondrial transcription initiation. *Nucleic Acids Res* **20**: 1053-1059
- Yang X, Li W, Prescott ED, Burden SJ, Wang JC (2000) DNA topoisomerase IIbeta and neural development. *Science* **287**: 131-134

References

Yasukawa T, Reyes A, Cluett TJ, Yang MY, Bowmaker M, Jacobs HT, Holt IJ (2006) Replication of vertebrate mitochondrial DNA entails transient ribonucleotide incorporation throughout the lagging strand. *Embo J* **25**: 5358-5371

Yasukawa T, Yang MY, Jacobs HT, Holt IJ (2005) A bidirectional origin of replication maps to the major noncoding region of human mitochondrial DNA. *Mol Cell* **18**: 651-662

Zhang H, Barcelo JM, Lee B, Kohlhagen G, Zimonjic DB, Popescu NC, Pommier Y (2001) Human mitochondrial topoisomerase I. *Proc Natl Acad Sci U S A* **98**: 10608-10613

Zhang H, Meng LH, Pommier Y (2007) Mitochondrial topoisomerases and alternative splicing of the human TOP1mt gene. *Biochimie* **89**: 474-481

Zhang H, Meng LH, Zimonjic DB, Popescu NC, Pommier Y (2004) Thirteen-exon-motif signature for vertebrate nuclear and mitochondrial type IB topoisomerases. *Nucleic Acids Res* **32**: 2087-2092

Zhang H, Pommier Y (2008) Mitochondrial Topoisomerase I Sites in the Regulatory D-Loop Region of Mitochondrial DNA. *Biochemistry*

7. Abbreviations

ATP	Adenosine triphosphate
2DNAGE	Two dimensional neutral agarose gel electrophoresis
a.a.	Amino acids
ADP	Adenosine diphosphate
ANT	Adenine nucleotide translocator
AntA	Antimycin A
BER	Base excision repair
bp	Base pairs
CD	Common deletion
COX	cytochrome c oxidase
CPT	Camptothecin
CTD	C-terminal domain
<i>D. Melanogaster</i>	<i>Drosophila melanogaster</i>
ddC	2'3'-Dideoxycytidine
D-loop	Displacement-loop
dsDNA	Double-stranded DNA
e.g.	Exempli gratia
EtBr	Ethidium bromide
FACS	Fluorescence activated cell sorting
FADH ₂	Reduced flavin adenine dinucleotide
FCS	Foetal bovine serum
Fig.	Figure
GSHPx	Glutathione peroxidase
HMG	High-mobility-group
HSP	Heavy-strand promoter
HSP1	Heavy-strand promoter site 1
HSP2	Heavy-strand promoter site 2
i.e.	Id est
IMM	Inner mitochondrial membrane
IRES	Internal ribosome entry site
kDNA	Kinetoplast DNA
LOHN	Leber's hereditary optic neuropathy

Abbreviation

LSP	Light-strand promoter
MELAS	Mitochondrial encephalomyopathy
min	minutes
MPP	Mitochondrial-processing peptidase
mtDNA	Mitochondrial DNA
mTERF	Mitochondrial transcription termination factor
MTS	Mitochondrial targeting signal
mtSSB	Mitochondrial single strand binding protein
NADH	Reduced nicotinamide adenine dinucleotide
NCR	Non coding region
NLS	Nuclear localisation signal
NTD	N-terminal domain
nts	Nucleotides
O _H	Origin of replication for the leading-strand synthesis
O _L	Origin of replication for the lagging-strand synthesis
OXPPOS	Oxidative phosphorylation
pac	Pyromycin-N-acetyltransferase
PCR	Polymerase chain reaction
PEO	Progressive external ophthalmoplegia
POLG	Mitochondrial DNA polymerase γ
POLGA	Mitochondrial DNA polymerase γ subunits α
POLGB	Mitochondrial DNA polymerase γ subunits β
POLRMT	Mitochondrial RNA polymerase
qPCR	Quantitative real time PCR
QRT-PCR	Quantitative real time reverse transcriptase PCR
RIs	MtDNA replication intermediates
RITOLS	RNA incorporation throughout the lagging strand
ROS	Reactive oxygen species
RRM	RNA recognition motive
<i>S. cerevisiae</i>	<i>Saccharomyces cerevisiae</i>
<i>S. Pombe</i>	<i>Schizosaccharomyces pombe</i>
SEM	Standard error of the mean
SOD	Superoxide dismutase
SOD-2	Mitochondrial superoxide dismutase
ssDNA	Single-stranded DNA
TFAM	Mitochondrial transcription factor A

TFB1M	Mitochondrial transcription factor B1
TFB2M	Mitochondrial transcription factor B2
TIM	Translocase of inner mitochondrial membrane
T _m	Melting Temperature
TOM	Translocase of outer mitochondrial membrane
Top1	Nuclear topoisomerase I
TOP1	Gene encoding Top1
Top1mt	Mitochondrial topoisomerase I
TOP1mt	Gene encoding Top1mt
W/v	Weight/volume
X-gal	5-Brom-4-chlor-3-indoxyl-β-D-galactopyranosid
YFP	Yellow fluorescent protein

8. Appendix

8.1 Plasmid maps

8.1.A pMC-2PS-delta HindIII-P

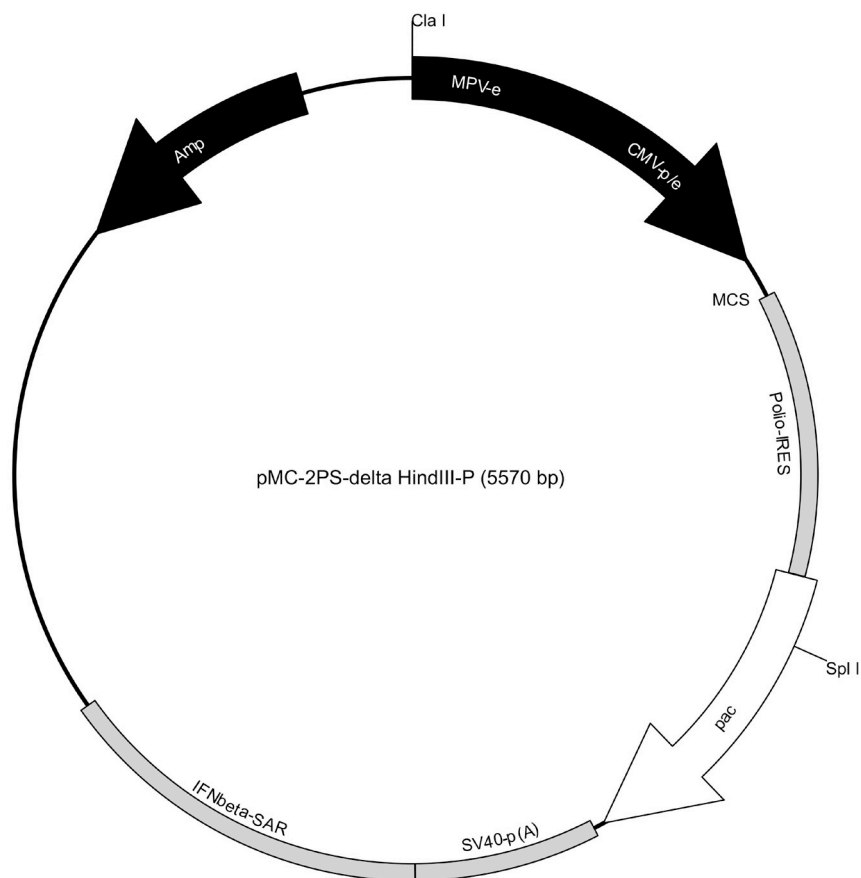


Fig. 8.1: Basic bicistronic expression plasmid pMC-2PS-delta HindIII-P (Mielke et al, 2000).
For details see 2.1.1.

8.1.B pMC-EYFP-P-N

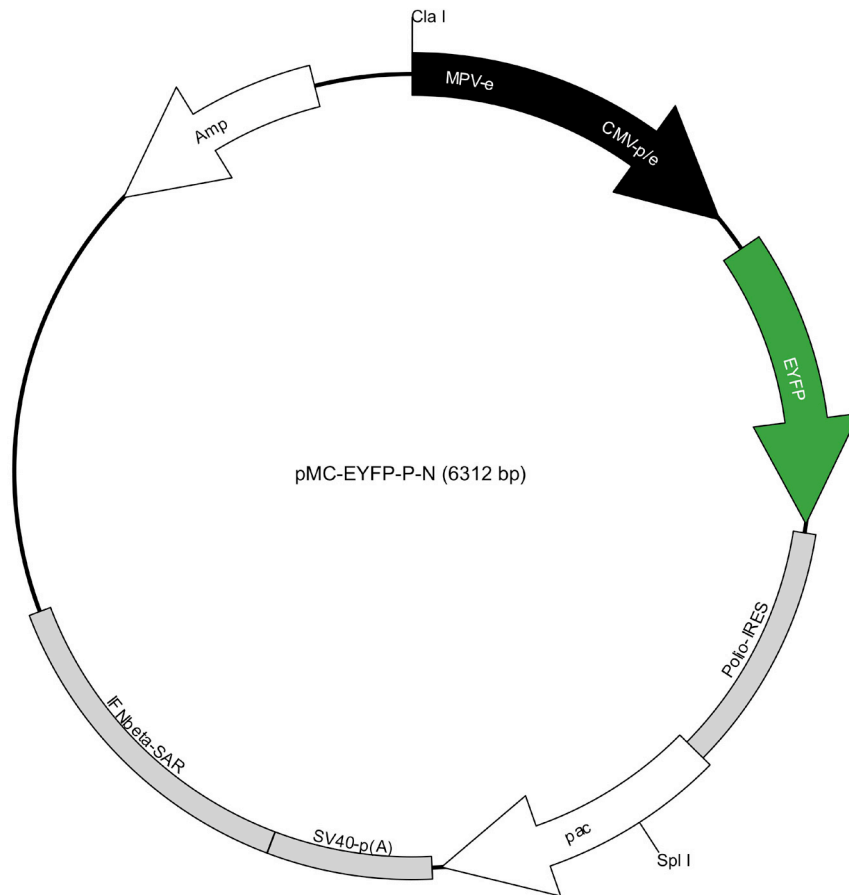


Fig. 8.2: Bicistronic expression plasmid pMC-EYFP-P-N. For details see 2.1.1.

8.1.C pCL1P3

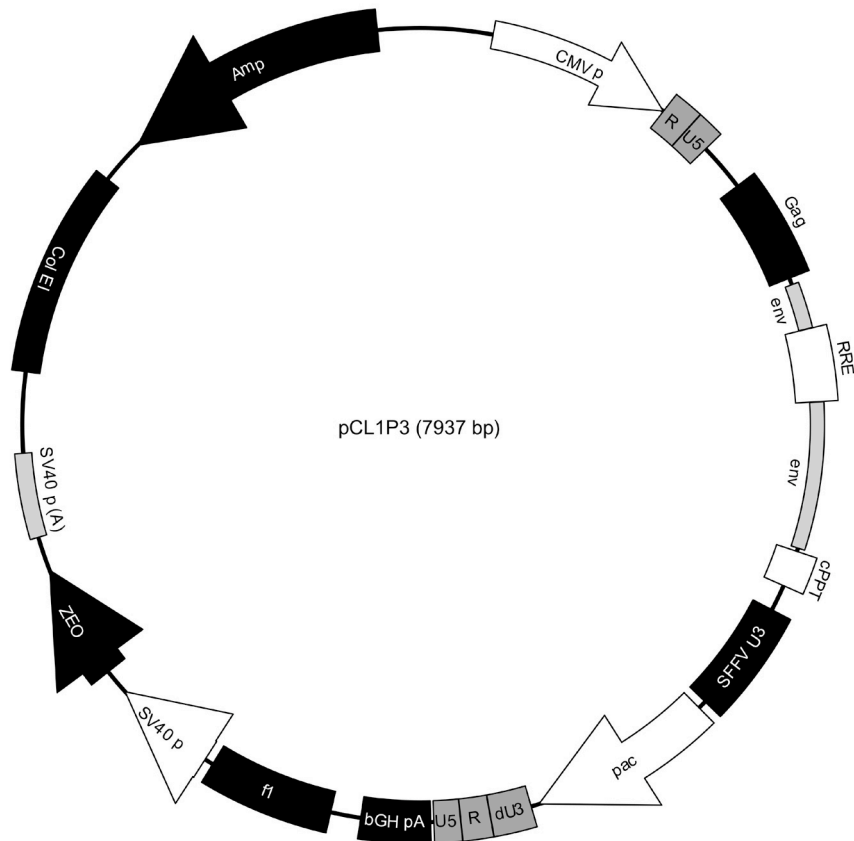


Fig. 8.3: Lentiviral vector pCL1P3 (see 2.1.2). pCL1P3 was kindly supplied by Prof. Hannenberg, Dep. of Pediatric Oncology, Haematology & Immunology Children's Hospital, Heinrich Heine University Düsseldorf.

8.1.D pMC-EYFP-P-N

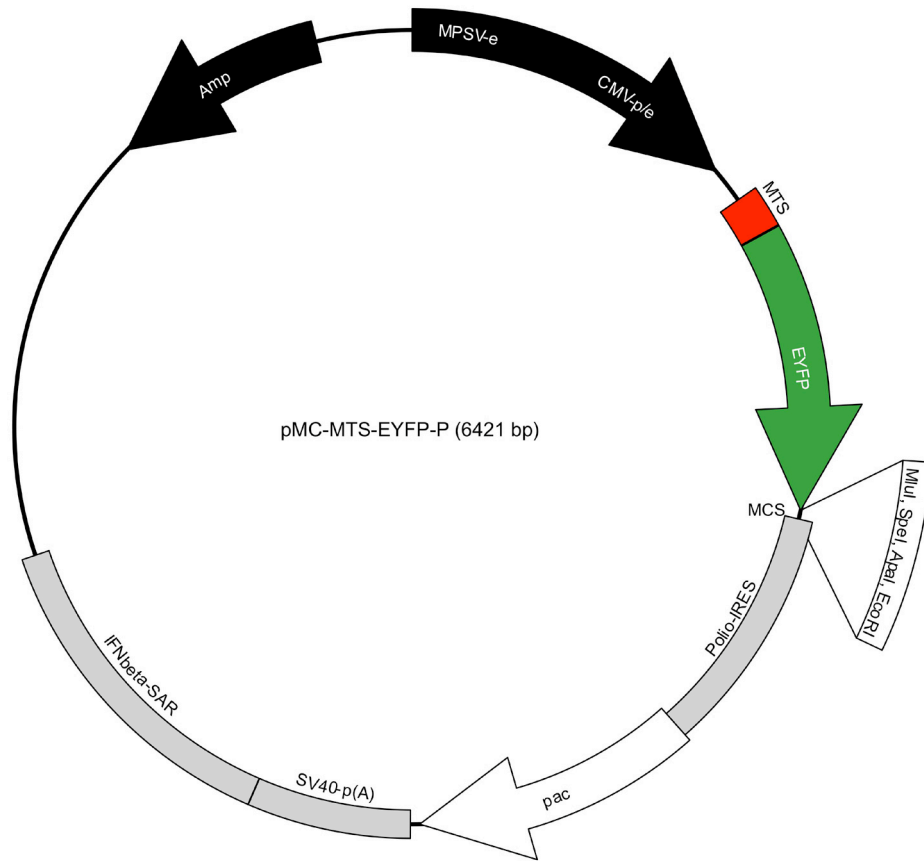


Fig. 8.4: Bicistronic expression plasmid pMC-MTS-EYFP-P. YFP (green) is fused at the 5' end with the MTS from subunit VIII of COX (red, see 3.1.1.1).

8.2 Top1/Top1mt alignment

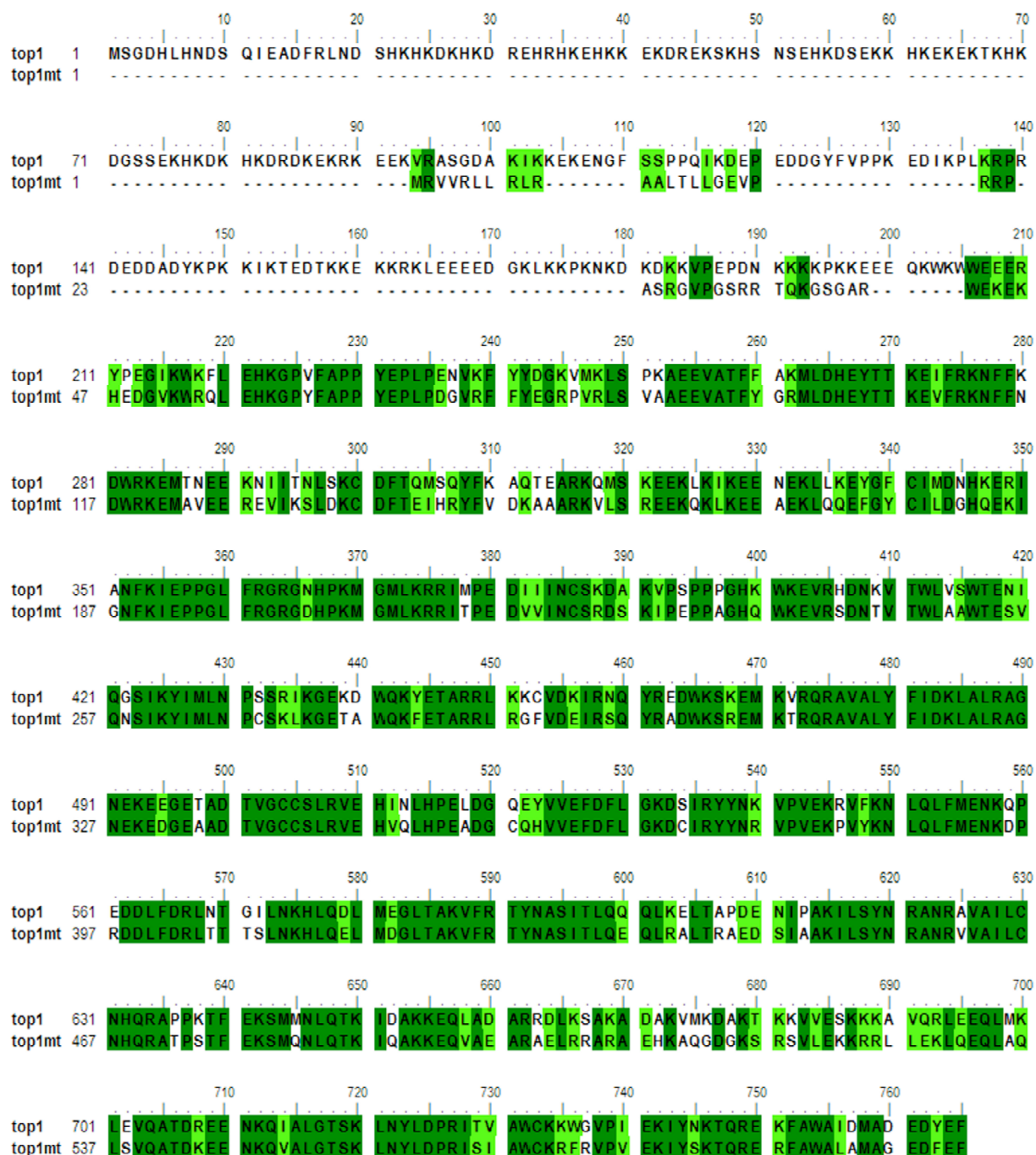


Fig. 8.5: Protein sequence alignment between Top1 and Top1mt. Identical and similar amino acids are shown in dark and light green, respectively. Alignment was performed using „ClustalW 1.81“ (Thompson et al, 1994) and graphically depicted using “BioEdit 7.053”.

9. Acknowledgments

First of all, I would like to thank Prof. Fritz Boege for giving me the opportunity to work in his laboratory and for the supervision of my PhD project. A special thanks goes to Dr. Morten Christensen who taught me almost all that I know in the lab: For your competent expertise, for the countless discussions and ideas about my project thank you very much! Many thanks go also to Dr. Christian Mielke for listening, all helpful advice and our pleasant chats.

I am also grateful to all other members of the Boege group: Beatrice, Björn, Birgit, Christoph, Ellen, Elke, Faiza, René, Said and Stefan (rigorously in alphabetical order) for the joking atmosphere in the lab and for their numerous German lessons. Special thanks go to Beatrice (my severest German teacher) for her friendship and empathy, to Faiza for her unconditional helpfulness and to René for sharing problems for a long time! Thanks to Stefan for our amusing cooperation and for performing the immunostains shown in Fig. 4.1.4 A and B.

I want to thank my collaboration partners Prof. Yves Pomier and Dr. Hongliang Zhang, from the NIH of Bethesda for supplying the Top1mt cDNA as well as Dr. Steffi Goffart from the Institute of Medical Technology of Tampere, for performing the 2DNAGE gels shown in Fig. 4.2.10. Many thanks also to Prof. Helmut Hanenberg, Melanie Wurm and Conny Wiek from the Children's Hospital of Düsseldorf who provided assistance with the viral transductions. I am also in debt to Verena Schildgen from the Institute for Virology of the University of Bonn, for providing some of the standard plasmids for qPCR and to Frank Essmann from the Institute of Molecular Medicine of the University of Düsseldorf who assisted me with the FACS analysis.

I would like to thank Prof. Johannes Hegemann for being my co-referee.

Many thanks to the Graduate program GK 1033 "Molekulare Ziele von Alterungsprozessen und Ansatzpunkte der Alterungsprävention" for the financial support and to my GK colleagues Silke, Janine, Tobi, Sonja and Holger for the pleasant conversations at dinner parties (Silke, I will never forget your tapas!) and the nice time together.

Acknowledgments

Finally, I would like to thank my family and all my Italian friends for being there in spite of the distance.... GRAZIE!

10. Curriculum Vitae

Personal information

Name	Ilaria Dalla Rosa
Date and place of birth	January 19, 1979, Bolzano (Italy)
Nationality	Italian
Address	68, Burghofstrasse, 40223 Düsseldorf, Germany
E-mail	ilaria.dallarosa@med.uni-duesseldorf.de

Education

September 1993- July 1998	High school: Liceo Scientifico Statale "E. Torricelli" Bolzano Italy School leaving examination: Maturità Scientifica, 52/60
October 1998- March 2004	"Alma Mater Studiorum" University, Bologna, Italy Undergraduate student of Biology First-class honours degree in Biology, 110/110 cum laude
March 2003- March 2004	Research Assistant at Department of experimental Pathology, "Alma Mater Studiorum" University, Bologna, Italy PI: Professor Novello Paglianti Francesco
September 2004- February 2005	Fellowships for abroad training activity awarded by "Alma Mater Studiorum" University of Bologna. Institute of Clinical Chemistry and Laboratory Diagnostics, Heinrich-Heine- University, Medical School
Since March 2005	Ph.D student at Institute of Clinical Chemistry and Laboratory Diagnostics, Heinrich-Heine-University, Medical School PI: Professor Fritz Boege

11. Erklärung

Hiermit erkläre ich, dass ich die vorliegende Dissertation eigenständig und ohne unerlaubte Hilfe angefertigt habe. Ich habe diese Dissertation in der vorgelegten oder in ähnlicher Form noch bei keiner anderen Institution eingereicht. Ich habe bisher keine erfolglosen Promotionsversuche unternommen.

Düsseldorf, den 21.1.2009

(Ilaria Dalla Rosa)